NOTICE

The quality of this microform is heavily dependent upon the quality of the original thesis submitted for microfilming. Every effort has been made to ensure the highest quality of reproduction possible.

If pages are missing, contact the university which granted the degree.

Some pages may have indistinct print especially if the original pages were typed with a poor typewriter ribbon or if the university sent us an inferior photocopy.

Reproduction in full or in part of this microform is governed by the Canadian Copyright Act, R.S.C. 1970, c. C-30, and subsequent amendments.

AVIS

La qualité de cette microforme dépend grandement de la qualité de la thèse soumise au microfilmage. Nous avons tout fait pour assurer une qualité supérieure de reproduction.

S'il manque des pages, veuillez communiquer avec l'université qui a conféré le grade.

La qualité d'impression de certaines pages peut laisser à désirer, surtout si les pages originales ont été dactylographiées à l'aide d'un ruban usé ou si l'université nous a fait parvenir une photocopie de qualité inférieure.

La reproduction, même partielle, de cette microforme est soumise à la Loi canadienne sur le droit d'auteur, SRC 1970, c. C-30, et ses amendements subséquents.

Modelling And Control Of A Variable Air Volume (VAV) System

Poi Ann Goh

A Thesis

in

The Centre for Building Studies

Presented in Partial Fulfilment of the Requirements
for the Degree of Master of Engineering at
Concordia University
Montréal, Québec, Canada

December 1990.

ISBN 0-315-64745-0

Canada

ABSTRACT

Modelling And Control Of A Variable Air Volume (VAV) System

Poi Ann, Goh

A dynamic model for controlling a variable air volume (VAV) system is developed. The overall model consists of the following sub-models: 1) a cooling and dehumidifying coil, 2) a chiller and storage tank arrangement, 3) a single zone environmental space, 4) a fan, and 5) the associate ductwork. The control variables are: a) the coil face and bypass dampers opening fractions, b) input energy to the chiller and c) supply air mass flow rate. The outputs of interest are: i) the zone air temperature and ii) relative humidity.

The model equations are described and open-loop tests are conducted to study the effect of changes in control variables (air mass flow rate, chilled water temperature) on zone air temperature and relative humidity.

Feedback control algorithms are implemented for controlling the input energy to the chiller, the position of the face and bypass dampers and the supply air mass flow rate. The operating performance of the VAV system is illustrated

using several simulated test cases. The results indicate that the control algorithms are capable of rejecting the disturbance (sensible and latent loads) effectively. This is shown in terms of time response characteristics to a step change in load as well as to typical daily load profile. In both cases, the control algorithm is able to maintain the zone air dry bulb temperature and relative humidity close to the respective setpoint values.

ACKNOWLEDGEMENTS

I wish to express my gratitude and appreciation to Dr. M. Zaheer-uddin for initiating this research and for his valuable guidance, criticism and suggestions throughout my graduate studies.

With respect, love and admiration, I sincerely thank my parents, brothers, sisters, and relatives for their encouragement and moral support.

And finally, special thanks and appreciation go to my fiancée Siew Hoon Ooi for her patience, understanding, encouragement and moral support throughout my graduate studies.

TABLE OF CONTENTS

TABLE OF CONTENTS

TABLE OF CONTENTS

TABLE OF CONTENTS

LIST OF FIGURES

LIST OF FIGURES

LIST OF FIGURES

LIST OF TABLES

NOMENCLATURE

a	constant
A	surface area, (m^2 or ft^2)
A_o	total outside heat transfer area, (m^2 or ft^2)
atm	atmospheric
b	constant
BHP	brake horse power
C_f	dimensionless flow coefficient
cfm	volume flow rate, (ft^3/min)
C_h	dimensionless pressure head coefficient
COP	coefficient of performance
C_p	specific heat, (kJ/kg.°C or Btu/lb.°F)
C_w	chilled water tank thermal capacity, (kJ/°C or Btu/°F)
CWFR	chilled water flow rate, (kg/s or lb/hr)
d	differential
$\bar{d}$	duct thickness, (m or ft)
D	diameter, (m or ft)
D_e	equivalent diameter, (m or ft)
D_h	hydraulic diameter, (m or ft)
e(t)	error term
E	power consumption, (kW or Btu/hr)
F	Fin
F_h	Fin height, (m or ft)
F_s	Fin spacing, (m or ft)
F_t	Fin thickness, (m or ft)

NOMENCLATURE

FFLP	fraction of full-load power
G	gain factor
h	enthalpy, (kJ/kg or Btu/h)
h	heat transfer coefficient, ($W/m^2 \cdot C$ or $Btu/hr \cdot F \cdot ft^2$)
$\hat{h}$	heat transfer coefficient per unit length, (W/m°C or Btu/hr°F.ft)
I_g	enthalpy of saturated water, (kJ/kg or Btu/lb)
J	Heat transfer factor defined in Equation (2.1)
K	constant
k_p	proportional constant
L or l	length, (m or ft)
Le	Lewis number
LMTD	log-mean temperature difference
m	mass flow rate per unit length, (kg/m or lb/ft)
M	mass flow rate, (kg/s or lb/hr)
$\hat{m}_w$	latent load, (kg/s or lb/hr)
mr	mechanical room
Ms	mass, (kg or lb)
N	rotation, (rps or rpm)
NTU	number of transfer units
Nu	Nusselt number
P	pressure, (kPa or inch of W.G)
$\bar{P}$	average perimeter, (m or ft)
P_D	Proportional constant defined in Equation (3.18)

NOMENCLATURE

PL	part load
PLC	percent of energy source input required
PLR	part load ratio
Pr	Prandlt number
Q or q	heat transfer rate, (W or Btu/hr)
R	thermal resistance, (m°C.s/kJ or ft°F.hr/Btu)
Re	Reynolds number
RPM	speed (rotation per minute)
RR	cooling tower temperature ratio
t	time, (s or hr)
T	temperature, (°C or °F)
T_d	derivative time
THROTL	throttling range
T_i	integral time
U_o	overall heat transfer coefficient, (W/m°C or Btu/hr.ft²°F)
U_a, U_c, U_{fd}	control variables
U(t)	control action defined in Equations (2.38) to (2.40)
V	velocity, (m/s or ft/hr)
V_{ol}	volume, (m^3 or ft^3)
W	humidity ratio, (kg_w/kg_a or lb_w/lb_a)
$\hat{W}$	work
x	water flow direction (coil), (m or ft)
y	air flow direction (coil), (m or ft)
z	length, (m or ft)

SUBSCRIPTS

a	air
c	conduit
ce	condenser entering
ch	chiller
cl	condenser leaving
com	compressor
con	condenser
cp	cooling plant
cs	between conduit and secondary fluid
ct	conduit thickness
CT	cooling tower
d	duct
ee	evaporator entering
el	evaporator leaving
eq	equipment
ev	evaporator
f	fan
fi	fin
fl	fluid
foul	fouling
i	inside
in	inlet
inf	infiltration

SUBSCRIPTS

int	internal
lt	latent load
m	mixed
max	maximum
mech	mechanical
min	minimum
mot	motor
o	outside
out	outlet or leaving
r	rated or design
R	refrigerant
rf	refrigerant
s	supply
set	setpoint
sol	solar
st	sensible load
sur	surroundings
sys	system
t	tube
to	outside tube
tost	outside tube saturated temperature
ts	tube spacing
v	vapour

SUBSCRIPTS

w	water
wr	return chilled water
z	zone or space
∞	sink

SUPERSCRIPTS

$*$	optimal

GREEK

η	efficiency
η_{cov}	overall wetted fin efficiency
η_s	dry fin efficiency
η_{sov}	overall dry fin efficiency
ρ	density, (kg/m^3 or lb/ft^3)
Δ	difference
τ	time constant
γ_s	ratio of specific heats
λ	constant as defined in Equation (2.9)
σ	constant as defined in Equation (2.9)

CHAPTER 1

INTRODUCTION

1.1 Introduction

When fossil fuel was plentiful at reasonable prices and our ecology seemingly undamaged, the "forgiving" constant volume terminal re-heat (CV) systems were in (Procell 1977). The temperature, ventilation and humidity control in a controlled environmental space, it was believed, could only be assured with constant volume systems, until when "energy conservation" became the catch phrase of a new era in our history which started in 1973, when the OPEC nations declared economic war on the world (Geake 1980). The response to the challenge to conserve energy led to the development of new techniques to achieve the same levels of performance as we have previously known without the profligate waste we have previously indulged in. Consequently the concept of variable air volume (VAV) to meet the occupied space needs has emerged as one of the most popular methods of achieving the goals of low energy design. The VAV approach to air conditioning is certainly not new. In fact, there are installations which we know of that date back to 1964 in the United States. The concept can result in significant money savings both in first cost and in energy cost, a very important factor in today's marketplace. It also has a tremendous impact on the overall

system (McQuiston and Parker 1988, Lujan 1977). For example, the HVAC designer will now size the systems to take full advantage of load diversity instead of the peak demand basis. The results are smaller basic systems, lower energy demands, and smaller mechanical room space requirements. But, most important the VAV systems are capable of delivering different quantities of supply air to meet the occupied space needs in proportion to zone loads.

A central heating, ventilating and air-conditioning (HVAC) systems with its major components is shown by block diagram in Figure 1.1. The major components are

1. Heat exchanger(s) (heating and cooling coils)
2. Fan(s) (supply and return fan)
3. Duct system (supply and return duct, fittings)
4. Chiller
5. Boiler
6. Mixing boxes
7. Filter
8. Face and bypass dampers
9. Terminal boxes
10. Environmental space(s) and a
11. Control system

In terms of its working and method of control, HVAC systems are broadly classified into two categories, namely, 1)

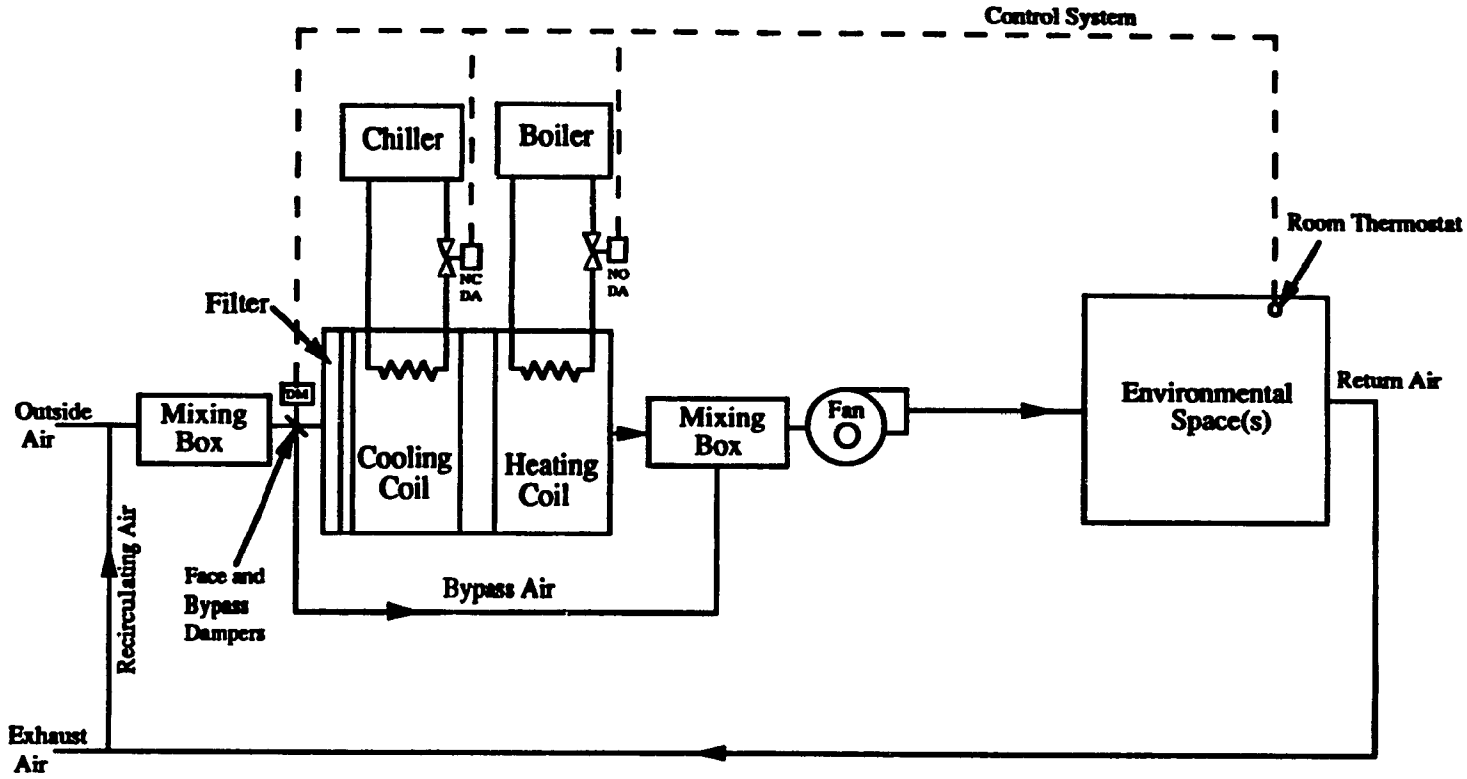

Figure 1.1 Schematic diagram of a central heating, ventilating and air-conditioning system.

constant volume (CV) systems and 2) variable air volume (VAV) systems (McQuiston and Parker 1988, Shuttleworth 1983).

1.2 Constant Volume Systems

Constant volume systems, as their name implies, supply constant quantity of conditioned air to the space and the conditions of the supply air (dry bulb temperature and humidity ratio) are varied in response to the changing in space loads. Thus, the CV systems are well suited when the load characteristics of different spaces are the same (ie. single zone systems, or for interior zones). On the other hand, since different spaces in large buildings are subjected to different loads at any given time, especially in the perimeter zones (Geake 1980, Procell 1980, Blankenbaker 1982), the single zone CV systems can not supply conditioned air at different temperatures to suit the needs of individual zones. Under these circumstances multi-zone CV systems must be used.

One draw back of the CV systems (single or multi-zone) is that the fan energy consumption remains the same irrespective of the zone loads (Spitler 1986, Brothers and Warren 1986, Blankenbaker 1982). The fan still circulates the same amount of air throughout the building, even though the space sensible heat load is reduced.

1.3 Variable Air Volume Systems

An alternative system which provides the supply air to different zones according to their needs while at the same time uses less fan energy at low loads is known as VAV system. Since the building HVAC loads generally vary considerably during occupied periods, especially in the perimeter zones, the HVAC system must be able to respond to these changes. The VAV systems are capable of supplying varying quantities of air to different zones. Since the quantity of supply air is proportional to the fan speed and fan power is proportional to cube of the speed, it is evident that at low loads only low quantities of air are required and hence considerable amount of fan energy could be saved.

Although VAV systems have definite advantages in reducing the initial and operating costs, they are also known to be difficult to control. One problem is that when the supply air quantities are reduced in response to decreasing load, the relative humidity of the air tends to be high unless additional control actions are taken. Furthermore, low air flow rates may lead to thermal discomfort due to inadequate air movements and poor indoor air quality which could be attributed to low ventilation rates. Under these circumstances the issue of designing control strategies for VAV systems become quite important.

In order to improve the indoor environment in buildings,

a knowledge of the dynamic interactions between the mechanical system, the building structure, and the indoor air space is necessary so that corrective actions can be taken with respect to design or operation of the building.

As pointed out by Guntermann (1986), many of the HVAC problems are summer air conditioning problems. So, in this study, only summer air conditioning (cooling and dehumidifying) case is studied. In the following chapter existing literature on modelling and control of HVAC system, in particular the VAV systems, will be reviewed. The merits and deficiencies of these studies will be pointed out. With this as the basis, the objectives of the present research will be defined and the statement of the problems as well as the methodology used to solve the problems will be proposed.

CHAPTER 2

LITERATURE REVIEW

2.1 Introduction

Extensive research has been conducted either through experiments or theoretical simulations on the dynamics of HVAC systems. However, the primary concern has been on the study of individual components of HVAC system stability, such as designing and tuning of PI controllers to control the coil discharge air temperature as discussed in references (Hamilton et al. 1974, Shavit and Brandt 1982, Metha 1987, Nesler and Stoecker 1984). Examination of the dynamic interaction between major HVAC system components as a whole has , however, received limited attention. This chapter will review the modelling of the individual system components of a summer air conditioning system as well as their interactions. Also the merits and deficiencies of the VAV system operation and control will be reviewed.

2.2 Component Modelling

Ever often the mechanical equipment for heating and air-conditioning systems are chosen on the basis of static (steady-state) performance characteristics. However, static

data provide little insight into such matters as system stability and short-term transient responses which occur as a result of sudden changes in heating or cooling loads. These matters are important to comfort and control issues. The heat exchanger dynamics are the most important and influential in air loop control (Gartner and Harrison 1965).

2.2.1 Heat Exchangers

Much literature is available on determining the transient response characteristics of the heat exchangers by use of governing equations (Ljung and Soderstrom 1983). One way of characterizing the dynamic response of a heat exchanger that has been studied extensively is to use the governing differential equations (Myers et al. 1970). In 1959, Dusinberge described a numerical method of finding transient response of a single-pass cross flow heat exchanger for a gas-turbine. Gartner and Harrison (1963) used energy balance principles to obtain the basic partial differential equations in space and time for a cross-flow heat exchanger. The method of Laplace transforms is used later to obtain transfer function relations for different coil parameters. Gartner and Harrison (1965) extended the above model to a fin tube cross-flow heat exchanger.

In 1964, Kays and London published a book on compact heat exchangers which contains a chapter summarizing the transient

performance primarily for counterflow dry sensible heating or cooling coils. Their results London et al. (1952), Kays (1949) and Kays and London (1950) were reported in the form of tables and graphs of J-factor and friction factor f, versus Reynolds number based on the air-side hydraulic diameter, D_h. Briggs and Young (1963) extended the work carried out by Ward and Young (1959) to correlate the published heat transfer data. The authors presented the following formula for the average heat transfer J-factor, in terms of the air flow Reynolds number and physical dimensions of the coil:

$$J = 0.134 Re^{0.319} \left(\frac{F_s}{F_h}\right)^{0.2} \left(\frac{F_s}{F_t}\right)^{0.1134} \qquad (2.1)$$

More cross-flow dry heating or cooling coils are studied by Myers et al. 1967, Gartner and Daane 1970, Tamm 1969 and Myers et al. in 1970 to determine the effect of coil construction on the response of the coil. A number of simplifications of this models for dry sensible heating or cooling coils were subsequently presented by Gartner 1972 and Tobias in 1973. Many studies have included experiments to verify the accuracy of the coil models also (Gartner and Harrison 1965, Tamm and Green 1973).

However, the dynamic characteristics of cooling and dehumidifying coils have received much less attention than the dynamic characteristics of sensible heating or cooling coils

as mentioned above. It is because of the unpredictability of the combined effects of heat and mass transfer. McCullagh et al. (1969) and Elmahdy (1977) presented a transient model of a chilled water cooling and dehumidifying coil. These equations are obtained by treating the time and space as independent variables and humidity ratio, air, water and tube temperatures as dependent variables. These model equations are given in Chapter 3.

This model accounts for the fin efficiency, air and water-side heat transfer coefficients, and parameters that were not included in other models. In 1978, McQuiston presented a solution of the fin efficiency during dehumidifying processes. He correlated the heat and mass transfer coefficients from experimental data and presented them in empirical form as a function of air flow rate Reynold number. In an another study, Pearson et al. (1974), O'Neill (1988) and Maxwell (1989) determined the cooling and dehumidifying coil gain and time constant through experiments.

2.2.2 Chillers

In summer cooling case, chillers are needed to provide chilled water to the cooling coils to extract heat (cooling load) from the air streams across the cooling coils, and cooling towers are typically used to reject heat from the condenser of a chiller to the outside environment. The chilled

water supply temperature is maintained by control of the chiller refrigerant flow through modulation of the compressor and expansion device. Therefore, a typical chiller plant consists of one or more chillers with integral condensers, primary chilled water pumps with distribution piping, and evaporative cooling towers with condenser water pumps (Haines 1988, Spethmann 1985, Wong and Wang 1989, and Johnson 1985, DOE 2.1A 1981).

Many researchers have concentrated on the study of optimizing of chiller plant's energy consumption utilizing central energy management and control system (Williams 1985) which includes direct digital control (Johnson 1985). Mitchell (1988) and Braun et al. (1987) studied the performance and control characteristics of a large variable speed drive chiller system. They concluded that the savings associated with the use of variable-speed control are very significant at part-load conditions (40% savings).

Wong and Wang (1989), Spethmann (1985), Waller (1988) and Kirshenbaum (1987) stated that the chiller operating characteristics, such as pressure, temperature, fluid flow, heat transfer, and power input, are mainly influenced by the following factors:

1. The refrigeration load ratio of the operating refrigeration load to the design full-load. Load ratio affects the rate of heat transfer at the evaporator and condenser. It also affects the operating efficiency of the compressor.

2. Temperature of condenser water entering the condenser.

3. Constructional characteristics of the chiller, and

4. Control characteristics of the chiller at part-load operation.

A simple mathematical equation representing transient characteristics of the evaporator and condenser can be derived by (Wong and Wang 1989) using heat balance principle. In the following h represents the enthalpy of the refrigerant, q_w and q_{sur} the rate of heat transfer to or from the water and the surroundings, t the time, M_{rf} and Ms_{eq} the mass of refrigerant flow and the equipment, and $C_{p,eq}$ the specific heat of the metal. The energy balance at the evaporator and condenser was expressed as

Heat being absorbed or released from the refrigerant	=	Heat transfer to or from the water	+	Heat being absorbed or released from the equipment	+	Heat loss or gain from the surroundings

or

$$Ms_{rf}\frac{dh_{rf}}{dt} = q_w + \sum_{n=1}^{k} Ms_{eq}C_{p,eq}\left(\frac{dT}{dt}\right) + q_{sur} \qquad (2.2)$$

The transient equations for water and air temperature at the evaporator and condenser were also derived by applying energy balance principles. The heat capacity rate of water q_w is far greater than the equipment heat storage, the second term of the right-hand side of Equation (2.2), and its magnitude is

often less than 1% of the magnitude of q_w; hence, it is usually neglected. Similarly, the heat loss or gain from the surroundings is also ignored due to its negligible effect compared with the heat transfer to or from the water. Therefore, the rate of heat transfer (Q) at the evaporators and the condensers are usually expressed in steady state equation based on the log-mean temperature difference between the refrigerant and water and an overall heat transfer coefficient that includes a water fouling coefficient, the conduction coefficient in the tube wall, the water-side heat transfer coefficient for water flowing in the tube, and a condensing or boiling heat transfer coefficient respectively (Wong and Wang 1989, Jackson et al. 1987, and Braun et al. 1987).

$$Q = A_o U_o LMTD \tag{2.3}$$

The overall heat transfer coefficient is expressed as

$$U_o = \frac{1}{\frac{1}{h_w} + \frac{1}{h_{foul}} + \frac{1}{h_{wall}} + \frac{1}{h_R}} \tag{2.4}$$

and the Log-mean temperature different between the refrigerant and the water for evaporator $LMTD_{ev}$ and condenser $LMTD_{con}$ is given as

$$LMTD_{ev} = \frac{(T_{ao} - T_{ev}) - (T_{al} - T_{ev})}{\ln\left[\frac{T_{ao} - T_{ev}}{T_{al} - T_{ev}}\right]} \tag{2.5}$$

$$LMTD_{con} = \frac{(T_{con} - T_{ce}) - (T_{con} - T_{cl})}{\ln\left[\frac{T_{con} - T_{ce}}{T_{con} - T_{cl}}\right]} \qquad (2.6)$$

where

A_o : total outside heat transfer area, (m^2 or ft^2)
h_{foul} : water-fouling heat transfer coefficient, ($W/m^2 \cdot C$ or $Btu/hr.ft^2 \cdot F$)
h_R : refrigerant condensing or boiling heat transfer coefficient for the condenser or evaporator, ($W/m^2 \cdot C$ or $Btu/hr.ft^2 \cdot F$)
h_w : water-side heat transfer coefficient, ($W/m^2 \cdot C$ or $Btu/hr.ft^2 \cdot F$)
h_{wall} : tube wall conductive heat transfer coefficient, ($W/m^2 \cdot C$ or $Btu/hr.ft^2 \cdot F$)
T_{ee}, T_{el}: temperature of chilled water entering and leaving the evaporator, (°C or °F)
T_{ce}, T_{cl}: temperature of condenser water entering and leaving the condenser, (°C or °F)

The water-side fouling factor has a significant influence on the rate of heat transfer in the evaporator and condenser. The type of water circuit, degree of water treatment, and other operating characteristics affect the magnitude of the fouling factor on the water-side of the heat exchanger. Table 2.1 lists the water-side fouling factors which are recommended for various shell-and-tube-type evaporators and condensers having conventional treatment (Table 2.1, Wong and Wang 1989).

The water-side heat transfer coefficient, h_w can be obtained by using Nusselt's correlation equation for a length-to-diameter ratio of $L/D_h < 400$.

$$Nu = 0.036\, Re^{0.8}\, Pr^{0.33}\, \left(\frac{D_h}{L}\right)^{0.055} \qquad (2.7)$$

where

D_h : hydraulic diameter, (m or ft)
L : length of the tube, (m or ft)

Table 2.1 Fouling factors for shell-and-tube-type heat exchangers (Wong and Wang 1988).

Chilled water in evaporator	Fouling factor	
	$m^2 \cdot C/W$	$hr.ft^2 \cdot F/Btu$
Closed circuit	.000044	.00025
Open circuit for air washer	.00018	.001
Condenser water		
Without brush cleaning system, water from cooling tower	.00018	.001
With brush cleaning system, water from cooling tower	.000035	.0002
Seawater, without heat exchanger	.00018	.001
Seawater, with heat exchanger	.000044	.00025

Then, the condensing heat transfer coefficient on the outside low finned tubes based on correlations from Beatty and Katz (1948) is normally used

$$h_{con} = 1060\left[\frac{1}{D_o \Delta T}\right]^{\frac{1}{4}} \tag{2.8}$$

and the boiling heat transfer coefficient is expressed as

$$h_B = \lambda \Delta T^{\sigma} \qquad \left[\frac{W}{m^2 C}\right] \tag{2.9}$$

where ΔT is the average temperature difference between tube wall and refrigerant, D_e is the equivalent diameter, and λ and σ are constants. Dougherty and Sauer (Wong and Wang 1989) had shown that the exponential index σ is approximately equal to 0.7 for oil-free R-11 and λ can be taken as 6.5 by Ariai et al. (Wong and Wang 1989).

The cooling tower water temperature (T_{ce}) entering the condenser is a function of the combined effect of part load ratio (PLR), average outdoor air wet-bulb temperature ($T_{o,a,wb}$), and the number of transfer units (NTU) of the cooling tower, and can be expressed as (Wong and Wang 1989)

$$T_{ce} = T_{o,a,wb} + 4\, K_{PLR}\, K_{T_{o,a,wb}}\, K_{NTU} \qquad (2.10)$$

and

$$K_{PLR} = \frac{1}{4}\,(0.4 + 3.6\,PLR)$$

$$K_{T_{o,a,wb}} = \frac{1}{4}\,(8.2 + 0.025\,T_{o,a,wb} - 0.00625\,T_{o,a,wb}^2) \qquad (2.11)$$

$$K_{NTU} = \frac{1}{4}\,(11.77 - 12.05\,NTU + 3.94\,(NTU)^2)$$

where

K_{PLR} : coefficient of load ratio
$K_{To,a,wb}$: coefficient of outdoor wet-bulb
K_{NTU} : coefficient of cooling capacity

DOE-2.1A (1981) simulated the cooling tower exit temperature as function of cooling tower setpoint temperature ($T_{CT,set}$), the

temperature throttling range (THROTL) and the ratio of design temperature of the cooling tower (RR) as shown below

$$T_{CT,out} = T_{CT,set} + [THROTL(RR - 0.5)] \qquad (2.12)$$

The actual power input (E_i) to the compressor motor can be simulated as a function of compressor efficiency (η_{com}), mechanical efficiency (η_{mech}) and motor efficiency (η_{mot}) respectively

$$E_i = \frac{M_{rf}\hat{W}_i}{\eta_{com}\eta_{mech}\eta_{mot}} \qquad (2.13)$$

where M_{rf} is the mass of the refrigerant flow and $\hat{W}_i$ is the work input to the compressor. The overall cooling plant load can be simulated as (BESA 1987)

$$q_{cp} = PLC\frac{q_{sys}}{COP} \qquad (2.14)$$

where

PLC : percent of energy source input required for q_{sys}/COP output
q_{sys} : cooling load from the coil, (W or Btu/hr)
COP : plant coefficient of performance.

2.2.3 Air Duct

The transient performance of heating or cooling distribution (ductwork) system depends on the temperature of

surroundings, the thermal capacitance of the duct itself and the transport delay. Therefore, models for the duct air temperature response should account for thermal losses to the surroundings, the thermal capacitance of the duct and the transport delay.

The study of the energy consumption in townhouses at Twin Rivers, NJ has lead to the conclusion that only about 50% of the energy entering a duct actually emerged from the register (Harrje, Socolow and Sonderegger 1977, Harrje 1976, and Grot and Harrje 1981). This discrepancy was explained by taking into account the heat storage effects of the duct system and the heat transfers to the surroundings.

If the temperature of the air surrounding a conduit such as a pipe and a duct is assumed to be constant and uniform, then the temperature of a fluid flowing through it at any distance, can be described by the following equations (Harriott 1964, and Gartner and Harrison 1963):

$$\rho A C_{p,f1}\frac{dT_{f1}}{dt} + M C_{p,f1}\frac{dT_{f1}}{dy} + \hat{h}_1 (T_{f1} - T_c) = 0 \qquad (2.15)$$

$$m C_{p,c}\frac{dT_c}{dt} + (\hat{h}_1 + \hat{h}_o)\, T_c - \hat{h}_1 T_{f1} = 0 \qquad (2.16)$$

The subscripts fl and c stand for fluid and conduit. The transfer function can then be derived from the partial differential equations by taking the Laplace transform. Grot and Harrje (1981) and Tobias (1973) used this principle to determine the partial differential equations which characterize the dynamic response of the duct surface and air temperature. However, in their simulations the dynamic terms of the duct ($k.\tilde{d}.d^2T_d/dz^2$, $\rho_a.C_{p,a}.A.dT_a/dt$) are ignored. This is done by making the assumption that the heat propagation along the duct by conduction is negligible compared to that caused by the moving air. Equations (2.17) and (2.18) are the two governing differential equations which characterize the duct surface and air temperature response.

$$\rho_d C_{p,d} \bar{d} \frac{dT_d}{dt} = U_o (T_o - T_d) + U_i (T_a - T_d) \qquad (2.17)$$

$$\rho_a C_{p,a} A V \frac{dT_a}{dz} = \bar{P} U_i (T_d - T_a) \qquad (2.18)$$

and

$$U_i = \frac{1}{(R_i + \frac{1}{h_i})} \qquad (2.19)$$

$$U_o = \frac{1}{(R_o + \frac{1}{h_o})} \qquad (2.20)$$

where

ρ_a : mass density of the air, (kg/m^3 or lb/ft^3)
ρ_d : mass density of the air, (kg/m^3 or lb/ft^3)
$C_{p,a}$: specific heat of air, (J/kg°C or Btu/lb°F)
$C_{p,d}$: specific heat of duct, (J/kg°C or Btu/lb°F)
A : duct cross section area, (m^2 or ft^2)
d : duct thickness, (m or ft)
V : air flow velocity, (m/s or ft/hr)
P : average duct perimeter, (m or ft)
U_e : overall exterior thermal conductance, (W/m^2 °C or Btu/hr°F ft^2)
U_i : overall interior thermal conductance, (W/°C m^2 or Btu/hr°F ft^2)
T_a : duct air temperature, (°C or °F)
T_d : duct temperature, (°C or °F)
t : the time, (s or hr)
z : distance of the duct, (m or ft)
R_e : exterior insulation thermal resistance, (°C m^2/W or hr°F ft^2/Btu)
R_i : interior insulation thermal resistance, (°C m^2/W or hr°F ft^2/Btu)
h_e : exterior air film heat transfer coefficient, (W/°C m^2 or Btu/hr°F ft^2)
h_i : interior air film heat transfer coefficient, (W/°C m^2 or Btu/hr°F ft^2)

Equations (2.17) and (2.18) must be solved with the initial and boundary conditions:

$$T_d(z,0) = X(z)$$

$$T_a(0,t) = f(t)$$

where $f(t)$ is the inlet air temperature. $T_d(z,t)$ and $T_a(z,t)$ are respectively the duct metal and the air temperature at a distance z from the inlet and at time t.

Clark et al. (1985) used a different approach to present an approximate model which accounts for transport delay and air temperature distribution in the duct. This model is used in HVACSIM+. This is a fifth order time-dependent polynomial

model to describe the temperature distribution in a duct as follows.

$$T(z,t) = \sum_{i=0}^{5} a_i(t)\, z^i \qquad (2.21)$$

where
a_i : time dependents of the polynomial
z : normalized position in duct.

2.2.4 Fan Models

The fan is an essential component of almost all heating and air-conditioning systems or air handling units. Except in those uses where free convection creates air motion, a fan is used to move air through ducts and induce air motion in the space.

Many researchers have done a comparison between different methods for controlling the air flow in VAV systems. They investigated energy consumptions, stability and sound level at part-load conditions (Spitler et al. 1986, Brothers and Warren 1986, McClive 1974 and BLAST 1979). The most common methods for modulating the variable air flow are static pressure control with inlet dampers or discharge dampers, inlet vanes, motor speed control, run-around or scroll bypass control and blade pitch control (Patterson 1977, ASHRAE 1988). Table 2.2 lists the recommended minimum air flow fractions for several

common types of fans and fan controls (BLAST 1979).

Table 2.2 Fan power coefficients and the recommended minimum air flow rate fractions (BLAST 1979).

Type	C_0	C_1	C_2	C_3	C_4	Recommended min. air frac.
2-speed back inclined blade fan	.4561	-4.446	9.968	-7.11	2.110	.40
Variable pitch vaneaxial fan	41.68	-142.1	160.24	-62.71	1.849	.40
Inlet vanes on backward inclined centrifugal fan	1.208	5.7902	15.027	15.978	6.551	.35
Damper control with forward curved centrifugal fan	.4891	-.5553	1.0891	0.0	0.0	.30
Damper control with backward inclined centrifugal fan	-.099	2.243	-1.421	.283	0.0	.35

The three important variables in the fan model simulation are the temperature rise across the fan, the fan energy consumption at full and part-load conditions and the pressure rise in the air stream (HVACSIM+ Jan. 1985, Brothers and Warren 1986). Fan efficiency is required to compute the temperature rise across the fan, as well as fan power consumption, and can be obtained from dimensionless performance curves (Figure 2.1). In general, the supply air and return air fan heat gain are ignored (Miller 1982) or not integrated in fan-duct model. Only larger and more detailed programs such as HVACSIM+ (1985), DOE-2.1A (1981), BLAST

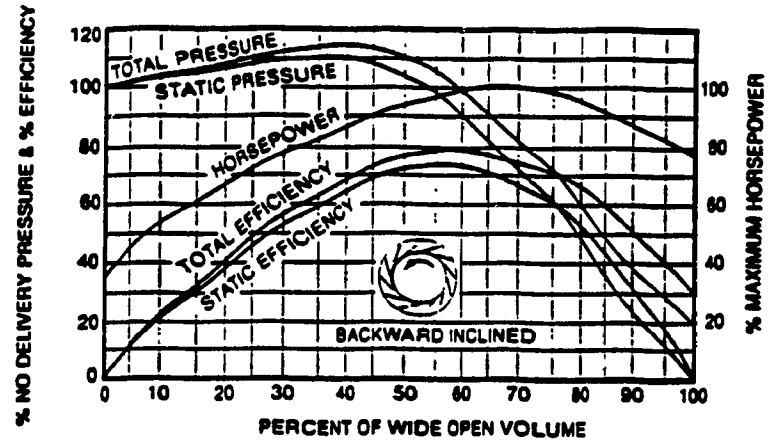

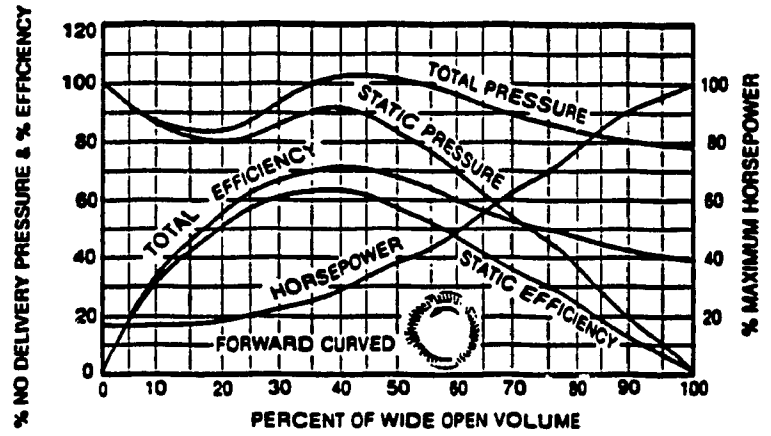

TYPICAL NORMALIZED CURVES FOR CENTRIFUGAL FANS

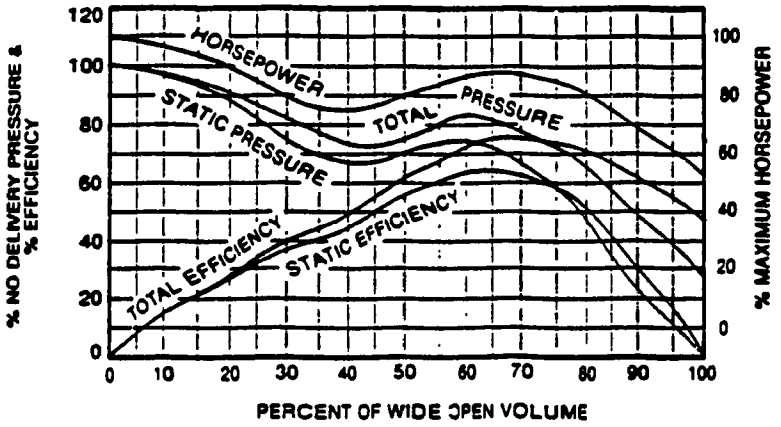

TYPICAL NORMALIZED CURVE FOR AN AXIAL FLOW FAN

Figure 2.1 Typical fan dimensionless performance curves (AMCA 1985).

(1979) and BESA (1987) have used the fan model by correlating one of the above three variables to the air mass flow rate, efficiency and the size of the fan.

HVACSIM+ (1985) calculates the air temperature rise across the fan and fan energy consumption. This requires fan efficiencies and air pressure, calculation of the dimensionless flow coefficient and the dimensionless pressure head coefficients. These are defined as follows:

$$C_f = \frac{M_a}{\rho_a N D^3} \tag{2.22}$$

$$C_h = a_0 + a_1 C_f + a_2 C_f^2 + a_3 C_f^3 + a_4 C_f^4 \tag{2.23}$$

where

C_f	:	dimensionless flow coefficients
C_h	:	dimensionless pressure head coefficient
D	:	diameter of blades or impeller, (m or ft)
N	:	rotation speed (rps or rpm)
M_a	:	air mass flow rate (kg/s or lb/hr)
ρ_a	:	air density (kg/m^3 or lb/ft^3)

and efficiency (η_f) is written as:

$$\eta_f = e_0 + e_1 C_f + e_2 C_f^2 + e_3 C_f^3 + e_4 C_f^4 \tag{2.24}$$

The a_i and e_i coefficients can be obtained from fan dimensionless performance curves (Figure 2.1) for the given fan type. The inlet pressure is obtained from

$$P_i = P_o - 0.001\, C_h\, \rho_a\, N^2\, D^2 \qquad (2.25)$$

where

P_i : inlet pressure (kPa or inch W.G)
P_o : outlet pressure (kPa or inch W.G)

and $\Delta P = P_i - P_o$. The efficiency is used to compute power consumption (Equation 2.24), and the temperature rise is calculated on the assumption that all the heat lost is gained by the fluid. The air temperature leaving the fan is expressed as

$$T_o = T_i + \frac{(P_o - P_i)}{\rho_a C_{p,a}} \left(\frac{1}{\eta_f} - 1\right) \qquad (2.26)$$

$$E = \frac{M_a\, \Delta P}{\eta_f\, \rho_a} \qquad (2.27)$$

where

E : power consumption, (kW or Btu/hr)
$C_{p,a}$: specific heat of air (kJ/kg-C or Btu/lb°F)

The dimensionless flow coefficient (C_f) and e_i coefficients in fan efficiency equation take into account for the part-load performance.

The model used by BLAST(1979), BESA (1987) and DOE-2.1A (1981) requires air static pressures (ΔP_r) and fan efficiencies ($\eta_{f,r}$) to be specified and assumes that all fan energy consumption causes an air-stream temperature rise.

At design load, the steady state air temperature rise for supply fan ΔT_r is as follow:

$$\Delta T_r = DT_r * k_1 \qquad (2.28)$$

where

$$DT_r = \frac{\Delta P_r}{\eta_{f,r}}$$

and k_1 is a constant which is function of the supply air humidity ratio W_s. While the power consumption is:

$$E_r = \frac{M_{a,r}\, DT_r}{k_2} \qquad (2.29)$$

where $M_{a,r}$ is design supply air mass flow rate and k_2 is a conversion factor.

At part-load conditions, the part-load fan power for VAV systems is computed using fan power coefficients. Fan power coefficients determine the fraction of full-load fan power consumption for variable air volume systems according to the following equation:

$$FFLP = C_0 + C_1 PLR + C_2 PLR^2 + C_3 PLR^3 + C_4 PLR^4 \qquad (2.30)$$

where

FFLP : the fraction of full-load power
PLR : the part-load ratio defined as the delivered air flow (M) in any time step divided by the design air flow rate ($M_{a,r}$) for the fan, and

$$PLR = \frac{M_a}{M_{a,r}}$$

c_i are the five fan power coefficients and any of these coefficients can be zero. Table 2.2 is the recommended fan power coefficients from BLAST (1979) and DOE-2.1A (1981). This ratio is used to calculate the temperature rise and energy consumption at part-load conditions. The fan energy consumption can be calculated as

$$E_{PL} = E_r * FFLP \qquad (2.31)$$

and the air temperature rise is

$$\Delta T_{PL} = \Delta T_r * PLR \qquad (2.32)$$

The best means of determining the part-load power consumptions would be from actual motor curves. However, this information is not always available, but the following method described by Cooper (1976) can be used to get an approximate estimate. Thus, the actual power required for the variable speed drive is

$$\frac{IkW}{kW_f} = \eta_f \frac{BHP}{BHP_f} + FL + VL + IFL + IVL \qquad (2.33)$$

It is equal to the summation of the motor and inverter fixed losses (FL, IFL) and those vary with load (VL, IVL) are the major losses for fan motor. The BHP value must be determined in accordance with actual VAV-fan-duct system requirements.

2.2.5 Room Models

The last few years have seen a growing interest in the mathematical modelling of the dynamics of HVAC systems. This is partially due to the recognition that the poor design of a control loop may adversely affect the comfort level, and lead to increased use of energy, by forcing the HVAC system to operate in an uneconomic manner. The room often has a stabilizing influence on the control loop. It is, therefore, of significant interest to choose closely the room dynamics.

Metha (1980) and Woods (1980) formulated a model for the dynamic response of a room assuming a uniform mixing of the room air. The heat capacity of the furnishings is added to the room air heat capacity. Metha stated that in his analysis the thermal capacity of the walls is neglected. However, the capacity is eventually taken into account by linearizing the experimental results around different operating points. The term for the infiltration heat compensates for the thermal capacity.

Borresen (1981) studied several dynamic room models, which account for the interaction between the wall and room air in three different ways, and are described by the following equations:

$$\frac{dT_z}{dt} Ms_a C_{p,a} = q + M_a C_{p,a} (T_i - T_z) \tag{2.34}$$

$$\frac{dT_z}{dt} Ms_a C_{p,a} = q + M_a C_{p,a} (T_i - T_z) + \sum_{Walls} UA (T_{out} - T_z) + \sum_{Windows} UA (T_{out} - T_z) \tag{2.35}$$

$$\frac{dT_z}{dt} Ms_a C_{p,a} = q + M_a C_{p,a} (T_i - T_z) + \sum_{Walls} UA (T_{wall} - T_z) + \sum_{Windows} UA (T_{out} - T_z) \tag{2.36}$$

where

T_z : room air temperature, (°C or °F)
M_a : mass flow rate, (kg/s or lb/hr)
Ms_a : mass of air in room, (kg or lb)
t : time, (s or hr)
$C_{p,a}$: specific heat of air, (J/kg-C or Btu/lb°F)
q : convective heat flow (flux), (W or Btu/hr)
T_i : inlet supply air temperature, (°C or °F)
$\Sigma U A$: overall U-value, (W/C or Btu/hr°F)
$\Sigma h A$: overall h-value, (W/C or Btu/hr°F)
T_{out} : outdoor air temperature, (°C or °F)
T_{wall} : wall temperature, (°C or °F)

Borresen simulated a room in three different ways, from very simple dynamic model (Equation 2.34, Model I) that neglects the influence of the walls. Model II takes into account of the overall U-value of the walls, and Model III takes the temperature response of the walls into account. Borresen

stated the choice of the simplification level employed depends on how closely the long-term responses and steady-state values are to be fit to the actual room response. For modelling short-term dynamic responses, a simple time constant corresponding to the air change rate of the room is usually adequate.

Thompson (1981) pointed out that the model describing the thermal behaviour of the building vary widely in complexity from simple, first order ones that consider only the air mass and account approximately for the thermal properties of the enclosure (Borresen 1981, Zhang and Warren 1988), to very detailed one that take into account of the effect of solar radiation and thermal effects. The model used by Thompson does not consider radiation nor distinguish between latent and sensible heats. A program that handles the coupled effects of solar radiation-conduction heat transfer in detail is BEEP (Athienitis et al. 1986, Athienitis 1988). This program is capable of predicting the energy conservation and reduction of room temperature swings resulting from large solar and other radiant gains.

There are few detailed building energy analysis programs which are capable of taking into account the effect of radiation and other thermal effects such as DOE-2.1A (1981), BLAST (1979), and TARP (Walton 1983). A detailed model of a single zone house was developed and validated in a study by

Zaheer-uddin, and subsequently modified to take into account the latent loads (1986). The air infiltration component was modelled using the air change method and solar gains were computed using the models described in reference by Liu and Jordan (1960), and Hay (1976). The energy balance equation describing the to and from nature of the heat fluxes between different elements and the room air was described by

$$\rho_a C_{p,a} V_{ol} \frac{dT_z}{dt} = \sum_{i=1}^{N} UA\,(T_z - T_d) + h_1 A_1\,(T_z - T_1) + h_d A_d (T_z - T_d) + q_{inf} + q_{sol} + q_{int} \qquad (2.37)$$

where the term on the right hand side indicate respectively: heat gain through resistive walls and ceiling, heat exchange from lumped capacity elements, heat exchange from the distributed capacity elements, air infiltration heat gain (q_{inf}), solar heat gain (q_{sol}), and internal gains (q_{int}) all interacting with room air T_z.

The outputs of interest from the space load model were the time dependent sensible, latent loads and the space air temperature. It is apparent that whether it is with respect to energy consumption or thermal comfort, HVAC system behaviour depends strongly on the building dynamics and therefore, HVAC system operating behaviour depends on the building's dynamic characteristics.

2.2.6 Design And Simulation Of Control Systems In HVAC

To obtain a more accurate control, a feedback control action is required to correct the error (ie. the air temperature differences between the output and the setpoint). To satisfy the need for various kinds of control response, a number of types of control actions are used. It can range from most simple on/off control action (like thermostat) to more complicated Proportional plus Integral plus Derivative (PID) control action. Table 2.3 lists the most common control actions.

Table 2.3 Type of control actions.

	Control action
1.	On-Off (Two position) control action
2.	Two-position action with dead band
3.	Floating control action
4.	Integral control action, (I)
5.	Proportional action, (P)
6.	Proportional Plus Integral, (PI)
7.	Proportional Plus Derivative, (PD)
8.	Proportional Plus Integral Plus Derivative, (PID)

Each control action has its characteristic advantages and limitations. The selection or design of the control actions are dependent on system complexity. In general, the more

difficult a process is to controlled, the further down in the foregoing list one must go to find the best-suited control action. However, many building system processes are rather simple and the control requirements "not very severe", by standards in the process control industry. The controllers extensively used in HVAC industry are Proportional (P) and Proportional Plus Integral (PI).

For example, Stoecker et al. (1978) studied the air temperature control loop with P controller. Shavit and Brandt (1982) simulated a discharge air temperature control system using analog proportional plus integral controllers. They concluded that PI controller was the best with optimum integral gain, but higher gain may cause the system to take longer to reach the setpoint. The optimum gain and throttling range has to be selected on the basis of experience, analysis, and/or experimentation. Nesler and Stoecker (1984), and Nesler (1986) described a procedure for selecting the PI constants (time constant, proportional gain, integral time etc.) in the direct digital control of discharge air temperature. Pinnella et al. (1986) designed an integral-only control action for fan static pressure control systems. They concluded that the integral control is able to give a stable system response for fan static pressure.

Also, a number of researchers have used numerical simulations in their studies of HVAC control and HVAC process

dynamics. These studies typically cover such a wide range of control situations that performing all the tests experimentally would be impossible. For example, Miller (1982) described a simulation for HVAC process dynamics. Each Major HVAC element (each major portion of the HVAC system) is simulated and implemented as individual subroutines in parallel with the main program to form a complete control system simulation. It provides a flexible way of analyzing the dynamics and interactions of many different HVAC process. The simulation has been used to study a number of aspects of HVAC process dynamics and control methods, including energy use and control tuning. The results show that significantly different responses are possible as the result of process interactions and nonlinearities.

Cherchas et al. (1985) used bilinear mathematical model to simulate a direct digital control algorithm for controlling the dry bulb temperature and moisture content of a single environmental space. The algorithm includes feedback and feedforward terms in a manner respecting the bilinear nature. They concluded the design of a suitable direct digital control algorithm for a process can be aided by use of system dynamic response. Subsequent use of the estimated load in a feedforward control algorithm results in temperature error control that is significantly better than that achieved using feedback control alone. Most recently, Park and David (1983),

Brandt (1986), and Borresen (1981) discussed adaptive control simulation and implementation methodology used in HVAC system application.

The control actions can be designed as some function of the output and input or error, thus, the following few paragraphs present the three most common control actions. The equation for proportional control action can be written (Kuo 1987)

$$U(t) = k_p e(t) \tag{2.38}$$

While, the proportional plus integral control action are described by the following differential equation:

$$U(t) = k_p e(t) + \left(\frac{k_p}{T_i}\right) \int e(t)\, dt \tag{2.39}$$

The differential equation for proportional plus integral plus derivative controller can be written as

$$U(t) = k_p e(t) + \left(\frac{k_p}{T_i}\right) \int e(t)\, dt + k_p T_d \left(\frac{de(t)}{dt}\right) \tag{2.40}$$

2.3 Operation And Control Problems In HVAC System

One of the most important requirements in a built

environment is to satisfy the occupants' thermal comfort and it is believed that HVAC systems are installed to increase comfort. Thus, the criteria to assess the performance of HVAC system is based on thermal comfort issues. The major parameters which affect thermal comfort have been shown to be (ASHRAE Standard 55-1981, ASHRAE Fundamental 1989, Fanger 1972 and Yilmaz 1987)

i) Air temperature

ii) Air motion too much or too little

iii) Relative humidity and

iv) Lack of ventilation.

In this section, the performance of HVAC system in maintaining the above parameters within the desired limits will be discussed and the operating problems found will be pointed out. It will be noted that, although the literature review is based on the above four parameters, the scope of the thesis is limited to the VAV system performance in terms of controlling air temperature and relative humidity. The major review will be concentrated onthese two outputs from variable air volume systems.

2.3.1 Air Temperature Problem

The most common cause of an environmental problem is the HVAC system and many of the HVAC comfort problems are summer air conditioning problems. People are more sensitive to

temperature changes. Knudsen and Fanger (1990) concluded that occupants are more sensitive to temperature step-changes away from the neutral conditions (setpoint values) than toward it. It has been also shown that there is greater sensitivity to cold steps than to warm steps (Gagge et al. 1967). The uneven temperature in occupied space is usually due to the unequal air distribution causing high local temperature difference (draft or cold spot, Gupta 1987). However, the HVAC systems are able to maintain air dry bulb temperature close to the desired setpoint (Guntermann 1986). Figure 2.2 shows the acceptable range of temperature and humidity recommended by ASHRAE Standard 55-1981 for winter and summer seasons for persons clothed in typical summer and winter clothing, at light, mainly sedentary, activity (< 1.2 met).

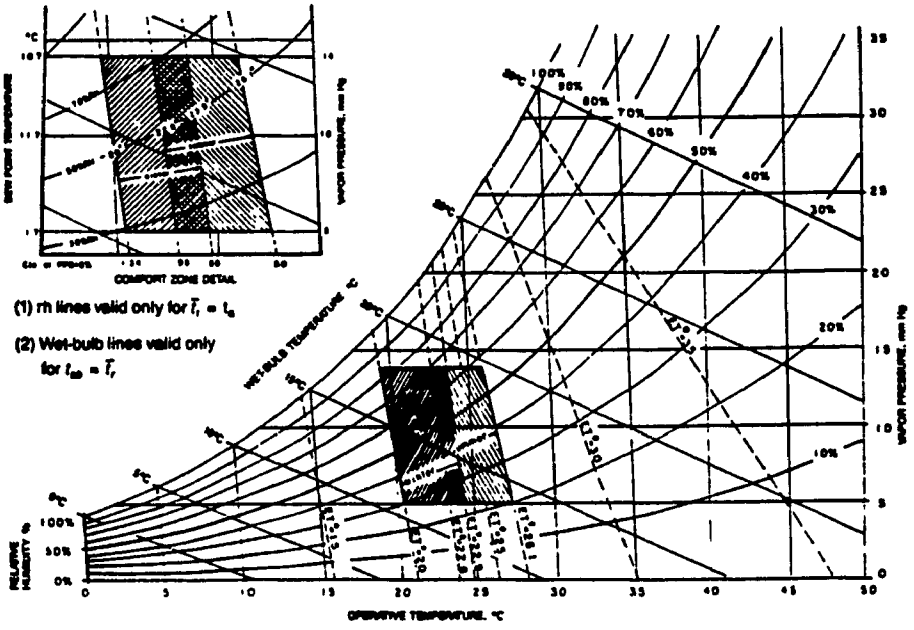

Figure 2.2 Standard effective temperature and the ASHRAE comfort zones (ASHRAE Standard 55-1981).

For example, at 50% relative humidity, where occupants are engaged in light or sedentary activity and are wearing light clothing, the temperature recommended by ASHRAE (1981) is 24.4°C (76°F) in summer, and 21.7°C (71°F) in winter.

2.3.2 Relative Humidity Problem

As discussed, a VAV system is designed to satisfy the air temperature, humidity and ventilation requirements of each zone. However, the only condition affecting comfort that is directly controlled is the space air temperature, which is set at the air handling unit and the amount of air introduced into each zone as controlled by the zone thermostat (Brickman 1987). All other conditions affecting comfort result from a combination of factors and are not directly controlled.

The relative humidity in the zone is affected by the apparatus dew point, the amount of air introduced into the space and the sensible heat ratio. These must be considered not only at peak load, but at any anticipated part load. As the cooling load in a space decreases from the design load, it is necessary to use some means for controlling the quantity of cooling being done at the space. In a single-zone system and some fan-coils units, it is common practice to use the bypass control technique for reducing the quantity of cooling available at the space. As the sensible load in the space decreases, the room thermostat responds by bypassing some of

the air being circulated around the coil and then mixing it with air coming off the coil in order to satisfy the reduced sensible load on the space. In these control systems, the relative humidity in the space will change as the space sensible load changes and the quantity of bypass air increases. As pointed out by Howell (1989) and Flanagan (1990) higher room relative humidities at part-load are as a result of high bypass ratio.

The combined effects of higher space temperatures, low air motion, and increased space relative humidity can occur simultaneously with majority of HVAC systems. This may result in occupancy discomfort even though all the criteria are in the acceptability ranges. One temperature control strategy used to increase comfort and air flow is resetting the supply air temperature up at low load conditions. This is done by raising the cooling coil water temperature. However, this can have a negative impact on comfort since raising the supply air by increasing the cooling coil water temperature with throttling or bypass valves reduces or even eliminates the dehumidification capability of the cooling coil as pointed out by Guntermann (1986), and Braun and Mitchell (1987). This is probably responsible for at least some of the occupancy comfort complaints caused in modern buildings. The studies done by Canadian Federal-Provincial Working Group (Healthy Building Manual 1988) suggests that humidity levels should be

maintained between 40% and 60%. Humidity levels above 60% results in inhabiting of mould, fungi and mites that may cause allergies, and on the other hand, long periods of low relative humidity are believed to cause dryness of the skin and mucous membranes, which may lead to chapping and irritation. Figure 2.2 shows the acceptable range of humidity ratio recommended by ASHRAE (1981).

2.4 Summary Of Problems And Causes In HVAC Systems

Variable air volume systems have become popular for providing heating, air-conditioning and ventilation in office buildings in the last two decades. The primary reason the systems have become popular are (ASHRAE Handbook 1987, Gupta 1987)

1. The concept can result in significant money savings both in first cost and in energy cost compare to constant volume.
2. The versatility of VAV system in individual zone controlled space.
3. Generally, the systems are energy-efficient, by design analysis.
4. The systems do not require reheating, which conventional systems (CV) may require in order to maintain dry bulb temperature.
5. The systems are suitable for partial operation during weekends or after hours, thus providing flexibility in operations.

However, whereas these systems are efficient, supposedly easy to design and provide energy conservation, in some buildings there are numerous problems when VAV systems do not function as intended. Some of the problems given by researchers are (Gupta 1987, Roberts 1987, Wessel 1987, Brickman 1987, Waeldner 1987, and Int-Hout III 1987)

1. Uneven temperatures and lack of temperature and humidity controls.
2. Uneven air distribution, causing lack of air motion in space.
3. Lack of fresh air, especially during the in-between seasons.
4. Energy savings do not meet expectations.
5. Lack of supply and return fan sequencing, causing negative pressure in the building.
6. Some VAV systems are difficult to balance.
7. Some VAV systems are difficult to operate and maintain.
8. Only condition affecting comfort that is directly controlled is the space dry bulb temperature.
9. Further, many of the advances in VAV system design and control are not widely understood and used.

One may ask why do the above problems exist ? As pointed out by several researchers, generally, the reasons can be attributed to many factors -- both technical and non-technical. It is difficult to pinpoint one single reason; however, some of the possibilities include:

1. The complexity of the design. Sometimes innovative design engineers, in the name of energy conservation, design too complicated a system and forget about future maintenance.

2. Misapplication.

3. The selection of improper equipment (such as variable air volume boxes, variable speed drives, air distribution devices, and supply air fans), automatic controls, poor duct design, and the selection of inappropriate duct material.

4. Poor installation and air balance, and lack of coordination.

5. Poor or no maintenance.

6. Present-day demand for computers because occupants are no longer the primary variable load in many offices. Personal computers often produce three times as much as heat as their operator, but are not always on. This means that higher space load variation.

7. Rapid changes in technology, reflected in the many types of controls and necessitating their coordination, multiple choices of variable air boxes, and numerous types of fans and fans modulating drives.

8. Lack of standardization.

For example, James Woods (IAQU 1990), has investigated and reported on common deficiencies in HVAC systems. In buildings he investigated, he found that 75% of the system design often provided inadequate outside air and inadequate air distribution to occupied spaces. He also found that 90% of the operational problems come from inappropriate control strategies, 75% due to inadequate maintenance and 60% caused by thermal and contaminant load changes.

2.5 Limitation Of The Studies Done On VAV Systems

From the literature review in previous sections, it is evident that variable air volume system is the best to investigate because of its energy efficiency, low initial and energy cost, and versatility. However, there are still many problems existing in HVAC system design and operation as listed in section 2.4. Furthermore, there are not many studies on the relationships which include the dynamics and interactions of the supply, distribution, and control processes in HVAC systems. As James Woods (IAQU 1990) found that 90% of the HVAC systems failed to operate satisfactory because of inappropriate control strategies. In order to address some of these issues the following objectives are proposed.

2.6 Objectives Of The Present Work

1. To develop component models of a VAV system and solve the individual model equations and study their transient response characteristics.
2. To integrate the component models to develop an overall model of a VAV system and find numerical solution to the model equations.

3. To study the transient response characteristics of the overall VAV system by carrying out open-loop simulation tests.
4. To implement feedback control algorithms on the VAV model and study the closed-loop system response to step changes in space-loads.
5. To simulate typical daily operating performance of the system and examine the controller response in maintaining room air temperature and humidity levels close to the desired setpoint values.

In the following, the physical model of the VAV system used in this study will be described and mathematical models of the component systems and the description of the overall system will be introduced in Chapter 3. The sensitivity results of major HVAC system components will be presented in Chapter 3. The open-loop test response of the integrated VAV system will be introduced in Chapter 4 to study the dynamic interactions between VAV system and the environmental space. The control algorithms will be implemented in Chapter 5. The results obtained through computer simulation runs will be presented and discussed in the same chapter. Conclusions and recommendations will be given in Chapter 6.

CHAPTER 3

COMPONENT MODELS AND SIMULATION RESULTS

3.1 Introduction

The HVAC system is made of many different components, and each has its own operating characteristics. To study the dynamic characteristics of the individual HVAC system components, it would be necessary to develop mathematical models which characterize the dynamic behaviour of the sub-systems. Energy balance principles or first law of thermodynamics to a control volume are used to obtain these basic governing partial differential equations in space and time. Then, numerical methods are used to solve the model equations. In the end, the transient response to a step changes in input variables is used as a way of finding the systems' dynamic characteristics.

In this chapter, 1) individual models of the sub-systems of a VAV system are developed, and 2) their step-response to changes in input is examined.

3.2 Component Models Of A VAV System

Figure 3.1 shows the schematic diagram of the VAV system used in this study. The major elements of the system are i) a

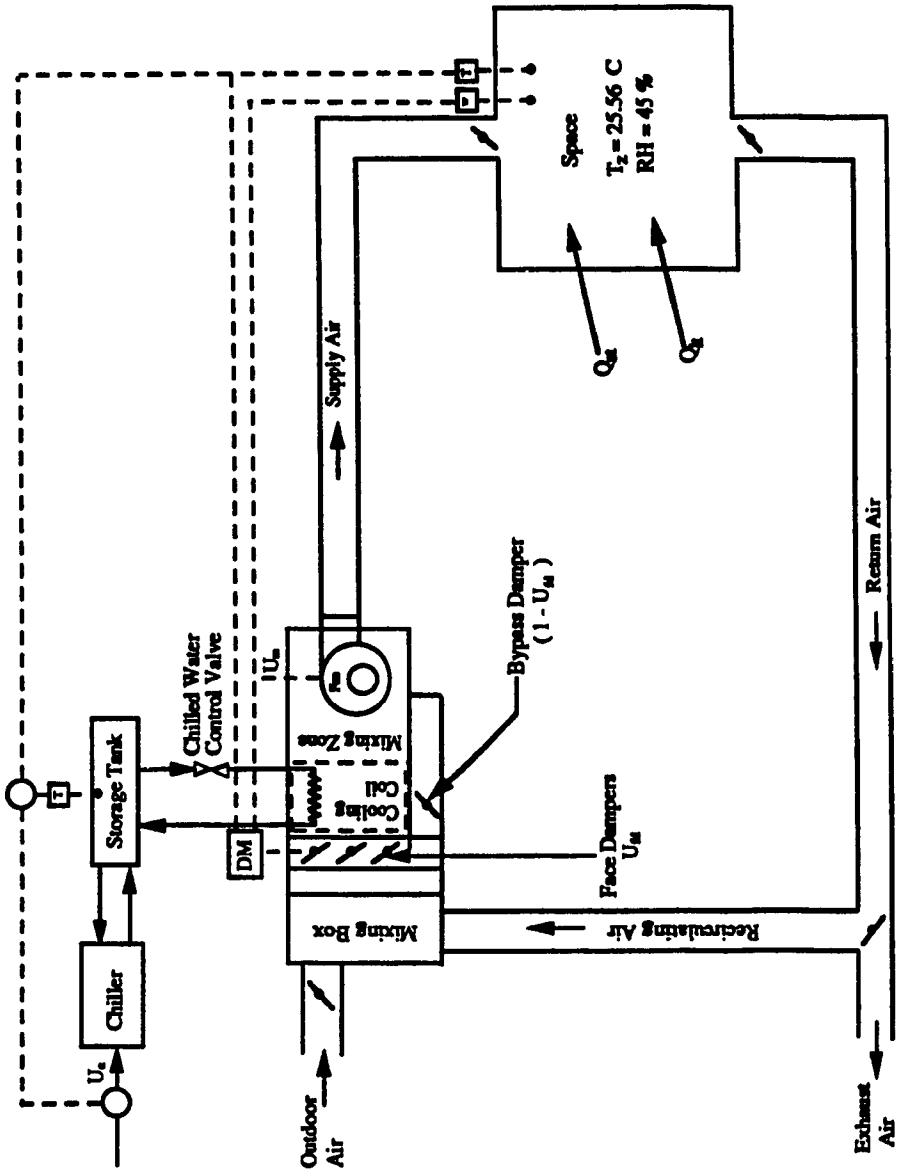

Figure 3.1 Schematic diagram of a variable air volume (VAV) system.

single zone environmental space, ii) a cooling and dehumidifying coil, iii) a chiller and a storage tank, iv) face and bypass dampers, v) a fan, vi) a distribution ductwork and vii) a feedback control system. The operation of VAV system can be understood by tracing the path of air around the loop.

For example, the air from the zone (space) returns through the return duct, a portion of this air is exhausted and the remaining air is mixed with the intake fresh outside air at mixing box. This mixed air which is hot and humid (considering summer cooling case only) is cooled and dehumidified in the cooling coil. The cooling coil receives chilled water from the chiller and storage tank arrangement shown in the figure. The supply air must be at appropriate conditions (in terms of dry bulb temperature and humidity ratio) in order to satisfy the cooling load requirements of the zone. In a variable air volume system, the air flows are typically adjusted depending upon the supply air temperatures to maintain fixed zone temperatures. Therefore, for a good control of zone air temperature and humidity ratio, the rate of supply air and its conditions (temperature and humidity ratio) must be continuously modulated. This is accomplished by the feedback control system (broken lines in Figure 3.1).

As shown in the figure there are three control variables that can be varied in order to improve the overall

performance. For example, the quantity of supply air ($U_m M_{a,r}$) is controlled by increasing or decreasing the fan speed. The supply air conditions are controlled through a combination of face and bypass damper setting (U_{fd}) and by controlling the temperature of the chilled water flowing in the cooling coil. A third control action deals with the regulation of input energy (U_c) required to run the chiller as a function of cooling load.

All these three control actions require feedback signals from the thermostat (T) and the humidity sensor (W). For example, when the room temperature (T_z) increases because of an increase in cooling load, the difference between the setpoint and the actual values of the outputs (temperature and humidity ratio) increases. This is known as error which is fed back to the controllers in order to initiate the control action. Typically in this case (that is, when the cooling load increases) i) the fan speed is increased to increase the supply air mass flow rate ii) the bypass dampers ($1-U_{fd}$) are partially closed and hence the face dampers (U_{fd}) are opened so that a higher fraction of air passes through the cooling coil iii) the chiller energy consumption is controlled such that it is just sufficient to meet the increased cooling load (sensible and latent). It must be noted that all three control actions are coupled in the sense the action of one influences the other. Therefore, the effect of changing loads on the

overall performance of the system must be carefully incorporated into the control strategy.

Also, as shown in Figure 3.1, the conditions of air must be determined i) just after the exhaust air damper, ii) at the mixing box, iii) after the cooling and dehumidifying coil and iv) after the fan. During each calculation cycle (along the air control loop), the air properties such as

1) Enthalpy (h),
2) Humidity ratio (W),
3) Temperature (dry-bulb and wet-bulb),
4) Relative humidity (RH), and
5) Specific volume (v)

are computed at the above locations by calling the psychometric subroutine (Witt 1972, Kusuda 1969). This means, the enthalpy and humidity ratio of the air are changing continuously while the air is circulated in the ductwork. For example, the enthalpy of the air changes i) all along the ductwork due to heat gains from the surrounding unconditioned space, ii) at the mixing box due to the addition of outdoor air, iii) after the cooling and dehumidifying coil and iv) at the fan due to sensible heat gain. Therefore, it is evident that models for i) cooling and dehumidifying coil, ii) chiller and storage tank iii) fan, iv) ductwork and v) mixing box are required. In the following, the dynamic models for these systems are described for a single zone environmental space.

3.2.1 Single Zone Environmental Space

Accurate prediction of indoor air temperature and humidity levels require the dynamic or time-dependent approach to building simulation. A simple mathematical equation represent the dynamic characteristics of a zone can be derived by using energy balance principle. Let V_{ol} be the volume of the zone, h_z and h_s the enthalpy of the zone and supply air, W_s and $M_{s,r}U_s$ the humidity ratio and mass flow rate of the supply air, the rate of change of enthalpy and humidity ratio on a single zone environmental space (Figure 3.2) can be written as:

$$\rho_a V_{ol} \frac{dh_z}{dt} = -M_{s,r} U_s (h_z - h_s) + Q_{st}(t) + Q_{lt}(t) \qquad (3.1)$$

$$\rho_a V_{ol} \frac{dW_z}{dt} = -M_{s,r} U_m (W_z - W_s) + \dot{m}_v(t) \qquad (3.2)$$

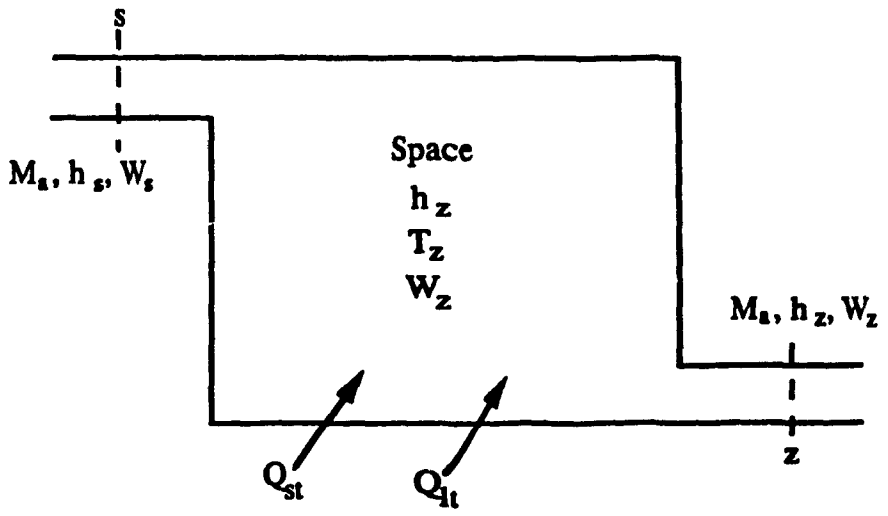

Figure 3.2 Energy balance on a single zone environmental space.

heat extracted from the space $M_{a,r}U_a(h_z-h_s)$ and the rate of sensible ($Q_{st}(t)$) and latent ($Q_{lt}(t)$) loads on the zone. Similarly, the rate of moisture change in the space is equal to the moisture removed from the space and the moisture load ($m_w(t)$) added on the zone. The enthalpy is related to dry bulb temperature (T_z) and humidity ratio (W_z). That is

$$h_z = C_{p,a}T_z + W_z(I_g + C_{p,v}T_z) \qquad (3.3)$$

if the specific heat C_{pa} and C_{pv} are assumed to be constant in the entire (cooling/heating) temperature range. In SI units, Equation (3.3) may be approximated as

$$h_z = T_z + W_z(2501 + 1.86T_z) \quad \frac{kJ}{kg} \qquad (3.4)$$

Equations (3.1) and (3.2) describe the enthalpy and mass balance on the zone. U_a is the mass flow rate control variable that the product of $M_{a,r}U_a$ is equal to M_a as shown in Figure 3.2.

3.2.2 Cooling And Dehumidifying Coil Model

The cooling coil is a significant element of most HVAC processes. It is the most important interface between the primary plant (eg. chiller) and secondary air distribution system. Also, its dynamics are the most influential in air

system. Also, its dynamics are the most influential in air control loop. Therefore, a number of models have been developed to study its transient response characteristics as reviewed in section 2.2.1 (heat exchanger). In this study, the transient model of a chilled water coil developed by Elmahdy (1975) was used. This model was used because in previous study (Zaheer-uddin and Goh 1990) the steady state version of the chilled water coil model (Elmahdy and Mitalas 1977) gave good results. Therefore, we had a good basis to compare the results obtained from the transient model (for $t \rightarrow \infty$) with that of the results obtained from the steady state model and thus ascertain the results from the present transient model.

Figure 3.3 shows a schematic diagram of a cooling and dehumidifying coil arrangement used in this study. The assumptions are described in the reference and in Figure 3.4. The cooling coil modeled is a typical counter-cross flow type with fitted either circular or continuous flat fins on the tubes. This model is capable of simulating different coil configurations such as varying the number of rows of tubes (4 rows and more) and the number of fins per inch of tube. Given the inlet temperature of the chilled water T_w and the conditions of the air entering the coil, the leaving conditions of air and water from the coil are described by the following equations.

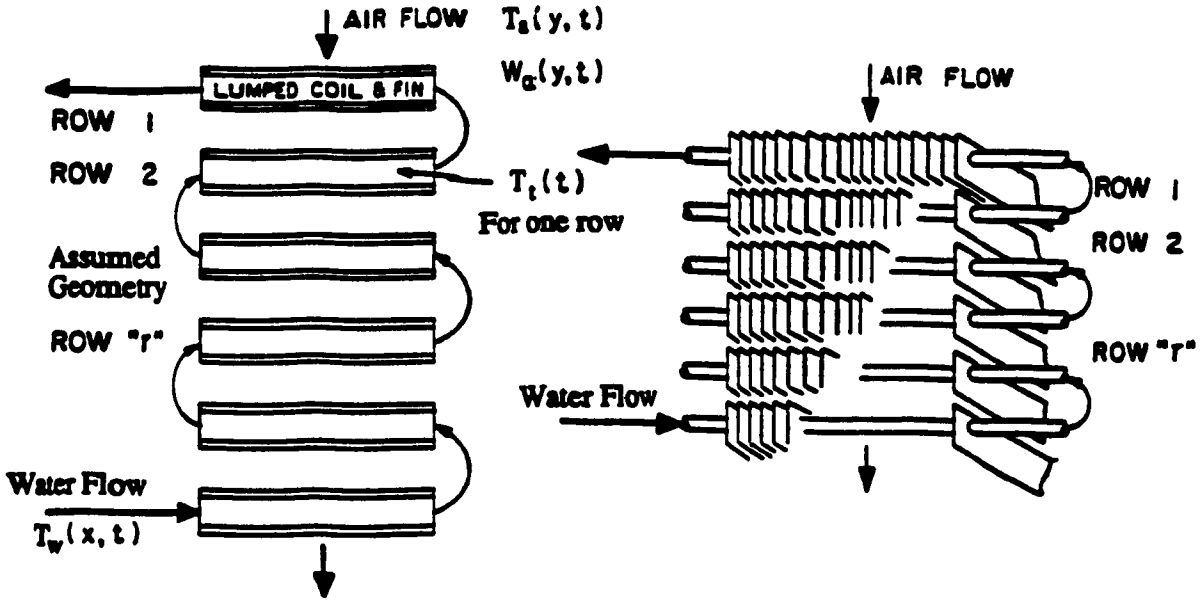

Figure 3.3 Cooling and dehumidifying coil arrangement.

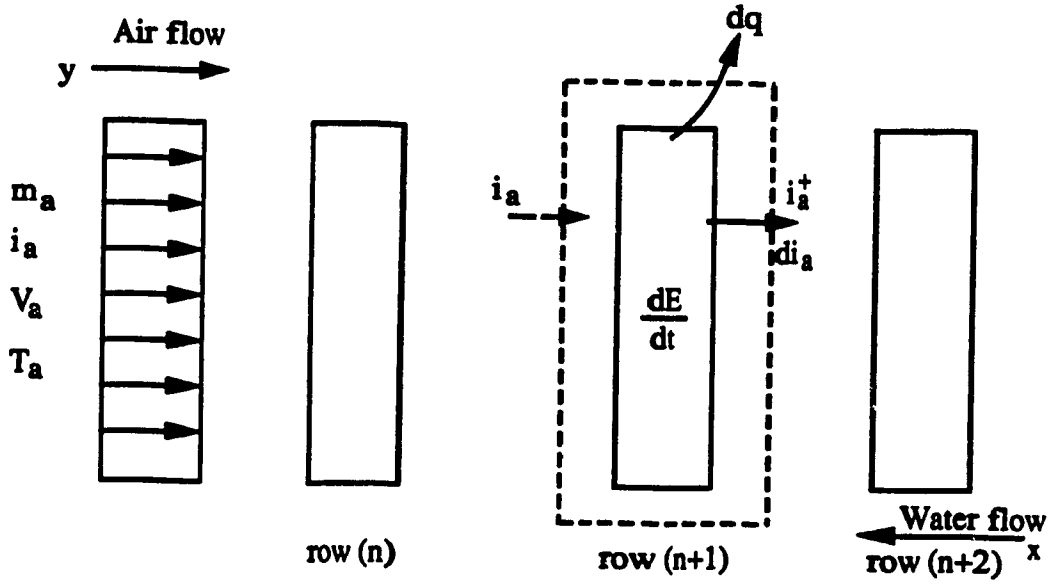

Figure 3.4 Energy balance on differential control volume of the coil.

Air-side

$$\frac{dT_a}{dt} + \gamma_a V_a \frac{dT_a}{dy} = -\frac{\gamma_a \eta_{aov}}{m_a C_{p,a} R_a} (T_a - T_{t,o}) + (\gamma_a - 1) \frac{dW_a}{dt} T_a \quad (3.5)$$

where

T_a	:	air temperature, (°C or °F)
t	:	time, (s or hr)
γ_a	:	ratio of specific heat of air by specific heat of vapour
V_a	:	air velocity, (m/s or ft/hr)
η_{aov}	:	overall dry heat exchanger efficiency
$T_{t,o}$	:	tube temperature, (°C or °F)
W_a	:	humidity ratio of the air, (kg_w/kg_a or lb_w/lb_a)
R_a	:	resistance to heat flow per unit length for the air side, (s.m°C/kJ or hr.ft°F/Btu)
y	:	air flow direction, (m or ft)
m_a	:	mass of air per unit length in the air flow direction, (kg/m or lb/ft)
$C_{p,a}$	:	specific heat of air, (kJ/kg°C or Btu/lb°F)

Water-side

$$\frac{dT_w}{dt} + V_w \frac{dT_w}{dx} = \frac{1}{m_w C_{p,w} R_w} (T_{t,o} - T_w) \quad (3.6)$$

where

T_w	:	chilled water temperature, (°C or °F)
V_w	:	water velocity, (m/s or ft/hr)
x	:	water flow direction, (m or ft)
R_w	:	resistance to heat flow per unit length, (s.m°C/kJ or hr.ft°F/Btu)
m_w	:	mass of water enclosed in control volume, (kg/m or lb/ft)

the tube temperature ($T_{t,o}$), air humidity ratio (W_a), and saturated humidity ratio (W_{sat}) in Equations (3.5) and (3.6) are given by

$$\frac{dW_a}{dt} + V_a \frac{dW_a}{dy} = \frac{1}{m_a C_{p,a} R_a Le} (W_a - W_{sat}) \qquad (3.7)$$

$$\frac{dT_a}{dt} + \frac{\eta_s + \frac{m_t C_{p,t}}{m_f C_{p,f}}}{1-\eta_s} \frac{dT_{t,o}}{dt} = \frac{\eta_{sov} (T_a - T_{t,o})}{R_a (1-\eta_s) m_f C_{p,f}} + \frac{\eta_{sov} I_g}{m_f C_{p,f} Le R_a C_{p,a}} \frac{W_a - W_{sat}}{1-\eta_s} - \frac{T_{t,o} - T_w}{R_a C_{p,f} m_f (1-\eta_s)} \qquad (3.8)$$

where

η_s : dry fin efficiency
η_{sov} : overall wetted fin efficiency
Le : Lewis number
I_g : Enthalpy of saturated water vapour, (kJ/kg or Btu/lb)
$C_{p,t}$: specific heat of tube material, (kJ/kg°C or Btu/lb°F)
$C_{p,f}$: specific heat of fin material, (kJ/kg°C or Btu/lb°F)

$$W_{sat} = -0.00793 + 0.00031 T_{t,o} + 0.0000075 (T_{t,o} - 53)^2 \qquad (3.9)$$

This model accounts for the fin efficiencies (dry and wet), air and water side resistances (R_a, R_w), mass flow of air and water per unit length, Lewis number (Le) and the heat storage in fins and tube.

Equations (3.5) through (3.9) were used to solve the

temperature T_a and humidity ratio W_a of the air leaving the coil. Equation (3.9) was an empirical relationship to calculate the air saturated humidity ratio at the given tube surface temperature (McCullagh et al. 1969). The inlet chilled water temperature to the coil was obtained by solving the chiller and storage tank model as follows.

3.2.3 Chiller And Storage Tank Model

If T_w is the chilled water temperature and C_w is the thermal capacity of the storage tank, the energy balance on the tank is written (Zaheeruddin and Goh 1990):

$$C_w \frac{dT_w}{dt} = - CWFR\, C_{p,w} \xi\, (T_w - T_{wr}) - U_c\, U_{2,max}\, COP + U_{ch} A_{ch}\, (T_{mr} - T_w) \qquad (3.10)$$

where the rate of energy stored in the tank is equated to the energy withdrawn from the tank $CWFR.C_{p,w}\xi(T_w-T_{wr})$, the rate of energy extracted from the chilled water $U_cU_{2,max}COP$ and the heat gains from the surroundings $U_{ch}A_{ch}(T_{mr}-T_w)$.

CWFR in Equation (3.10) is the mass flow rate of chilled water supplied to the cooling coil and U_c is the input energy (control variable) to the chiller. The coefficient of performance (COP) of the chiller was modelled as

$$COP = (COP_{max} - 1)\left(1 - \frac{T_w - T_s}{\Delta T_{max}}\right) \qquad (3.11)$$

where T_s is the sink temperature and ΔT_{max} is the maximum temperature differential the chiller is designed to work with.

3.2.4 The Fan Model

The fan is an essential component of almost all heating and air-conditioning systems. In general, the supply air and return air fan heat gain are ignored (Miller 1982) or is not included in air distribution system. However, the heat generated by the fan motor is part of the cooling load. Therefore, it must be added as sensible heat gain to the air stream. In order to calculate this component the fan model given in BLAST (1979), BESA (1987), and DOE-2.1A (1981) was used. The rate of heat delivered by the fan motor was expressed as a function of part-load-ratio (PLR) as follow

$$\Delta T_{PL} = \Delta T_r * PLR \qquad (3.12)$$

where

$$PLR = \frac{supply\ air\ flow\ rate}{rated\ flow\ rate\ of\ fan}$$

$$\Delta T_r = DT_r k_1$$

$$DT_r = \frac{\Delta P_r}{\eta_r}$$

$$k_1 = 0.3996 \frac{0.754\ (T_a+459.7)\ (1.0+1.605\,W_a)}{(0.24+0.444 W_a)\ 60.0\ P_{atm}}$$

As defined in Equation (3.12), the heat delivered to the air is equal to the product of rated temperature rise (ΔT_r) and the part load ratio (PLR). The rated temperature rise is the product of the ratio of rated static pressure (ΔP_r) to the rated fan efficiency (η_r) and k_1 which is function of the air temperature and humidity ratio and for English units only.

The fan chosen for this study is capable of producing a pressure of 0.5" water gauge (ΔP_r) at rated air flow rate of 1.6 m^3/s (3000 cfm). The fan speed and power consumption at part-load conditions were obtained from manufacture's catalogue (Cincinnati Fan 1989). Two fourth order polynomial equations were obtained from the catalogue data. These two correlation curves will be used in this study. The curves are shown in Figure 3.5, and the correlation equations are defined as:

$$RPM = a_0 + a_1\, cfm + a_2\, cfm^2 + a_3\, cfm^3 + a_4\, cfm^4 \qquad (3.13)$$

$$BHP = e_0 + e_1\,cfm + e_2\,cfm^2 + e_3\,cfm^3 + e_4\,cfm^4 \qquad (3.14)$$

where the coefficients a_i and e_i in equations (3.13) and (3.14) are listed in Table 3.1.

Table 3.1 Fan speed and brake horse power coefficients.

a_i, e_i	0	1	2	3	4
RPM	783.983	-1.19×10^{-1}	4.81×10^{-4}	-1.32×10^{-7}	1.41×10^{-11}
BHP	5.99×10^{-2}	-3.36×10^{-5}	8.57×10^{-8}	1.38×10^{-11}	2.75×10^{-15}

The maximum relative error for RPM correlation is 0.09% and the maximum relative error for fan blade horse power is 0.5% for the given volume flow range (800-3000 cfm).

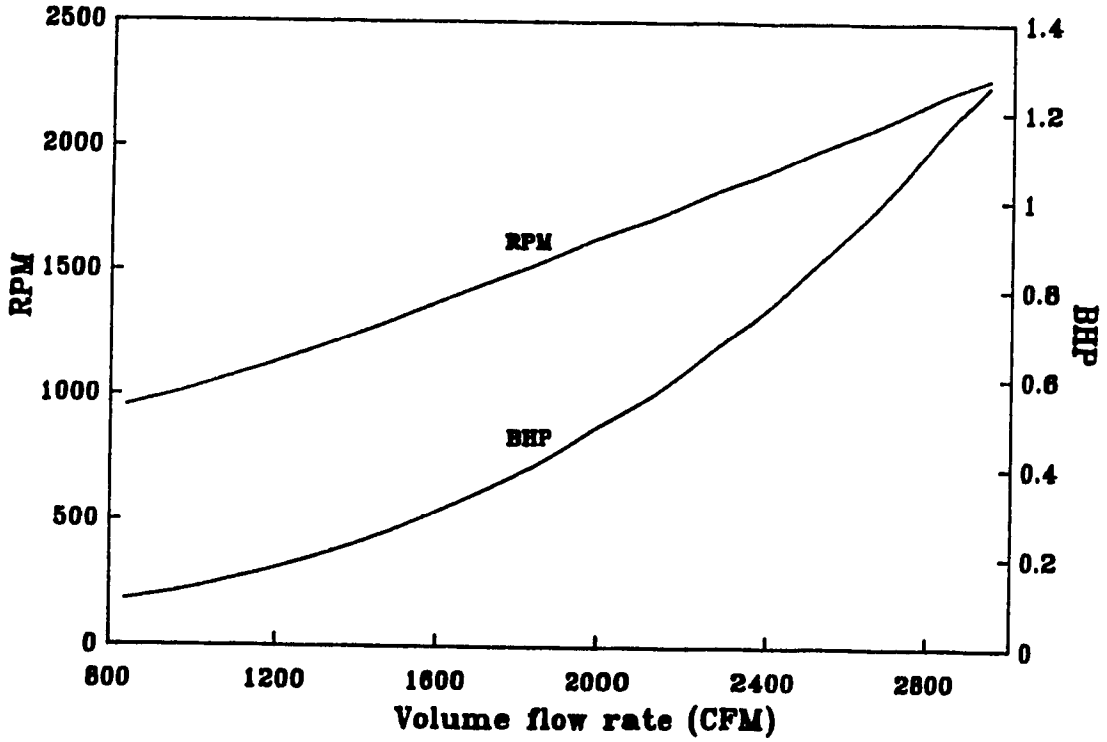

Figure 3.5 Fan speed and brake horse power curves

3.2.5 The Duct Model

A transient model for duct heat gain/losses developed by Grot and Harrje (1981) was used with the inclusion of the term $\rho_a C_{pa} A_d dT_a/dt$ in the duct air temperature equation (Equation 2.18). A simple mathematical model for the transient response of a duct can be derived by making three assumptions: 1) the duct is thin and therefore each cross section can be assigned a single temperature, 2) the air flow is well mixed, 3) propagation of heat along the duct by conduction ($k\bar{d}d^2T_d/dz^2$) is negligible compared to that caused by the moving air. The cross-section of the duct together with the nomenclature used is shown in Figure 3.6. The heat gain or loss from the duct was expressed as

$$\rho_d C_{p,d} \bar{d} \frac{dT_d}{dt} = U_o (T_\infty - T_d) + U_i (T_a - T_d) \qquad (3.15)$$

$$\rho_a C_{p,a} A_d \frac{dT_a}{dt} + \rho_a C_{p,a} A_d V_a \frac{dT_a}{dz} = \bar{P} U_i (T_d - T_a) \qquad (3.16)$$

where $\rho_d C_{p,d} d_t$ and $\rho_a C_{p,a} A_d$ are duct and air mass heat storage, the term $\rho_a C_{p,a} A_d V_a$ is forced convection term for the air stream. T_a is the air temperature and T_∞ is the temperature of the surrounding air. The interior (h_i) and exterior (h_o) thermal conductances are assumed to consist of two parts: one due to convection and the other due to the addition of insulation either externally or internally. Thus, h_i is

function of air flow velocity inside the duct and can be written as

$$h_i = \frac{0.024\, C_{p,a}\, (\rho_a V_a)^{0.8}}{D^{0.2}} \qquad (3.17)$$

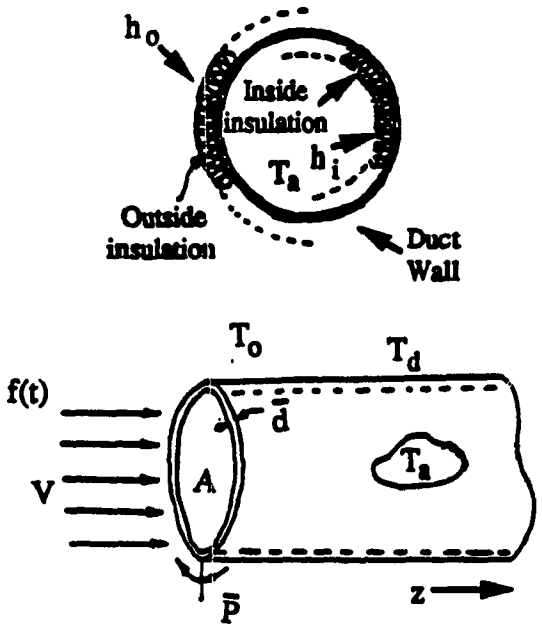

Figure 3.6 Arbitrary cross-section of duct indicating nomenclature used in the model.

and the overall interior (U_i) and exterior (U_o) thermal conductances can be found by using equations (2.19 and 2.20). Equations (3.15) and (3.16) must be solved with the initial and boundary condition:

$$T_d(z,0) = X(z)$$

$$T_a(0,t) = f(t)$$

where f(t) is the inlet air temperature. $T_d(z,t)$ and $T_a(z,t)$ are respectively the duct metal and the air temperature at a distance z from the inlet and at time t.

3.2.6 The Mixing Box Model

Air mixing such as that occurring at the outdoor air/return air dampers can be simulated if it is assumed that the mixing of the entry air is linear with respect to the damper position (P_D) and instantaneous. Then the mixed air outputs can be defined by the following equations

$$T_m = P_D T_1 + (1 - P_D) T_2 \qquad (3.18)$$

and

$$W_m = P_D W_1 + (1 - P_D) W_2 \qquad (3.19)$$

where T_m and W_m are the temperature and humidity ratio of the mixed air, T_1, T_2 and W_1, W_2 are the temperature and humidity ratio of entry air 1 and 2, and P_D is the mixing ratio or damper position. It ranges from 0 to 1 (from fully closed to fully open).

Apart from the model described above, a zone loads model is required in order to predict the sensible and latent loads on the zone (Q_{st}, Q_{lt}). For this purpose a modified version of the model developed in a previous study (Zaheer-uddin 1989) was used. It is a transient model and is capable of predicting

the sum of all the sensible heat loads (such as due to transmission loss, infiltration, solar and internal gains) and the latent loads due to infiltration and occupants. For simplicity outputs from that zone loads model were used in this study. That is, the loads $Q_{st}(t)$ and $Q_{lt}(t)$ in Equation (3.1) were computed from the zone loads model.

To this end, the next step is to study the open-loop response characteristics of the sub-systems. The open-loop tests not only provide a check on the adequacy of the component models, but they can also be used to determine the time required (for the variables of interest) to reach steady state values.

3.3 Numerical Technique And Simulation Results

In this section, the results obtained from the individual sub-systems (such as coil, duct, environmental zone etc.) are described. The model equations were solved using Euler method for time stepping and backward finite difference method to discretize the equations in space. The integration time was selected based on CFL criterion

$$\frac{\Delta V * \Delta t}{\Delta x} \leq 1.$$

Each of this sub-systems was simulated and a subroutine was developed. For example, Figure 3.7 shows the flow chart for cooling coil simulation program. The procedure used in the program to predict the steady state value is explained through the diagrammatic sequence shown in the figure. A step change in input is used to study the dynamic behaviour of the models. For example, cooling coil simulation is performed after the required parameters and inlet air and water conditions are given. The steady state result is printed when the steady state condition is achieved.

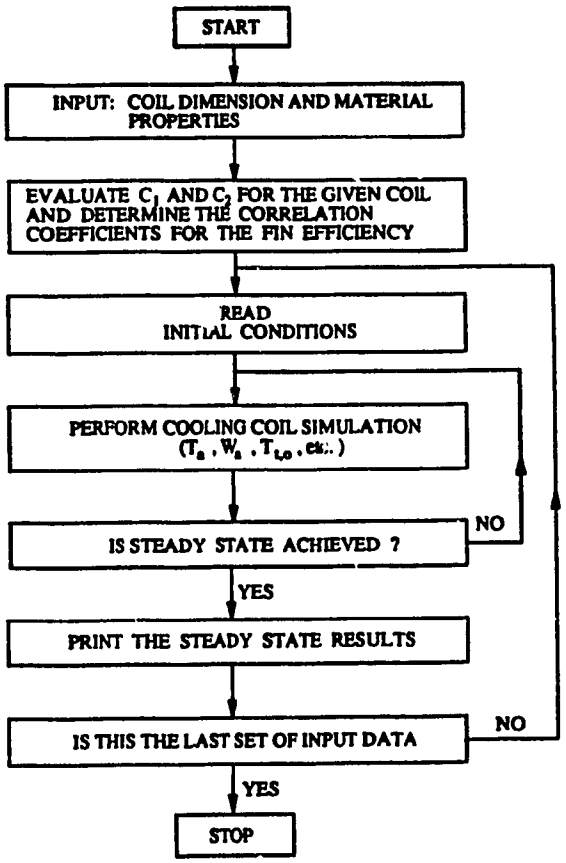

Figure 3.7 Flow chart for cooling coil simulation program.

3.3.1 Simulation Results From The Coil Model

Equations (3.1) to (3.5) were solved for a coil configuration, with the parameters given in Table 3.2. The dynamic characteristics of the coil have been simulated for changes in the inlet air and water temperature. For example, Figure 3.8 shows the leaving air and water temperatures from the coil as a function of time. It may be noted that starting from an initial temperature of 33.4°C (92°F) the air temperature decreased exponentially (decrease by almost 70% in the first 15 seconds) and reached a steady state value of about 11°C (51.8°F) in approximately 60s. Similarly, the water temperature raised from 8.2°C (46.8°F) to 10.5°C (51.2°F) during the same time period (that is 60s). This is a typical response expected from a cooling coil at constant air and water mass flow rate with the assumption that the air is well mixed between rows of the coils. This results show good agreement with the steady state results as listed in Table 3.3 with the same inlet air and water conditions.

Table 3.3 Comparison of temperatures from steady state and transient models.

Steady State Temperature, °C (°F,	Transient Model	Steady State Model
Coil dry bulb	10.8 (51.5)	10.2 (50.4)
Coil wet bulb	9.8 (49.6)	9.6 (49.4)
Chilled water	10.7 (51.4)	10.9 (51.6)

Table 3.2 Cooling and dehumidifying coil parameters

Configuration	Dimension
Coil depth: COID	27.94 cm (11 in)
Coil width: C_w	60.96 cm (24 in)
Coil height: C_l	60.96 cm (24 in)
Tube outside diameter: TD_o	1.59 cm (0.625 in)
Tube inside diameter: TD_i	1.46 cm (0.575 in)
Number of rows: NOR	8
Number of tubes per row: NTPR	16
Number of fins per inch: N_f	4.65 fins/cm (11.8 fins/in)
Fin thickness: F_t	0.01524 cm (0.006 in)
Row tube spacing: S_l	2.75 cm (1.083 in)
Column tube spacing: S_t	3.175 cm (1.25 in)
Coil face area: F_a	0.3716 m^2 (4.0 ft^2)
Primary area: A_p	3.614 m^2 (38.9 ft^2)
Secondary area: A_s	76.83 m^2 (827.0 ft^2)
Inside tube area: A_i	3.58 m^2 (38.5 ft^2)
Minimum flow area: FLFA	0.05 m^2 (.539 ft^2)
Fin material conductivity: FCON	0.2608 $W/in^2 \cdot C/m$ (128.2 $Btu/ft^2 \cdot F.hr/ft$)
Tube material conductivity: TCON	0.39856 $W/in^2 \cdot C/m$ (195.9 $Btu/ft^2 \cdot F.hr/ft$)
Lewis Number: Le	0.92

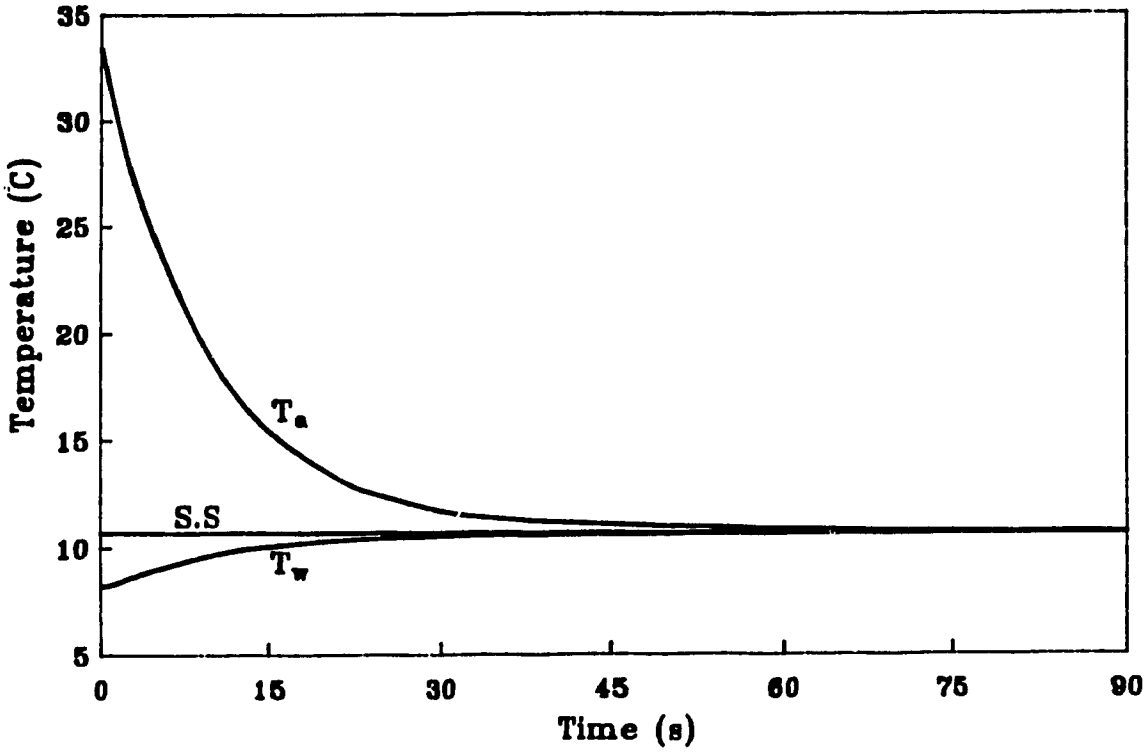

Figure 3.8 Air and water temperature responses from the coil model.

The effect of increasing/decreasing the chilled water mass flow rate on the time required by the leaving air to reach steady state is shown in Figure 3.9. In each test, a small step change in water flow rate was imposed on the chilled water coil. With each step change in water flow rate giving a different final value a curve was plotted as shown in the figure. The first thing to note from the figure is the fact that for water mass flow rates in the range of 0.01-0.05 kg/s (1.5-6 lb/min) the decrease in the steady state time is

rather sharp and beyond 0.25 kg/s (33 lb/min) the effect of mass flow rate of water is practically negligible. Of course, it is to be expected that a different response curve would be obtained by changing any of the coil parameters given in Table 3.2. From this result, it can be concluded that the outlet air temperature of the coil can be controlled as a function of chilled water flow rate. Often, this is the method used for controlling the air temperature leaving the coil to meet the zone loads.

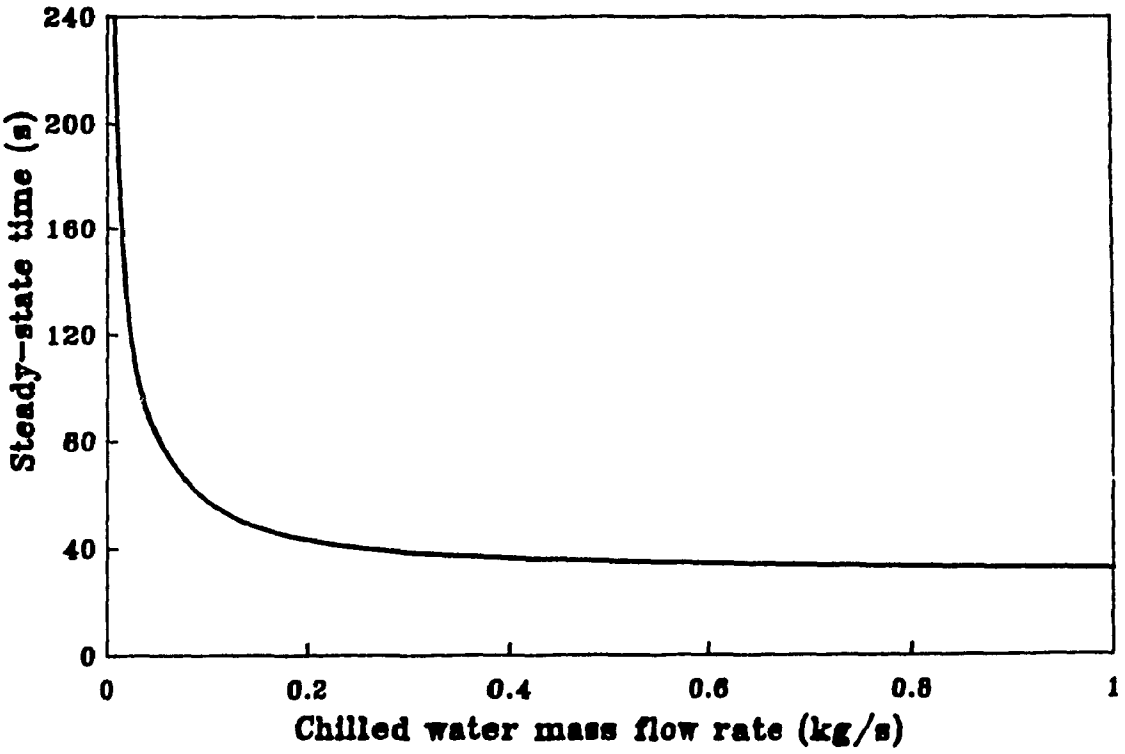

Figure 3.9 Steady-state time of the cooling coil.

Another method by which air temperature can be controlled is by varying the chilled water temperature entering the coil while keeping its mass flow rate constant. The results are presented in Figure 3.10 for three different water temperatures. In each case, the initial temperature of the air was kept the same which is 33.4°C (92°F). It is apparent from the results (Figure 3.10) that as the chilled water temperature is decreased, the leaving air temperature is decreased and vice versa. Furthermore the rate of leaving air temperature decrease increases as the water temperature is decreased. This effect is predominant during the first 15 to 20 seconds as shown in the figure. Note also that lower water temperature resulted in lower steady state values of leaving air temperature.

The effect of chilled water temperature on the humidity ratio of the leaving air is shown in Figure 3.11. Again three different inlet water temperature were considered. It is apparent that the humidity ratio can be decreased by decreasing the chilled water temperature. Also, it is understood that the rate of leaving air humidity ratio decreases as the water temperature is decreased. It can be concluded that the leaving air temperature and humidity ratio can be controlled by varying the chilled water temperature flowing into the coil.

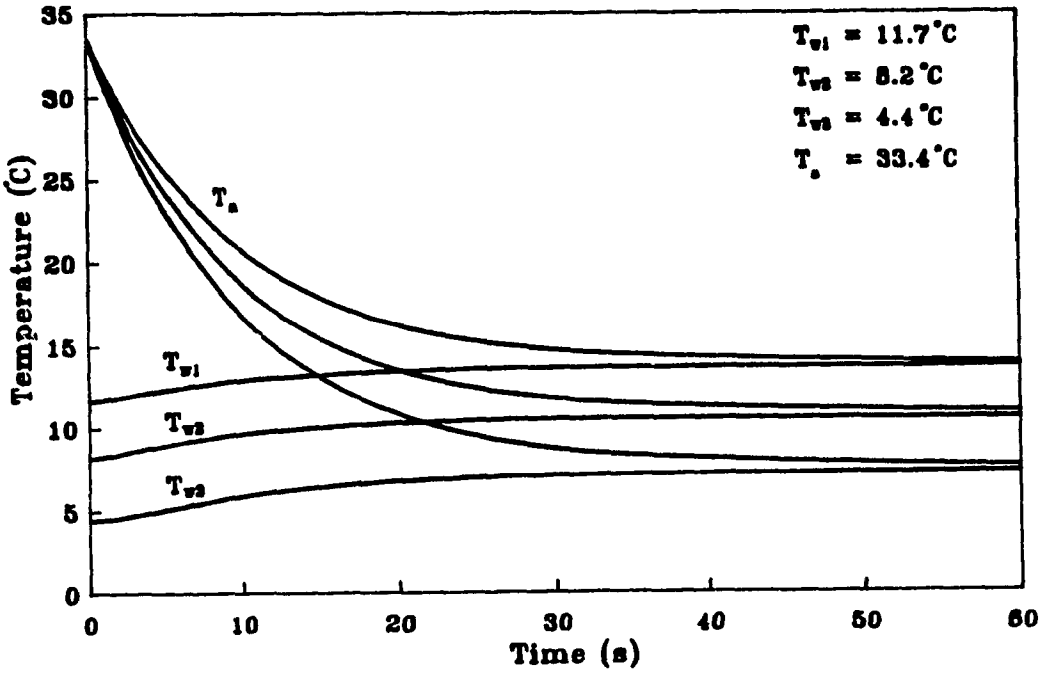

Figure 3.10 Air and water temperature responses from the coil model to step changes in chilled water temperature.

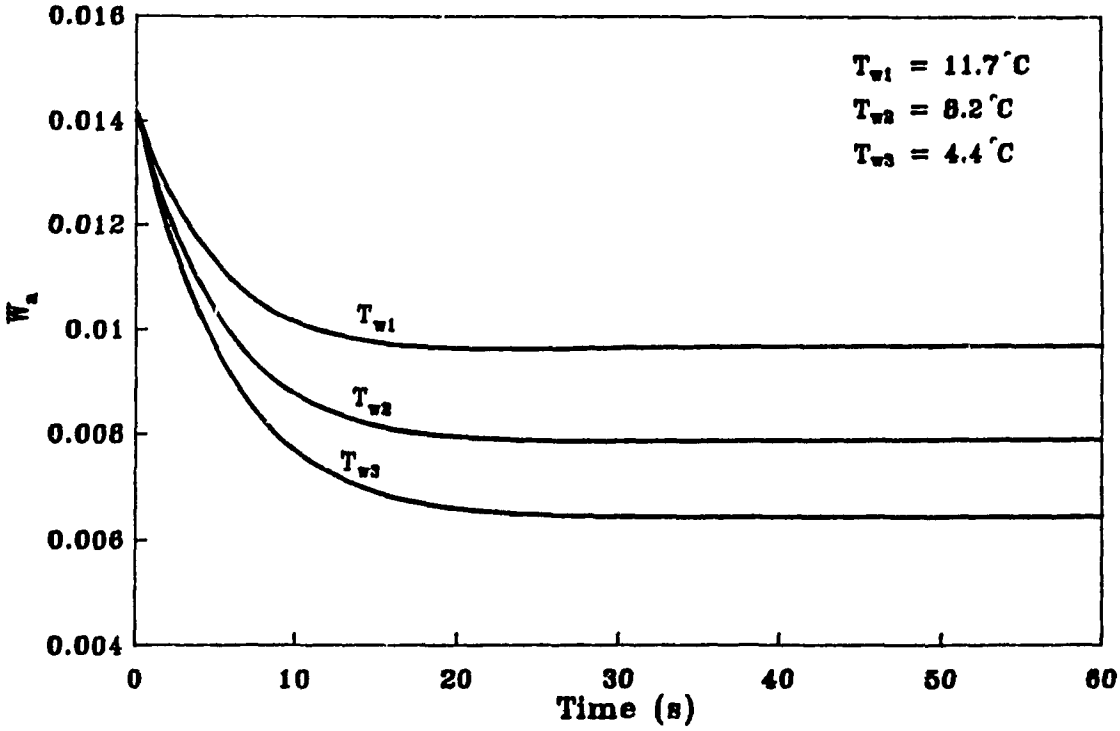

Figure 3.11 Air humidity ratio responses from the coil model to step changes in chilled water temperature.

More studies have been done for a step changes in inlet air mass flow rates (in term of coil face velocity for the given coil) and temperature into the coil while keeping the chilled water mass flow rate and temperature constant. These results are shown in Figures 3.12 and 3.13. It can be noted from Figure 3.12 that the leaving air temperature is decreased for higher coil air face velocity (higher mass flow rate) which also resulted in lower steady state time. It is apparent that the rate of decrease (in leaving air temperature) increases as the air velocity increased. Note also that lower inlet air temperature results in lower final values of leaving air and water temperatures as shown in Figure 3.13.

Furthermore, the coil model is also capable of simulating the dehumidifying process inside the coil and along the depth of the coil in the air flow direction. The results are shown in Figure 3.14. For example, at time τ=0., the coil is all wet along the depth of the coil and for the next instant time τ=0.3 s, the coil is partially wet and partially dry, and for the later instant time τ=0.6 s, the coil is all dry along the depth.

3.3.2 Simulation Results From The Duct Model

Figure 3.15 shows the leaving air temperature as a function of time. Equations (3.15) and (3.16) were solved for a square duct configuration with the parameters given in Table

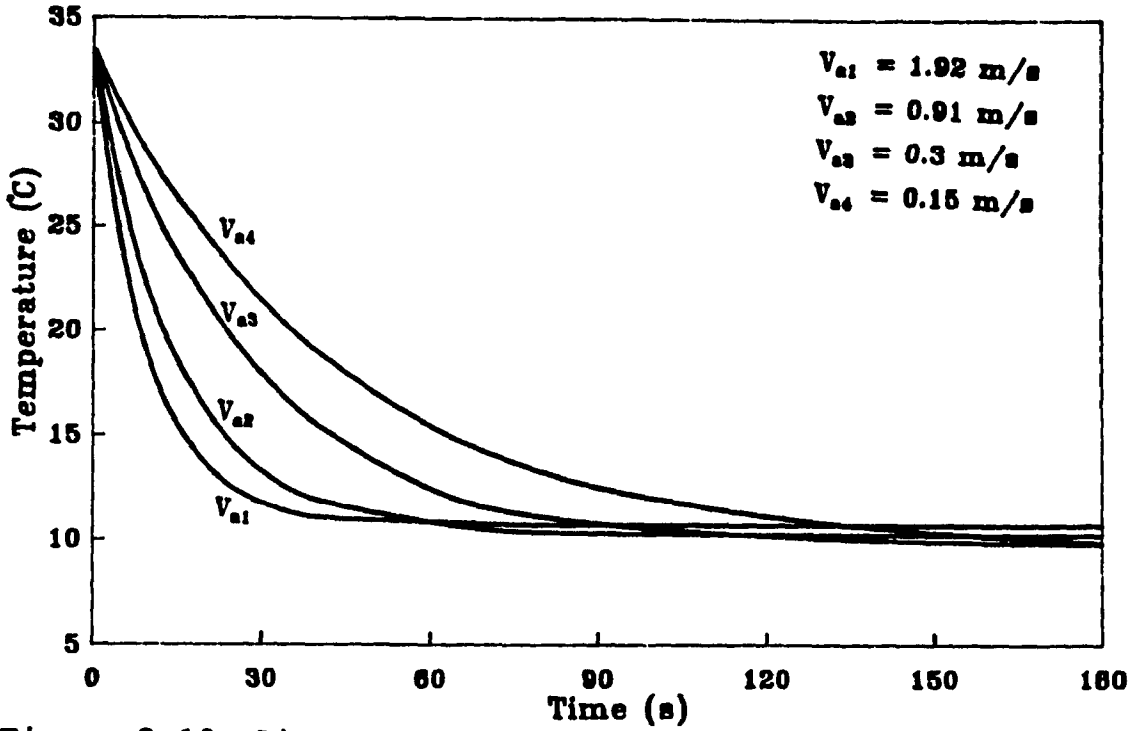

Figure 3.12 Air temperature response from the coil model to step changes in air mass flow rate (face velocity).

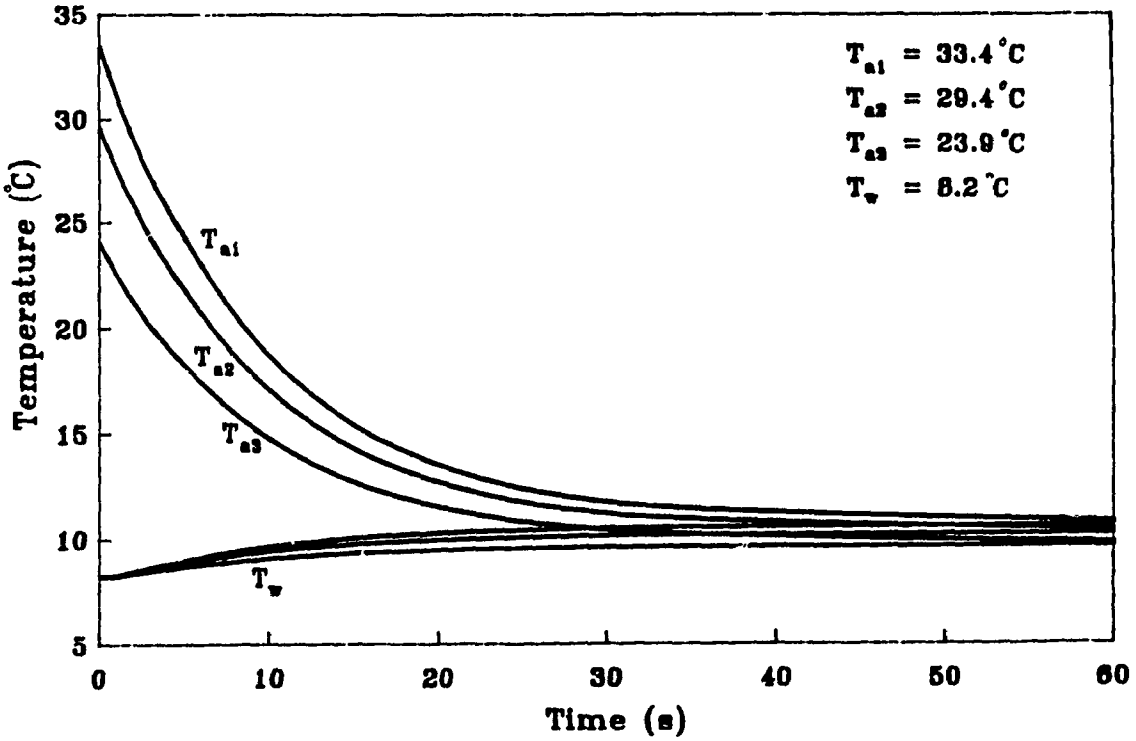

Figure 3.13 Air and water temperature responses from the coil model to step changes in inlet air temperature.

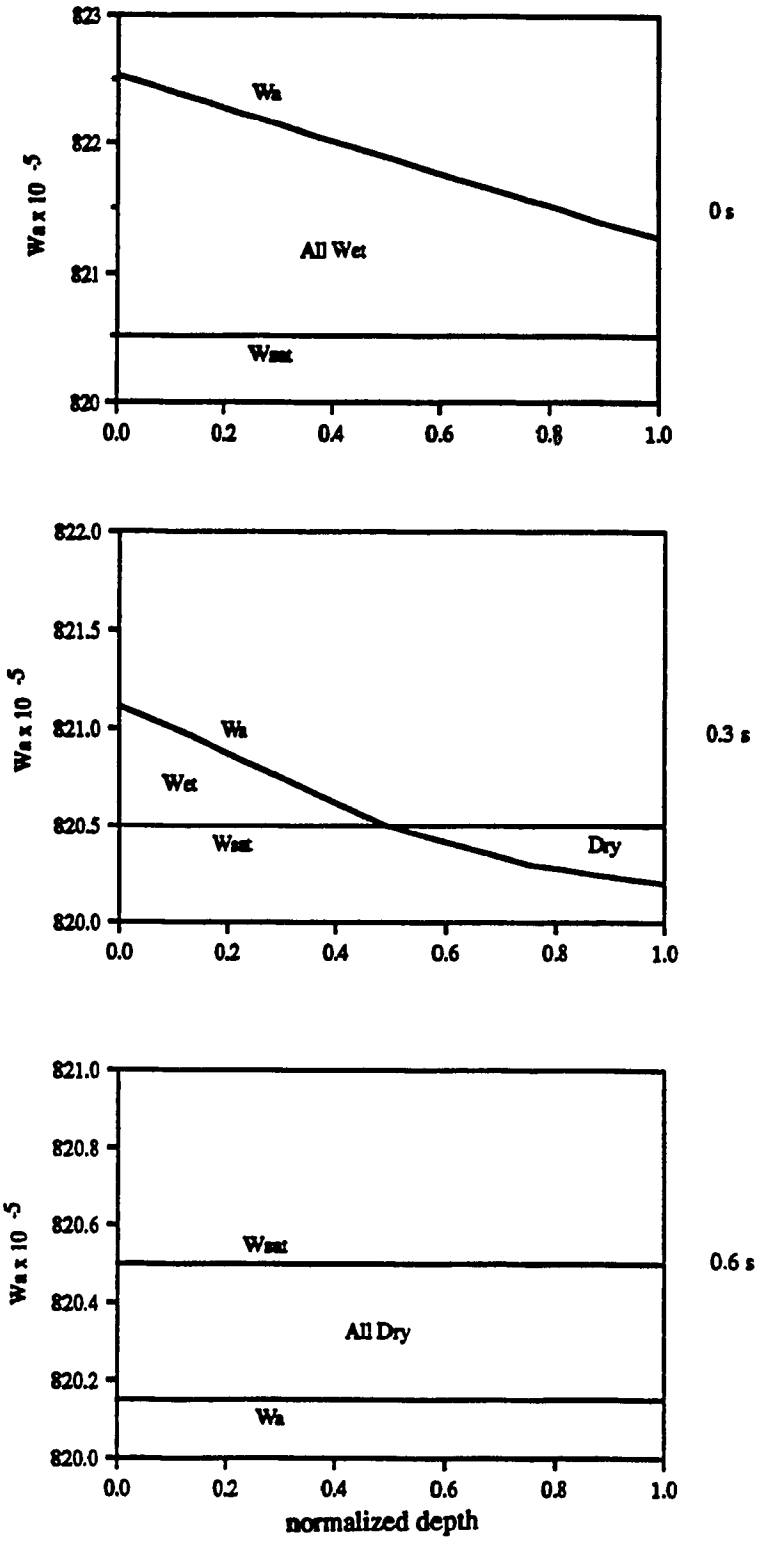

Figure 3.14 Cooling coil dehumidifying process along the depth of the coil.

3.4. A comparison between the steady-state results (Grot and Harrje 1981) and the transient results is depicted in Figure 3.15.

From the Figure 3.16, the first thing to note is that the heat gain through the duct with no external or internal insulation resulted in higher supply air temperature. For example, an increase of 4°C (7°F) in air temperature in about 100 seconds was observed. This is because the duct metal has high thermal conductivity which resulted in high heat gain through the bare duct metal. Hise and Holman (1977) found the overall heat transfer coefficient of a bare sheet metal duct was experimentally measured to be about 8.5 $W/m^2°C$ (1.5 $BtuH/ft^2$) per degree temperature differential between duct air and unconditioned surrounding air. This heat losses can account to 40% of heating/cooling cost under mild conditions and can easily be much greater under worst conditions. It is obvious that insulation is needed to increase the overall thermal resistance of the duct to reduce heating/cooling energy. According to ASHRAE Fundamentals (1977 Chapter 31) all duct systems, or portions thereof, shall be insulated if the temperature difference (ΔT) between the supply air and the unconditioned surrounding air temperature is greater than 14°C (25°F). The RSI (R) value recommended by ASHRAE (1977) is given by Equation (3.20) and in English units by Equation (3.21).

$$RSI = \frac{\Delta T}{47.3} \qquad [\frac{m^2 \cdot C}{W}] \qquad (3.20)$$

$$R = \frac{\Delta T}{15} \qquad [\frac{hr \cdot F.ft^2}{Btu}] \qquad (3.21)$$

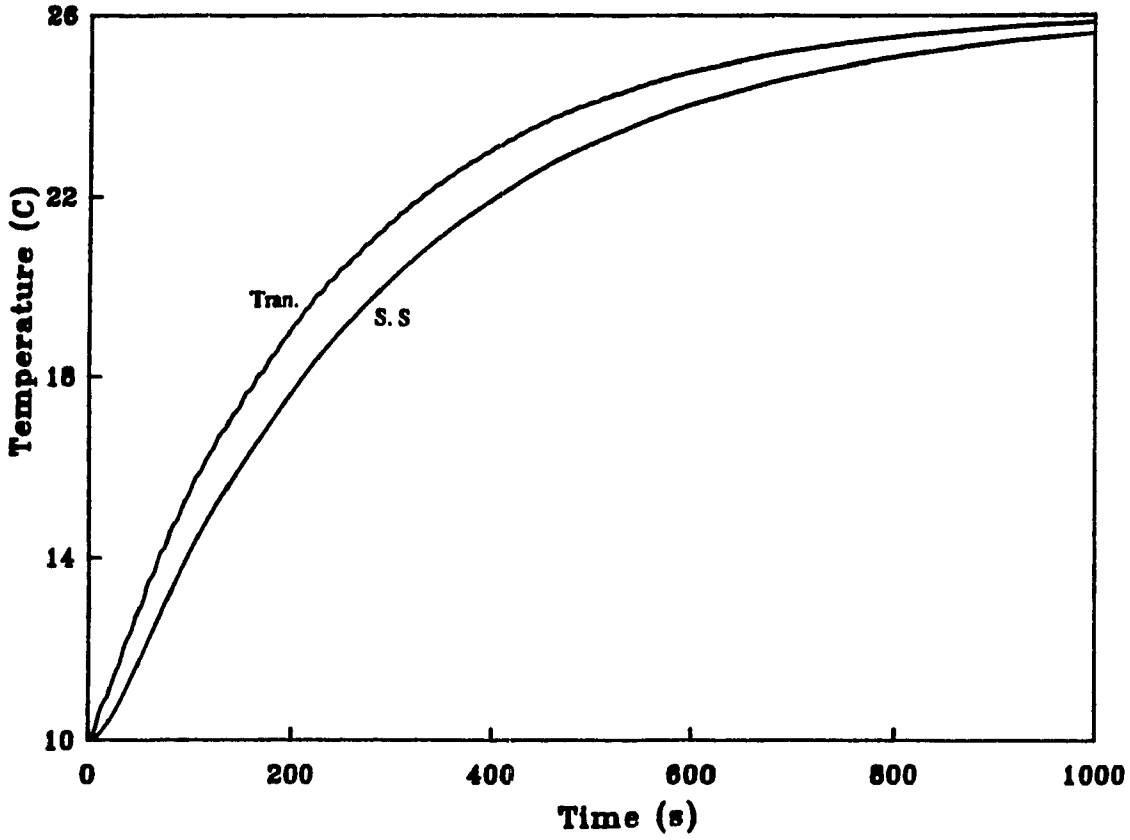

Figure 3.15 Air temperature response to step changes in inlet air temperature (duct model).

Table 3.5 lists the insulation thickness chosen for this simulation. The insulation thickness is expressed in inches because of its conventional use in the market. The effect of increasing insulation thickness on the leaving duct air to reach steady state is shown in Figure 3.16. As expected the rise in duct air temperature reduced significantly with insulation (thicknesses 1", 2" and 4") compared to the

Table 3.4 Duct parameters used in the simulation

Configuration	Dimension
Duct length	65.8 m (216 ft)
Duct width	0.508 m (20 in)
Duct height	0.508 m (20 in)
Duct metal thickness	0.08 cm (0.0316 in)
Duct specific heat, C_{pd}	0.4187 kJ/kg·C (0.1 Btu/lb·F)
Duct mass density, ρ_d	8009 kg/m^3 (500 lb/ft^3)
Air specific heat, C_{pa}	1.005 kJ/kg·C (0.24 Btu/lb·F)
Air mass density, ρ_a	1.17 kg/m^3 (0.075 lb/ft^3)
Exterior resistance, R_e	0.
Interior resistance, R_i	0.
Duct ambient temperature	28.3°C (83°F)
Volume flow rate	1.6 m^3/s (3000 cfm)

Table 3.5 Duct insulation thickness tested

Insulation thickness (inch)	RSI value (R value)
1	0.62 m^2·C/W (3.5 hft^2·F/Btu)
2	1.23 m^2·C/W (7.0 hft^2·F/Btu)
4	2.11 m^2·C/W (12. hft^2·F/Btu)

uninsulated duct (thickness 0"). For example, with 2 inch insulation the duct supply air temperature only increased by approximately 3°C (5.4°F) in 1000 seconds while it increased by 16°C (29°F) for uninsulated duct. It is apparent that significant amount of cooling energy can be saved by adding 2 inches of insulation. Also note from the figure that for the insulation thickness in the first 2 inches there is significant decrease in duct air temperature rise and beyond 2 inches the effect of increased insulation is not significant.

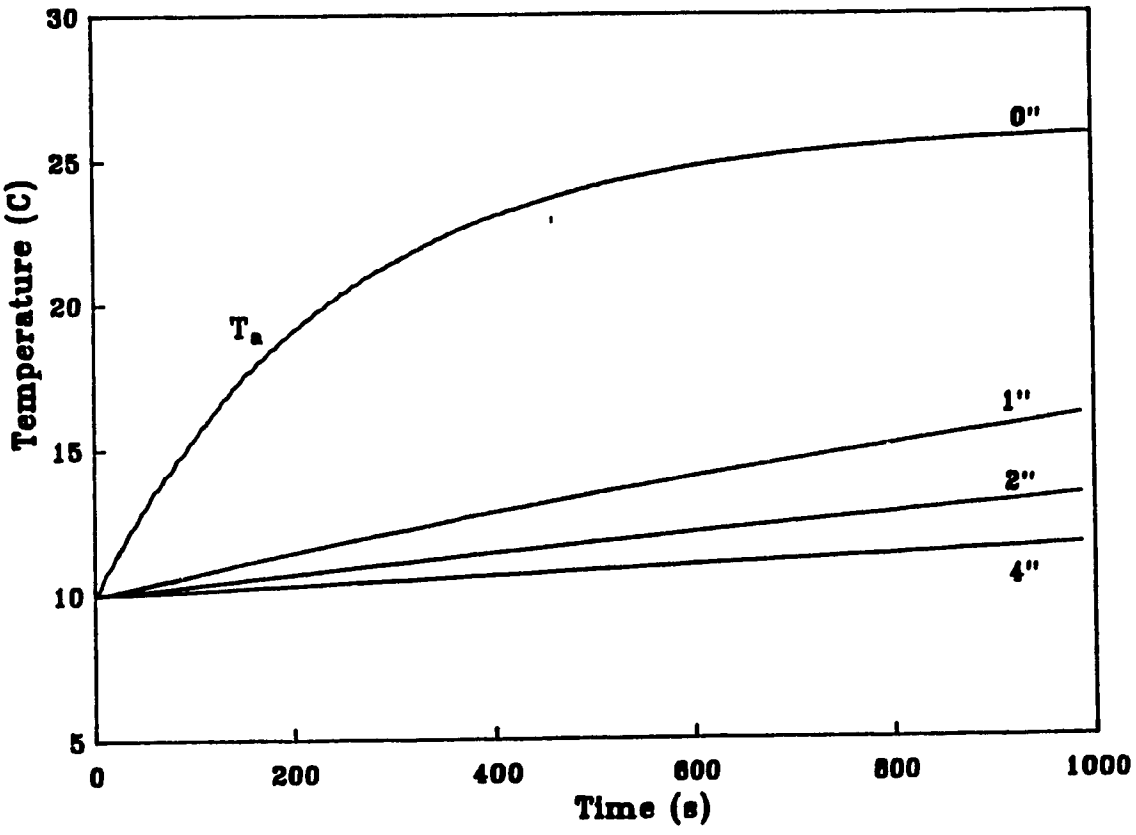

Figure 3.16 Air temperature response with insulated duct.

3.3.3 Simulation Results From The Environmental Space Model

Several simulations were conducted to study the dynamic response of the zone model. In this study, the zone volume was taken to be 673.1 m^3 (22500 ft^3), the rated supply air flow rate was taken to be 1.6 m^3/s (3000 cfm) and the initial conditions of the zone air were set arbitrarily at $T_z(0)=31.8°C$ with a relative humidity of 52%. Equations (3.1) through (3.3) were solved for the zone air temperature and humidity (as a function of time) at four different supply air mass flow rates. The results are shown in Figures 3.17a (zone air temperature response) and 3.17b (relative humidity response). Note that the supply air conditions were kept constant during the test. The temperature (T_s) and humidity ratio (W_s) of the supply air were set at 11.1°C (52°F) and 0.0075 kg_w/kg_a (0.0075 lb_w/lb_a) respectively.

It can be noted from Figures 3.17 a and b that the zone air temperature and relative humidity are decreasing as the supply air mass flow rate is increased. At the rated mass flow rate (1.6 m^3/s, curve-1 in Figure 3.17a) the time required to bring T_z from 31.8°C to 25.5°C setpoint is about 300s. This response time is function of thermal capacity of the zone air volume and the heat extraction rate. Similarly, the time required to bring the relative humidity of the zone to the setpoint value is function of thermal capacity of the zone air and the mass extraction rate. Of course, these response

(a)

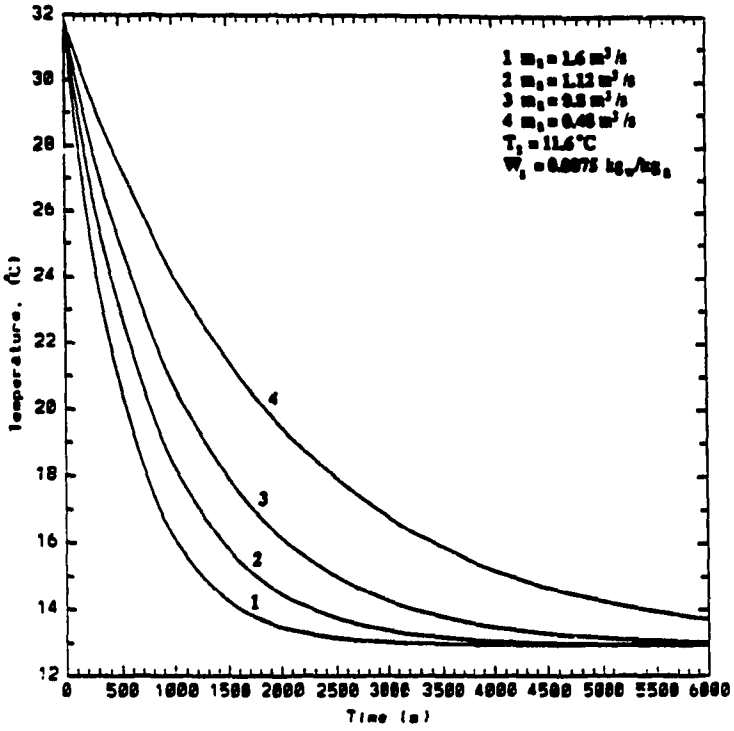

(b)

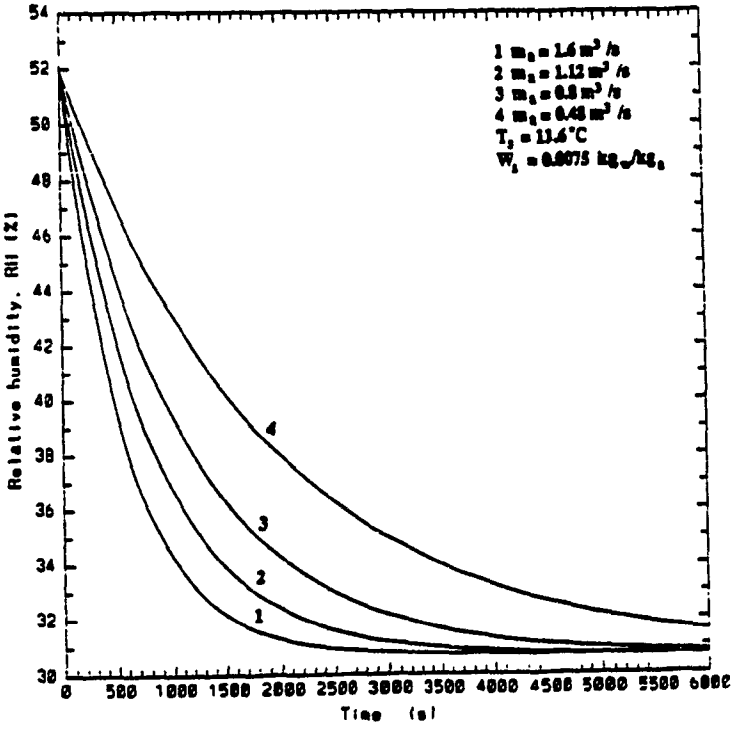

Figure 3.17a,b Zone air temperature and relative humidity responses to step changes in supply air flow rate.

characteristics change when feedback controllers are implemented. In the absence of any feedback control (as in the case shown in Figures 3.17a and 3.17b) the temperature and relative humidity decrease until they reach their respective steady state values which in this case are the supply air conditions. Thus, the steady state time at rated mass flow rate is more than 3000 seconds.

3.4 Discussion

It is apparent from the above studies performed that the responses of the sub-systems provide insight of the models' steady state time and the effect of control variables. For example, the results obtained from the system models tested can be summarized as follows.

1) The steady state time of the given coil configuration is in approximately 60 seconds, and this steady state time is function of chilled water mass flow rate. The leaving coil air temperature and humidity ratio can be controlled through varying i) the chilled water temperature entering the coil, ii) the air mass flow rate through the coil and obviously iii) by mixing of two air streams (leaving and bypass coil airs).

2) The rise in duct air temperature is reduced significantly with insulation, and

3) The response time of the space (zone) is function of its thermal capacity of the zone air volume and the rate of

heat and mass extracted from the zone. However, the steady state time for the selected zone is greater than 3000 seconds at the rated mass flow rate.

Thus, the results presented here have shown that the component models are successfully simulated and the responses from sub-systems are satisfactory. However, the important thing to note at this point is that individual sub-system responses can not provide adequate information regarding the relationships which include the dynamics and interactions of an integrated VAV system. In the next chapter, the study of the open-loop VAV system response test will be conducted.

CHAPTER 4

OVERALL VAV SYSTEM MODEL AND ITS OPEN LOOP RESPONSE

4.1 Introduction

In the preceding chapter the component models of a VAV system were developed. Also, the effect of several different parameters on the dynamic behaviour of each sub-model were investigated. In this chapter the objective is to develop an overall model of the VAV system (where all component models are integrated) and study the open-loop response of the system to step changes in control inputs.

Figure 4.1 shows the schematic diagram of a VAV system without feedback. Figure 4.2 shows the flow chart of the computer model developed for simulating the system shown in Figure 4.1. A main program is used to select the sub-programs required to represent the process of interest. The approach used in the program to calculate the supply air conditions is illustrated by the sequence shown in Figure 4.2. For example, the supply air conditions were updated while the air is being circulated in the duct via the duct model, in the coil via the coil model, at the fan via the fan model until it is delivered to the zone, and this completes one cycle. The psychometric properties of air at the above locations were computed by calling the available algorithms. Then, the conditions of air

(T_z and W_z) in the zone were determined by solving Equations (3.1) and (3.2).

Given such a system, the objective is to study its open-loop response. For this purpose, simulation tests will be conducted in which the control variables U_a, U_c, and U_{fd} will be set at constant values and the output responses of the system will be recorded.

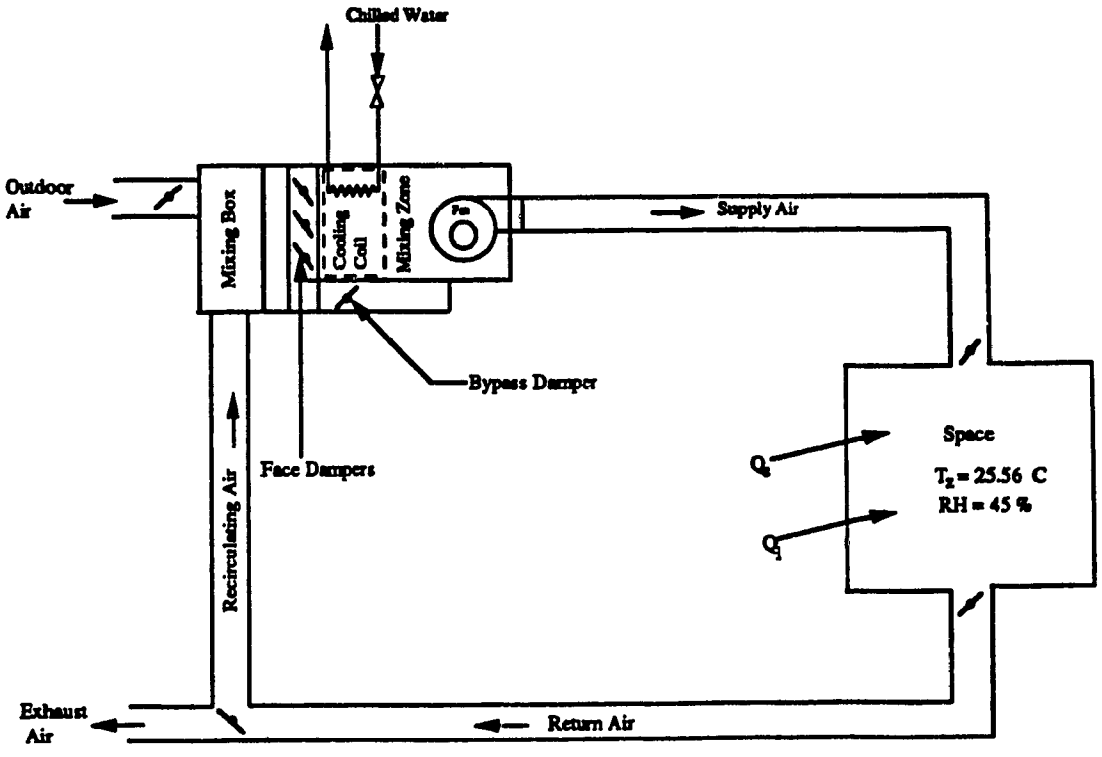

Figure 4.1 Schematic diagram of a variable air volume system without feedback.

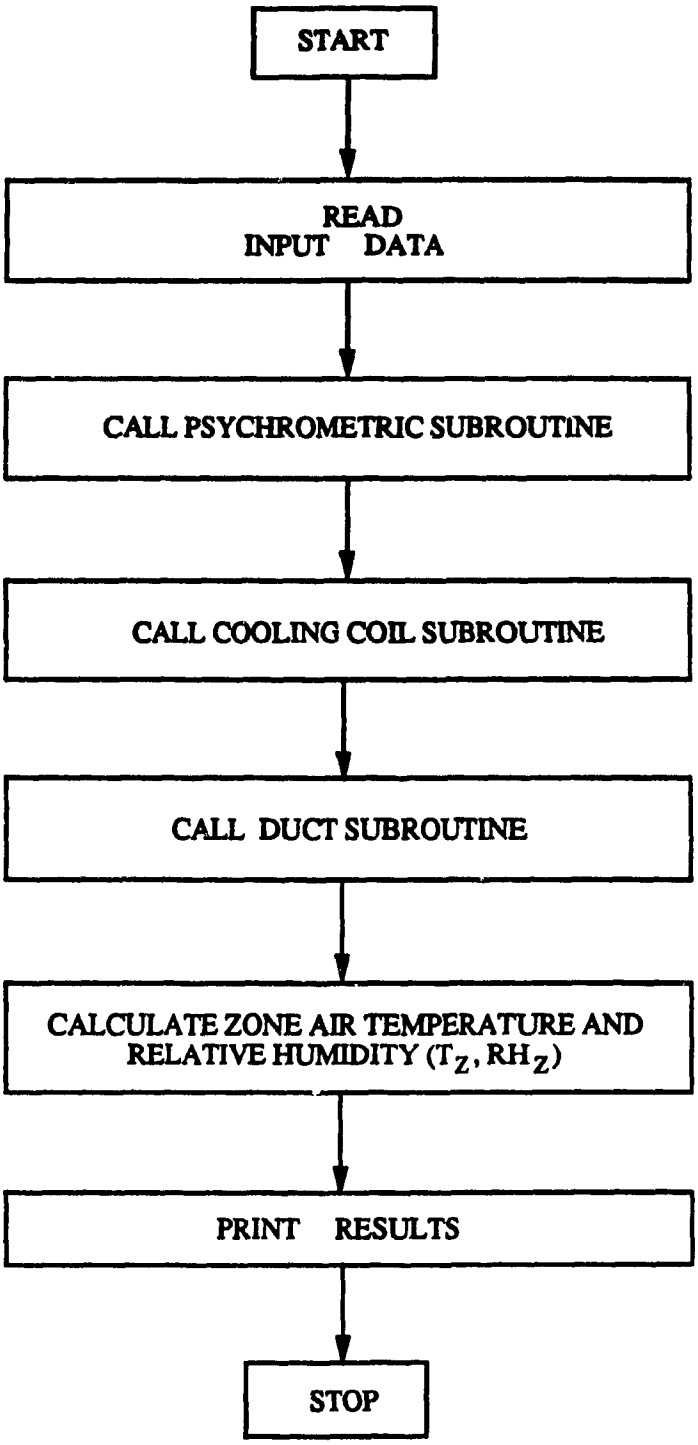

Figure 4.2 Flow chart of a variable air volume system without feedback.

4.2 Open-Loop Simulation Results

4.2.1 Input Data

The input data used in these simulation tests is given in the following Tables:

1) Cooling coil: Table 3.2 (page 66)

2) Duct: Table 3.4 (page 76)

3) Fan: Table 4.1

The length of the supply and return duct were taken as 47.7m (150 ft) and 28.48m (100 ft). The supply duct was insulated with two inches of insulation with RSl of 1.23 m^2°C/W (R=7. hft^2/Btu). The volume of the environmental space was 637.1 m^3 (22500 ft^3).

Table 4.1 Fan parameters used in the simulation.

Configuration	Dimension
Rated volume flow rate	1.6 m^3/s (3000 cfm)
Rated static pressure	0.5" W.G.
Maximum RPM	3834
Max BHP	1.5

The objective of the open-loop results in the following is to show the effect of adding one component model at a time and study its response until the overall system model is developed.

4.2.2 Simulation Results

It is instructive to start with the zone model. The temperature and relative humidity response from this zone model were given in Figures 3.17a and b (curve-1 in Chapter 3) at a fixed mass flow rate and supply air conditions. One may ask how these response curves look like when the coil model is added? Figures 4.3a and b show the open-loop response of the system (coil and space only) under similar set of conditions. The bottom curve (curve-1) in Figures 4.3a and b is the dynamic response obtained from the zone model. The upper curves (curve-2 in Figures 4.3a and b) show the temperature and relative humidity response with the addition of cooling coil. It can be noted that due to the dynamics of the coil the zone air temperature (curve-2) now lags behind curve-1. This difference is more clearly shown in Figures 4.4a and b by plotting the response for the first 100 seconds. This kind of behaviour is due to the short-term transient response of the coil which occur as a result of sudden changes in cooling load. This matter is important and influential criterion in air-control loop studies as pointed out by Gartner and Harrison (1965). It may also be noted from the figure that the zone air temperature and relative humidity gradually decrease and settle to steady-state values. The zone air temperature has settled to about 11°C (52°F) which is of course is less than the setpoint value (25.6°C or 78°F; Fig. 4.3). The

(a)

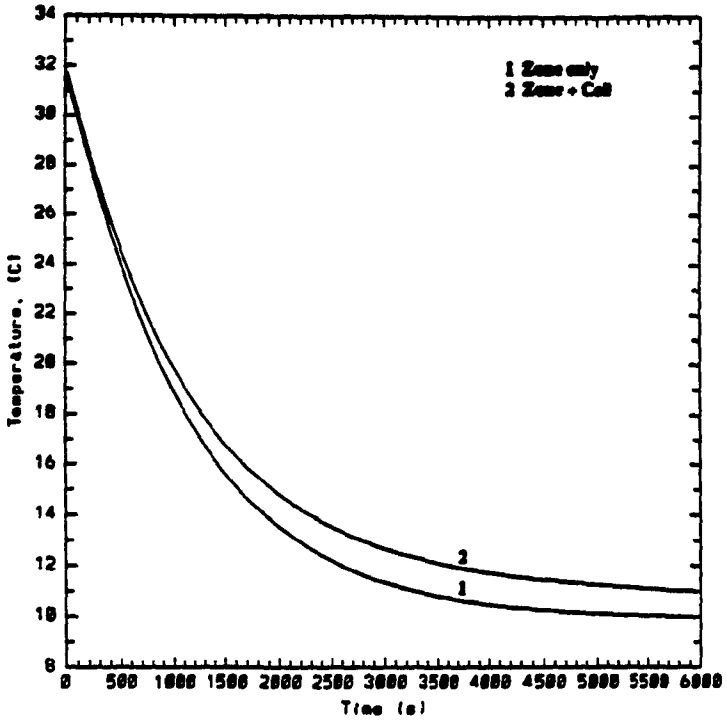

(b)

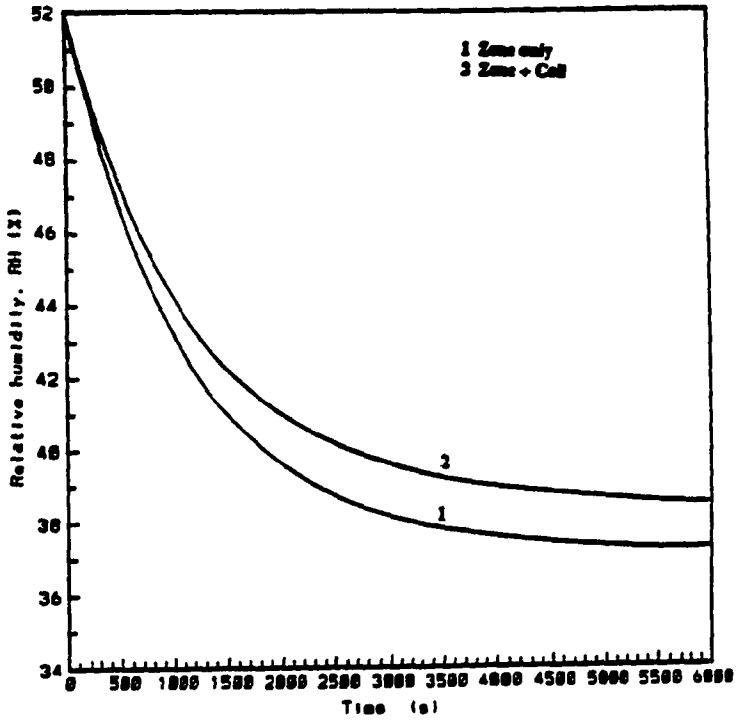

Figure 4.3a,b Open-loop zone air temperature and relative humidity responses (zone + coil models).

(a)

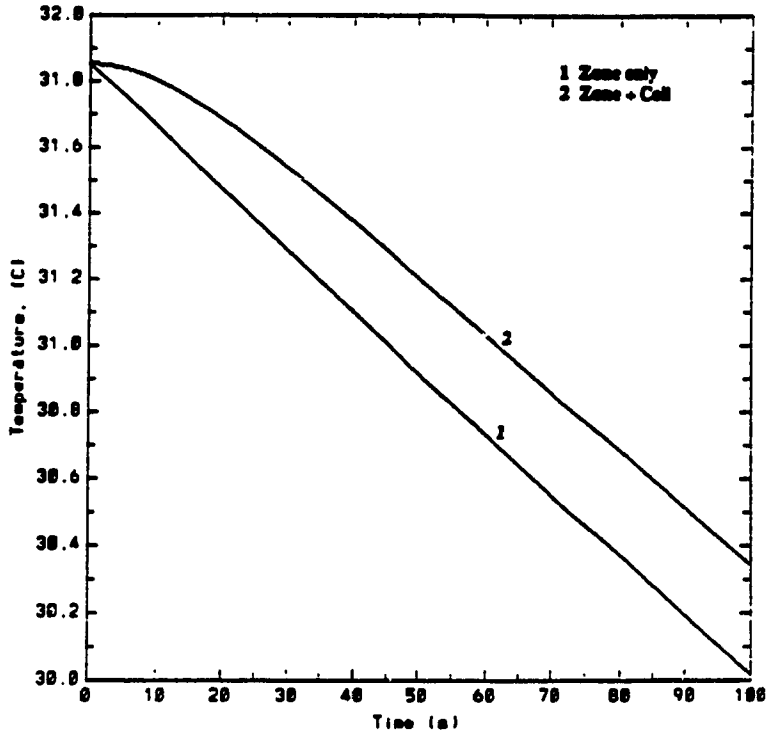

(b)

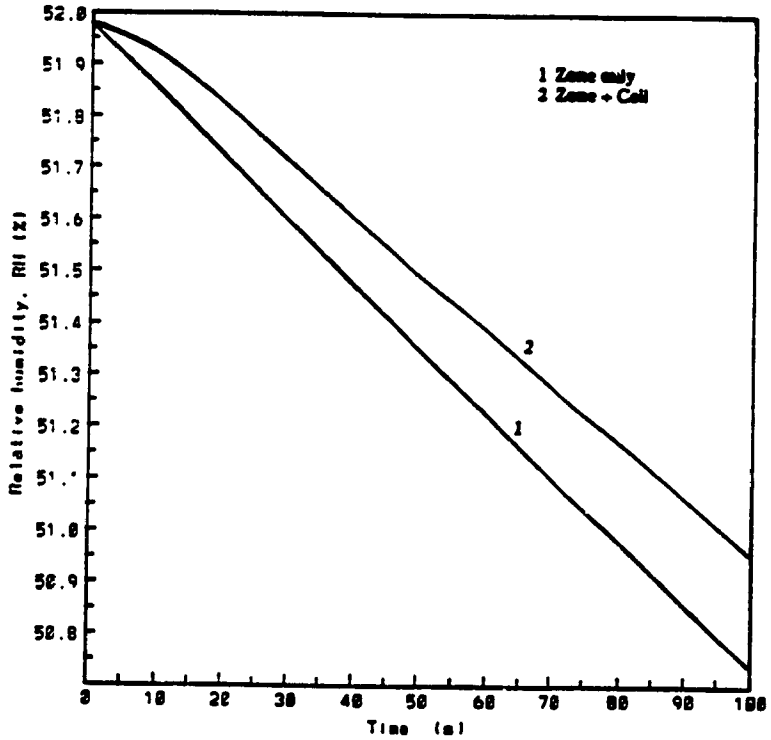

Figure 4.4a,b Open-loop zone air temperature and relative humidity responses for the first 100 seconds (zone + coil models).

relative humidity as shown in figure has settled to about 38% which is much lower than the setpoint value (45%). This is because of the temperature of the chilled water flowing in the coil which was set at a constant value and there is no feedback control to regulate the chilled water temperature. This constant chilled water temperature has the effect of over cooling and dehumidifying the supply air and thus the zone air temperature and relative humidity levels settled below the setpoint values.

Figures 4.5a and b show the zone air temperature and relative humidity responses for four different cases (labelled 1 through 4 in the figure). Curves 1 and 2 in Figure 4.5a were replotted from Figure 4.3a. Recall that curve-1 shows the open-loop response obtained from the zone model with constant supply air mass flow rate and its conditions. What happens when the coil model is added to the zone model is illustrated by curve-2. The zone temperature now takes longer time to reach steady state because of the dynamics of the coil. A further consequence of adding the duct model to curve-2 is shown in curve-3. Note that the ductwork not only introduces its time delay effects but it also adds heat gains from the surrounding spaces. For example, the difference in zone air temperature between curve-3 and curve-2 after one hour is 1.5°C. In other words, the 1.5°C rise in zone air temperature in curve-3 is due to heat gain from the bare surfaces of the

(a)

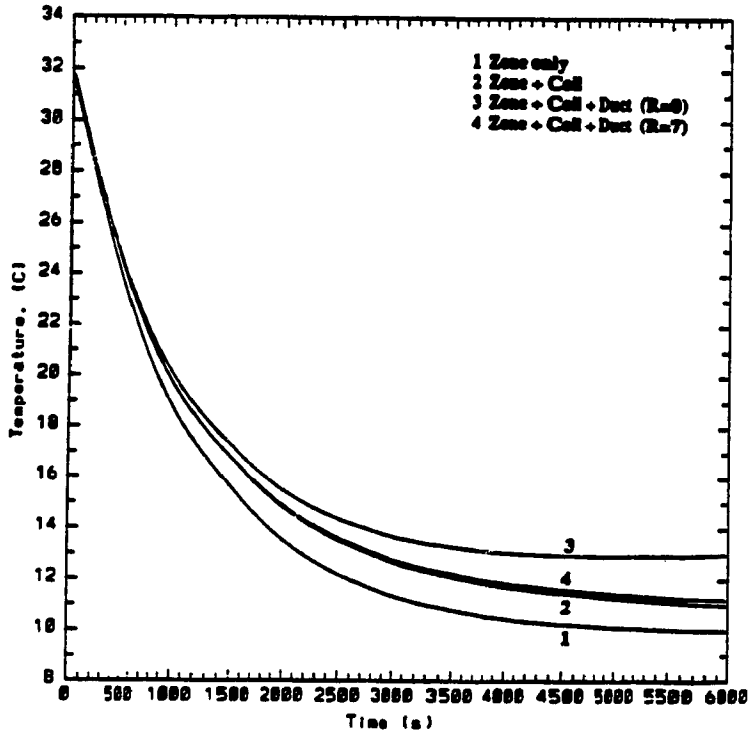

(b)

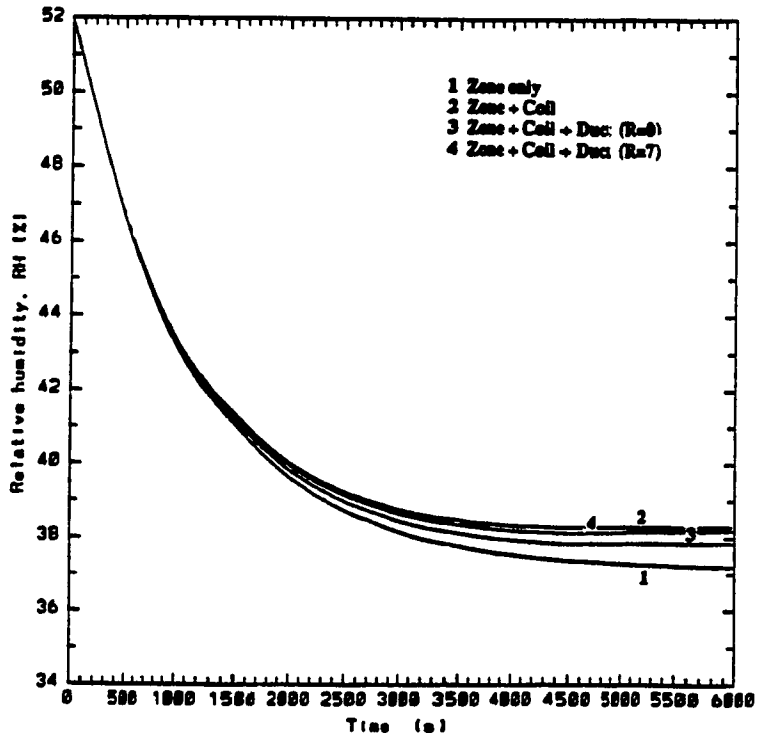

Figure 4.5a,b Open-loop zone air temperature and relative humidity responses (zone + coil + duct models).

ductwork. Of course, these heat gains can be reduced by adding insulation on the exposed surfaces of the duct. For example, the effect of adding a two inch insulation on the duct is shown in curve-4. It may be noted that the heat gains from the surroundings are considerably reduced. This can be seen by comparing the curves 3 and 4 at a fixed time such as one hour. It is apparent that the 1.5°C (2.7°F) difference noted earlier is reduced to less than 0.1°C (0.2°F). This represents a considerable saving in terms of cooling energy requirements and as such the results reiterate the importance of insulating the ducts. However, the space air temperature is settled to about 11.3°C (52.4°F) for insulated duct and to about 13°C (55.4°F) for the uninsulated duct.

Similarly, how the relative humidity in the zone varies as a function of time is depicted for four cases in Figure 4.5b. Case-1 represents the zone relative humidity response obtained from the zone model when constant rate of air at fixed conditions (temperature and relative humidity) was supplied. What happens when the coil and the duct models are added to the zone model is depicted by curve-3. It is apparent that because of the coil dynamics plus the duct heat gain, the supply air condition to the zone is no longer constant and therefore, the zone relative humidity response is slower than the response shown in case-1. For example, the zone relative humidity in curve-3 is about 1% higher than curve-1 at time

t=3600s. However, the relative humidity in curve-4 is about 0.5% higher than curve-3 at time t=3600s for insulated duct.

Finally, the fan heat gain is added into the air distribution system together with the insulated ductwork and cooling and dehumidifying coil. This completes the integration of all component models. The responses obtained now will be from the overall VAV model. The transient responses of the integrated VAV system are shown in Figures 4.6a and b (curve-4). It can be noted that the addition of fan heat resulted in a 0.5°C (1°F) increase in air temperature. The relative humidity did not change much as shown in Figure 4.6b (Curve-4) because the magnitude of sensible heat addition is small.

As we recall, the results from section 3.3.1 have shown that the supply air temperature and humidity ratio can be controlled by either by increasing/decreasing the air flow rate or the chilled water temperature. The effect of step changes in air flow rate and chilled water temperatures will be tested on the integrated VAV system.

Figures 4.7a, b show the zone air temperature and relative humidity responses to a step change in supply air flow rate. From the figures, we can conclude that for lower air flow rate (1.1 m^3/s or 2000 cfm) the rate of air temperature and relative humidity (curve-2) decrease is more gradual and the time needed for the zone air to reach steady state is longer. The zone air temperature and relative

(a)

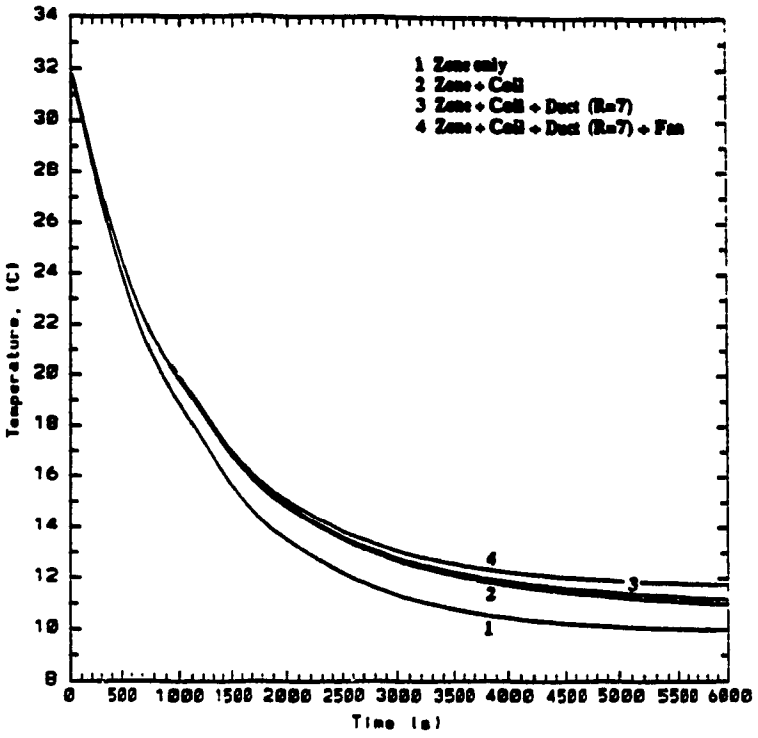

(b)

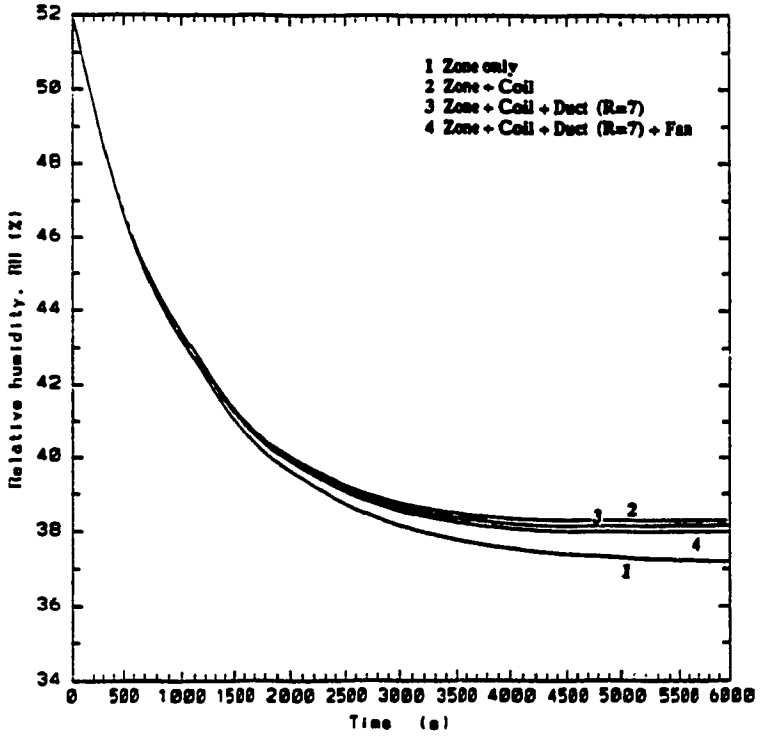

Figure 4.6a,b Open-loop zone air temperature and relative humidity responses (zone + coil + duct + fan models).

(a)

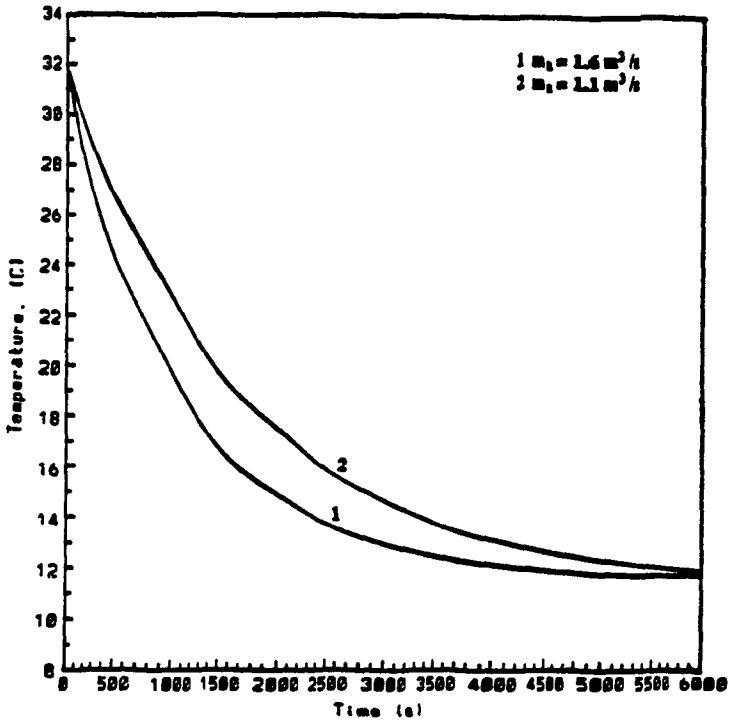

(b)

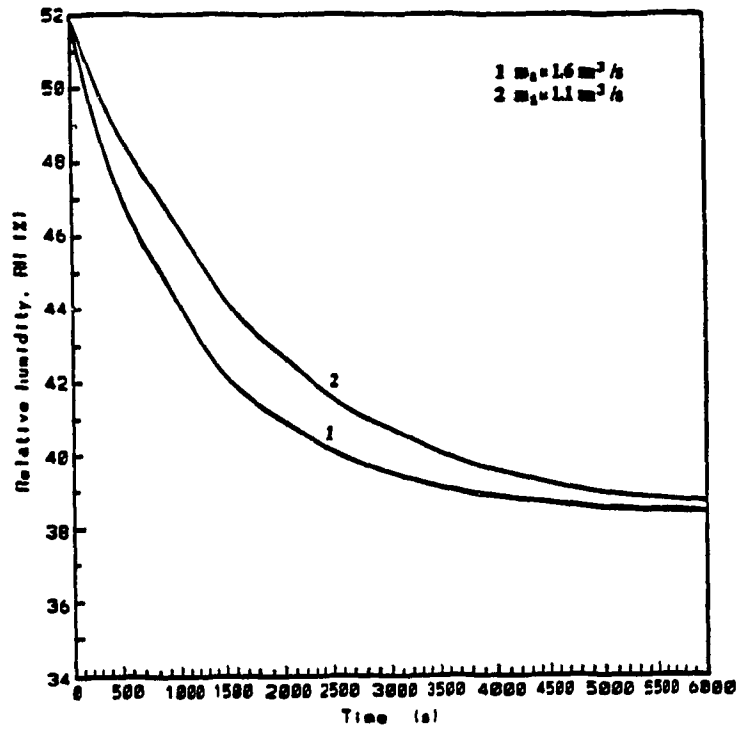

Figure 4.7a,b Zone air temperature and relative humidity responses of the VAV system to step changes in mass flow rate.

humidity response to a step change in chilled water temperature flowing into the coil are shown in Figures 4.8a, b. The temperature of the chilled water flowing into the coil was changed suddenly from 8.2°C (46.8°F) to 10°C (50°F). From the figures, it is apparent that increasing the chilled water temperature resulted in an increase the steady state zone air temperature and relative humidity (curve-2).

4.3 Discussion

The results presented in Figures 4.3 through 4.8 give an indication that the component models are properly integrated and the response from the integrated model is satisfactory. However, the important thing to note at this point is that the VAV model is responding to changes in input variables such as the supply air mass flow rate (U_m) and chilled water temperature (which can be varied by varying input energy (U_c) to the chiller) and/or its mass flow rate. The results indicate that the open loop VAV system performance can be improved if feedback capability is added to modulate either the chilled water temperature or the volume flow rate of supply air.

Now the major task is to control or regulate U_m, U_c and U_{df} such that the zone air temperature and relative humidity are maintained at the desired setpoints. Thus it is of

(a)

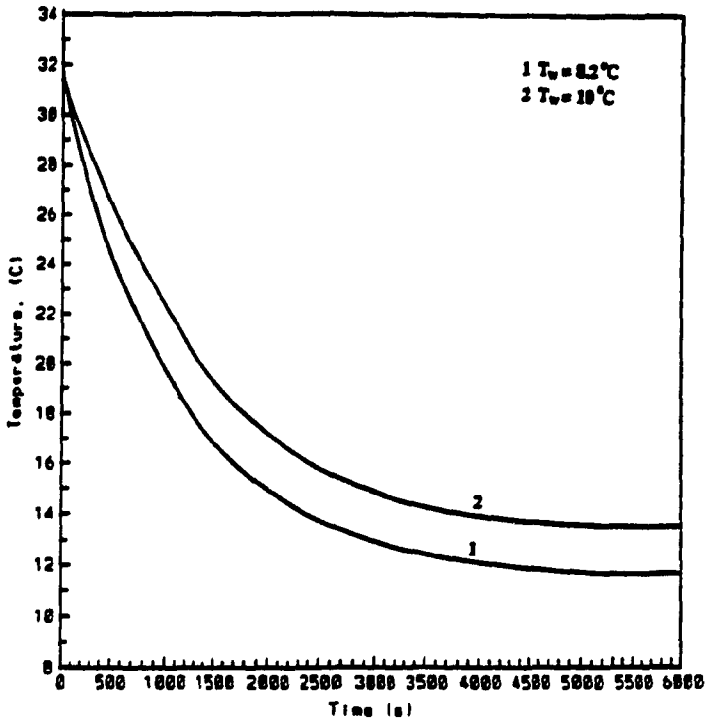

(b)

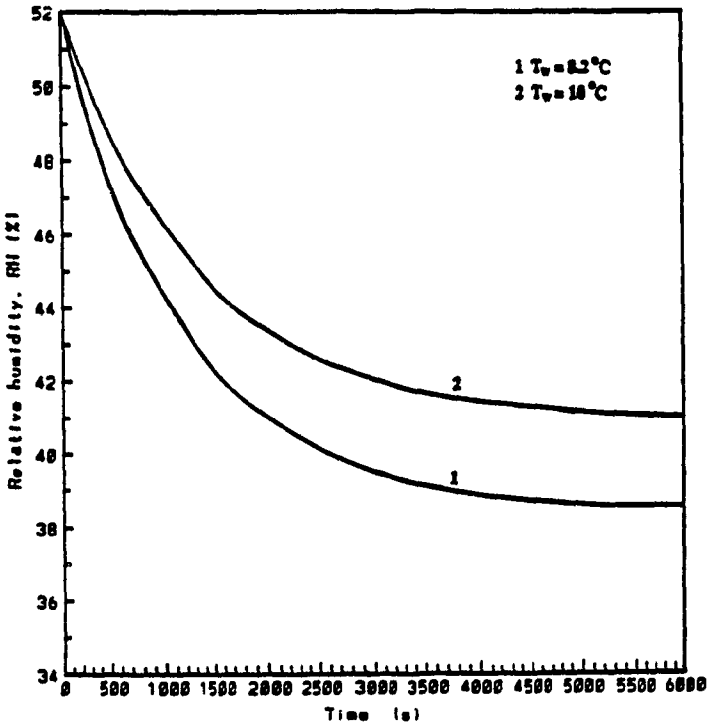

Figure 4.8a,b Zone air temperature and relative humidity responses of the VAV system to step changes in chilled water temperature.

interest to seek methods by which the inputs U_a, U_{fd} and U_c can be automatically varied through a feedback control algorithm and study the VAV system performance with feedback control.

CHAPTER 5

CLOSED LOOP RESPONSE AND DISCUSSION

5.1 Introduction

The open loop test results in Chapter 4 have shown that the steady state values of zone air temperature and relative humidity reached well below the setpoint values. The reason is that the temperature of the chilled water flowing in the coil was set at a constant value corresponding to the maximum peak load conditions. Furthermore there was no feedback to take corrective action. The chilled water temperature (constant at 8.2°C, 46.8°F) has the effect of over cooling and dehumidifying the supply air and thus the zone air temperature and relative humidity level dropped below the setpoint values. This indicates that a feedback control system is required to modulate either one or more of the control variables to remedy the errors and improve the overall VAV system response.

In this chapter, a feedback control strategy is used to improve the zone air temperature and relative humidity responses. The control strategy and its implementation will be given first, then transient response characteristics of the closed-loop VAV system will examined for unit step disturbances in space loads. Also tests will be conducted to study a typical daily operating performance of the VAV system.

5.2 The Control Strategy

The control strategy used in this study was designed in (Zaheer-uddin and Goh 1990) based on the methods presented in (Le et al. 1987, Zaheer-uddin 1989). The objective here is not the design of the control algorithms but rather their implementation on the VAV system and to examine the transient response of the VAV system under simulated load disturbances. For simplicity only three controllers were implemented in this study: namely, the settings for the coil face and bypass dampers (U_{fd}, $1-U_{fd}$), the control of input energy to the chiller (U_c), and supply air mass flow rate (U_m) as shown in Figure 5.1. The controller equations are given in the following.

5.2.1 Chiller Input Energy Controller (U_c)

The following control algorithm was used for regulating the input energy to the chiller.

$$U_c(t+1) = K_{c1}\,U_c(t) + K_{c2}\,G_c(t)\,[1 + T_w^* - T_w(t)] \qquad (5.1)$$

where K_{c1} and K_{c2} are constants, T_w^* is the optimal chilled water tank temperature and G_c is the dynamic gain factor, and T_w is the chilled water temperature in the storage tank. The optimal chilled water tank temperature T_w^* was defined as (Zaheeruddin 1989):

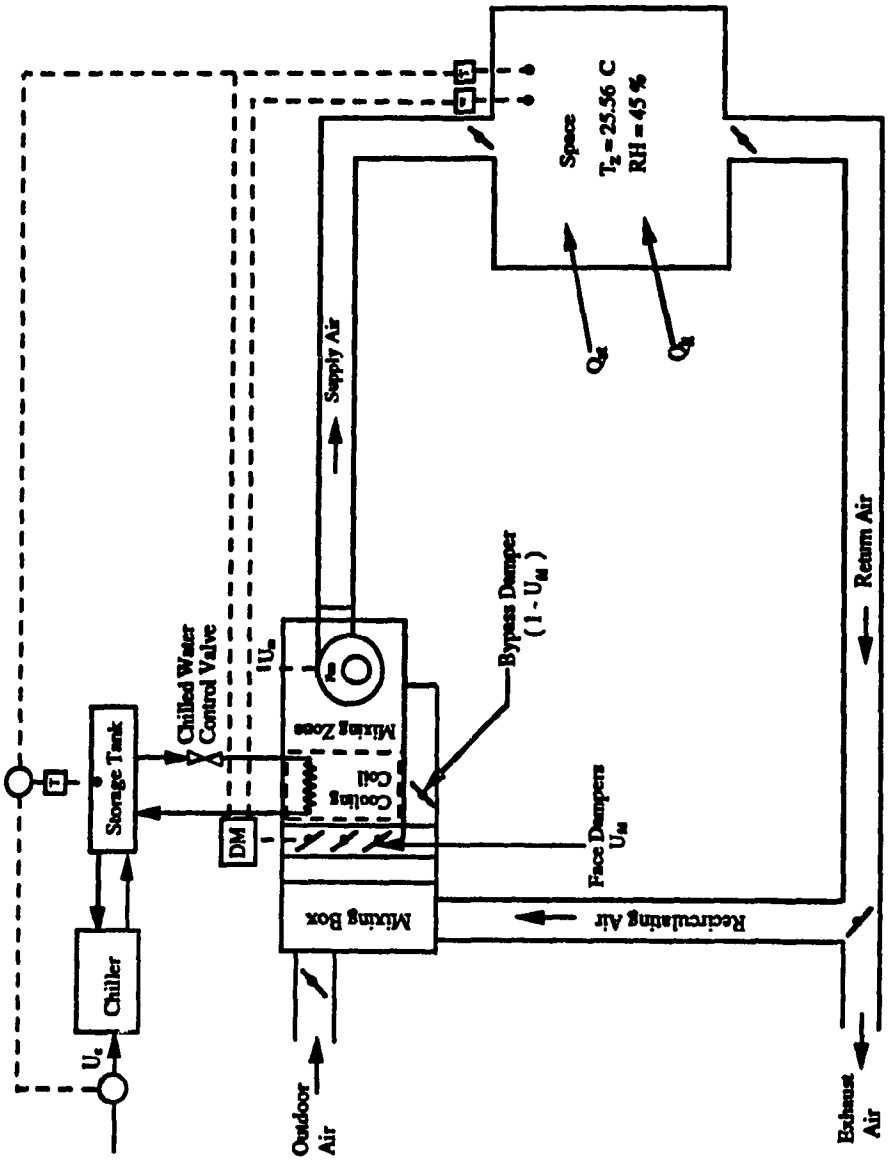

Figure 5.1 Variable air volume system with feedback control.

$$T_w^* = \begin{cases} T_{s,min} - \left(\frac{Q_{st}+Q_{lt}}{CWFR\, C_{p,w}}\right) & \text{if } T_{s,min} \le T_s \\ 5.5\,^{\circ}C\ (42\,^{\circ}F) & \text{if } T_s < T_{s,min} \end{cases}, \qquad (5.2)$$

and

$$G_c(t) = \frac{CWFR * C_{p,w}\eta_{ch}(T_{wr} - T_w(t)) + U_{ch}A_{ch}(T_{mr} - T_w(t))}{COP(t)\ U_{2,max}}. \qquad (5.3)$$

where

T_s	: supply air temperature, (°C or °F)
$T_{s,min}$	: minimum supply air temperature, (°C or °F)
T_{mr}	: sink air temperature, (°C or °F)
T_w	: chilled water temperature, (°C or °F)
T_{wr}	: return chilled water temperature, (°C or °F)
Q_{st}	: sensible space load, (kW or Btu/hr)
Q_{lt}	: latent space load, (kW or Btu/hr)
COP	: chiller's coefficient of performance
$U_{2,max}$	: chiller capacity, (kW or Btu/hr)
U_{ch}	: storage tank heat transfer coefficient, ($W/(m^2\ ^{\circ}C)$ or $Btu/(hr\ ft^2\ ^{\circ}F)$)
A_{ch}	: storage tank surface area, (m^2 or ft^2)
$C_{p,w}$	: specific heat of water, (kJ/kg°C or Btu/lb°F)
CWFR	: chilled water flow rate, (kg/s or lb/hr)

The equations for chilled water temperature (T_w) and the chiller coefficient of performance (COP) were defined in Equations (3.13) and (3.14).

Equation (5.1) is used to control the fraction of energy input to the chiller such that the temperature of chilled water T_w is made track the optimal chilled water temperature T_w^*. The lower bound of the optimal chilled water tank

temperature was set at 5.5°C (42°F). This is to avoid freeze-up in the chiller (according to ASHRAE System Handbook: Chapters 4 and 6, 1987). Generally, freezing occurs when the temperature falls to 0°C (32°F) but water can start freezing when the temperature falls below 4°C (39.5°F). For this reason, the chilled water tank temperature (T_w) was also set at 5.5°C (42°F) as its lower bound.

Normally, the supply air temperature for cooling is in the range of 10-11.6°C (50-53°F); thus, the minimum supply air temperature was set at 11°C (52°F). When the supply air temperature falls below 11°C, the optimal chilled water tank temperature was reset to 5.5°C.

5.2.2 Coil Face Damper Controller (U_{fd})

The zone relative humidity can be controlled by controlling the chilled water temperature and supply air conditions through bypass dampers. The following control algorithm for the coil face dampers position was used.

$$U_{fd}(t+1) = K_{f1}\, U_{fd}(t) + K_{f2}\, G_f(t)\, [1 + T_{wb,z} - T_{wb,z,set}] \qquad (5.4)$$

where K_{f1} and K_{f2} are constants, and G_f is the dynamic gain factor for the coil face damper controller and is given by

$$G_f(t) = \frac{M_a\, C_{p,a}\, (T_{a,in} - T_{a,out})}{CWFR\, C_{p,w}\, (T_{wr} - T_{w,in})} \qquad (5.5)$$

where

M_a : mass of air through coil, (kg/s or lb/hr)
$C_{p,a}$: specific heat of air, (kJ/(kg °C) or Btu/(lb °F))
$C_{p,w}$: specific heat of water, (kJ/(kg °C) or Btu/(lb °F))
$T_{a,in}$: air temperature entering coil, (°C or °F)
$T_{a,out}$: air temperature leaving coil, (°C or °F)
CWFR : chilled water flow rate, (kg/s or lb/hr)
T_{wr} : chilled water temperature leaving coil, (°C or °F)
$T_{w,in}$: chilled water temperature entering coil, (°C or °F)
$T_{wb,z}$: zone air wet bulb temperature, (°C or °F)
$T_{wb,z,set}$: zone air wet bulb temperature set, (°C or °F)

U_{fd} is used to position the face dampers. As shown in Equation (5.4) it positions the face dampers in order to minimize the error between the zone air wet bulb temperature and the setpoint wet bulb temperature ($T_{wb,z}-T_{wb,z,set}$). The range for U_{fd} is from 0 to 1. For example, when $U_{fd}=1$ it means that the face damper is fully opened and the bypass damper is fully closed and vice versa. The bypass damper position is given by $1-U_{fd}$.

5.2.3 Supply Air Mass Flow Rate Controller (U_m)

Similarly the following control algorithm for the supply air mass flow rate was used.

$$U_m(t+1) = K_{m1}\, U_m(t) + K_{m2}\, G_m(t)\, [1 + T_z - T_{z,set}] \qquad (5.6)$$

K_{m1} and K_{m2} are constants, and G_m is the dynamic gain factor which is given by

$$G_m(t) = \frac{Q_{st}+Q_{lt}}{M_{a,r}\,(h_z-h_s)} \tag{5.7}$$

and the rated air mass flow rate, $M_{a,r}$ is given by

$$M_{a,r} = \frac{Q_{st,r}+Q_{lt,r}}{h_{z,set}-h_{s,set}} \tag{5.8}$$

where

T_z	:	zone air temperature, (°C or °F)
$T_{z,set}$	:	zone air temperature set, (°C or °F)
$M_{a,r}$	:	rated air mass flow rate, (kg/s or lb/hr)
$Q_{st,r}$	:	peak sensible load, (kW or Btu/hr)
$Q_{lt,r}$	:	peak latent load, (kW or Btu/hr)

Ideally, a static pressure control system should be designed so that it can maintain the required static pressure in the duct via fan speed control mechanism. However, this was not attempted in this thesis. U_m gives the magnitude of supply air flow rates that should be maintained via fan speed control to reject the disturbance imposed by the cooling loads. The range of U_m was set between 0.3 to 1. This is due to the fact that ASHRAE/IES Standard 90.1A-1989 (section 9.5.2) prescribes a minimum supply rate during occupancy period at low load conditions as 30% of the peak (rated) supply air mass flow rate.

5.3 Implementation Methodology

In order to implement the control strategy given in section 5.2 (Equations 5.1, 5.4 and 5.6), first the space setpoint values necessary for thermal comfort in the built environment have to be selected and the optimal chilled water temperature (T_w^*) has to be calculated. The best source for selecting the preferred temperature and humidity level that are thermally acceptable to most of the occupants is the ASHRAE Comfort Standard 55-1981. These values are $T_{z,set}$=25.5°C with relative humidity level of 45%. The optimal chilled water tank temperature was computed according to Equation (5.2). Since the actual values of T_z, $T_{wb,z}$, and T_w are most likely to be off from the setpoint and/or desired optimal values, the control algorithm tries to reduce the error between T_z and $T_{z,set}$, $T_{wb,z}$ and $T_{wb,z,set}$, and T_w and T_w^*.

On the other hand in order to calculate T_z, $T_{wb,z}$, and T_w, the model equations described in Chapter 3 have to be solved.

5.4 Results And Discussion

Several simulation tests were carried out to study the time response characteristics of the controllers for a step change in total load on the zone. Also typical daily operating performance tests were conducted. The step disturbance tests,

will be presented in three stages. First, the VAV system response with air mass flow rate controller (U_m) in place will be given. In the second stage, the chiller input energy controller (U_c) will be added and the VAV system response with U_c and U_m will be studied. In the final stage all three controllers U_m, U_c, and U_{fd} will be implemented.

After the step disturbance tests, the performance of the VAV system for three typical days representing low to high values of sensible heat ratios will be investigated.

5.4.1 Implementation Of U_m Controller

Figures 5.2a, b and c show the unit step response obtained under the following conditions: i) a unit step change in total load on the zone was imposed, ii) the bypass control was set at $(1-U_{fd})=0.0$ which means all the air is passing through the coil, iii) the input energy to the chiller U_c was set at maximum (peak load T_w=8.2°C), and iv) the supply air flow rate was controlled through Equation (5.6). Under these conditions, how the single control action U_m was able to reject the disturbance created by a step change in total load is shown in the figures. It may be observed from Figure 5.2a that the zone air temperature changes rapidly at first (±0.6°C or ±1.1°F) and settles to near about the setpoint value in 20-25 minutes. The variation in mass flow rate is between 0.6-0.3

(a)

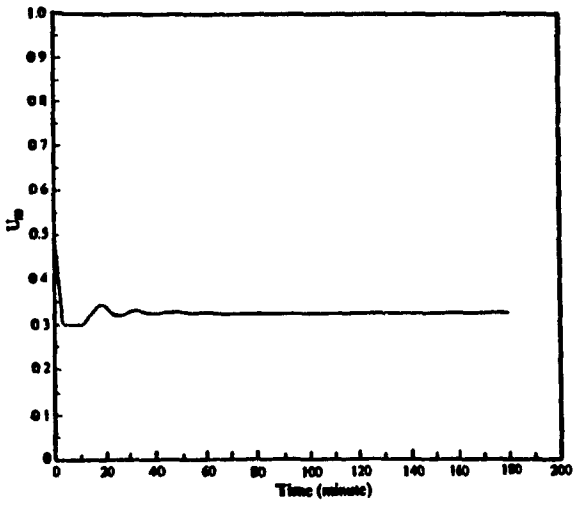

(b)

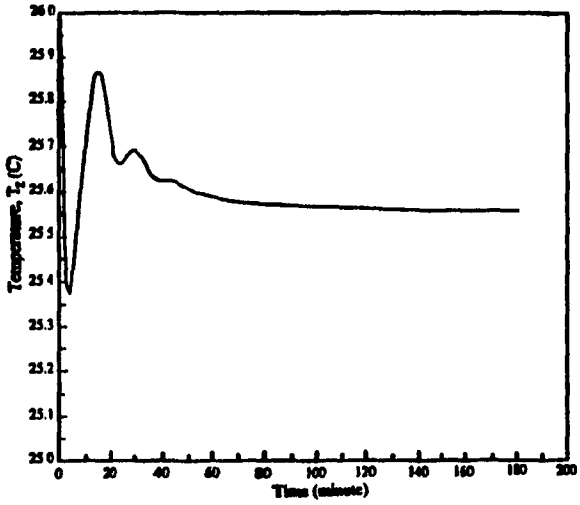

(c)

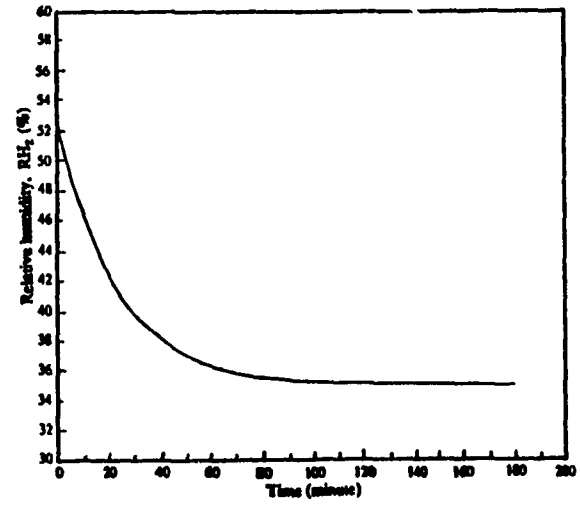

Figure 5.2a,b,c Closed-loop response with U_m
a) U_m response b) T_z response c) RH response

of the rated mass flow rate during the same time. At steady state U_m=0.32 and T_z is equal to $T_{z,set}$. It may be noted that the transient response characteristics of the system depend on the controller constants, K_{m1} and K_{m2}, and the dynamic gain factor in Equation 5.6. The constants chosen were 0.8 and 0.2 for K_{m1} and K_{m2} respectively. The relative humidity as shown in Figure 5.2c has settled to about 35% which is of course is less than the setpoint value. This is because of the fact that only one controller (U_m) is used in this case. Since the chilled water temperature used in the simulation was set at 8.2°C (46.8°F) which has the effect of dehumidifying the supply air and thus, the humidity level falls. Also note that, there is no face and bypass dampers to bypass the air as such good humidity control is difficult to achieve with only one controller in place.

5.4.2 Implementation Of U_m And U_c Controllers

It may be noted that the zone air temperature was maintained close to the setpoint value by controlling U_m. However, the relative humidity was still well below the desired setpoint value. This problem hopefully can be overcome by implementing the second controller (U_c) which can vary the chilled water temperature in response to the load on the system.

Figures 5.3a, b, c, d and e show the response of the VAV system to step change in total load when both controllers U_m and U_c are operating. The results shown in the figures have been obtained subject to the same conditions that were used in obtaining Figures 5.2a through 5.2c and in addition they also include the effect of controlling the input energy to the chiller (U_c) through Equation (5.1). The following values for K_{m1}=0.2, K_{m2}=0.8 and K_{c1}=K_{c2}=0.5 were found to give stable results. Figure 5.3a shows that the mass flow rate fluctuates rapidly at first and gradually settles at 0.35 following a step increase in total load. Figure 5.3b shows that the chiller input energy U_c fluctuates rapidly and gradually reaches to a steady state value of 0.33 in about 60 minutes. However, it has higher overshoot. This depends on the magnitude of the constants K_{c1} and K_{c2} in Equation (5.1). The chilled water temperature (T_w) response is shown in Figure 5.3c, and it can be noted that the chilled water temperature increases rapidly as U_c decreases (Figure 5.3b) and gradually settles to a value of 10°C (50°F). Initially, the chiller input energy (U_c) is decreasing, suggesting that the initial temperature of the chilled water in the storage tank is sufficiently low and that it can be used directly in the coil while operating the chiller at very low levels (Figure 5.3b). Figures 5.3d and e show the zone air temperature and relative

(a)

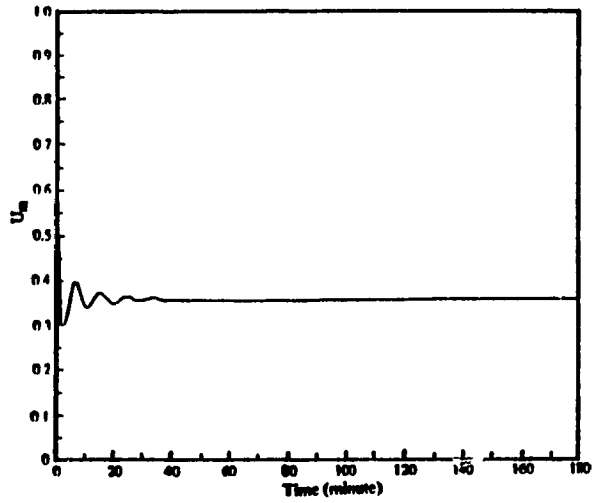

(b)

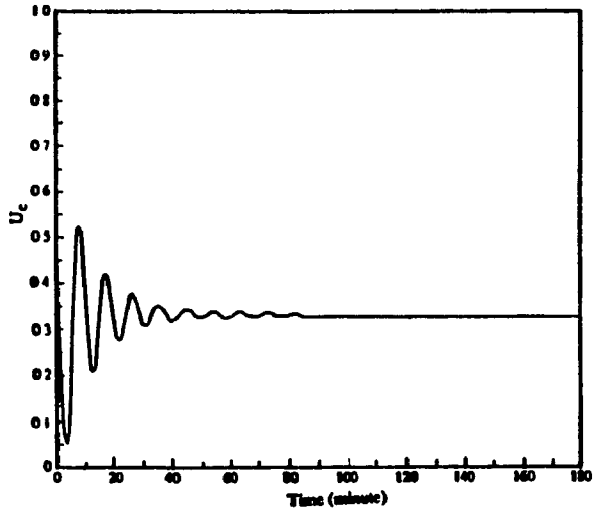

(c)

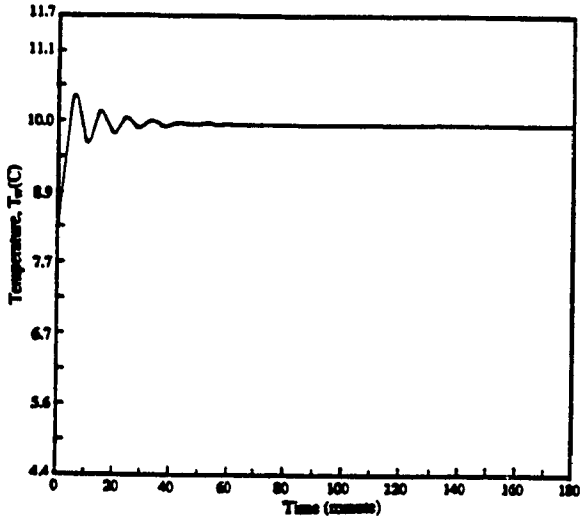

Figure 5.3a,b,c Closed-loop response with U_m and U_c
a) U_m response b) U_c response c) T_w response

(d)

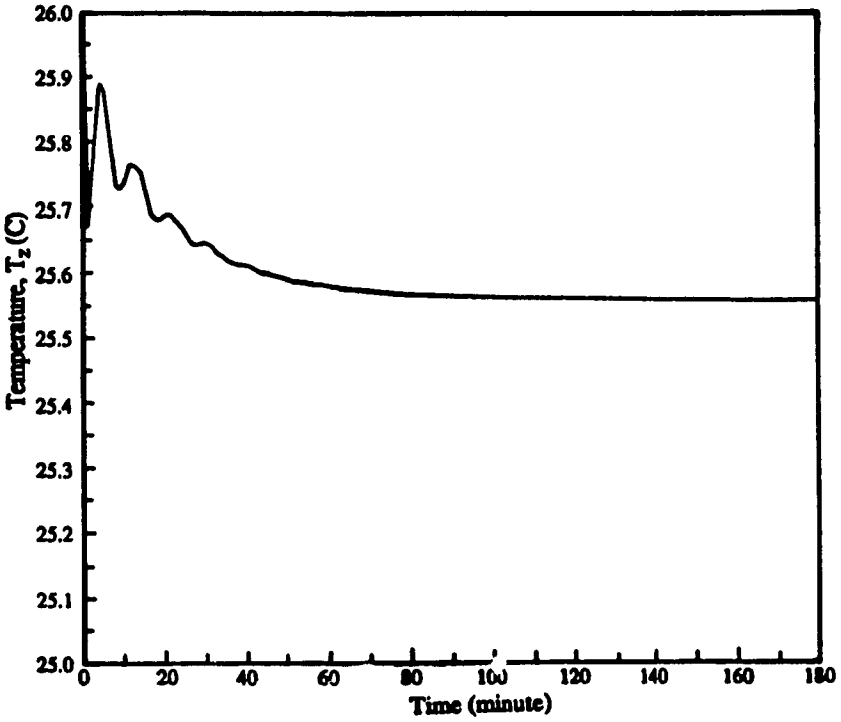

(e)

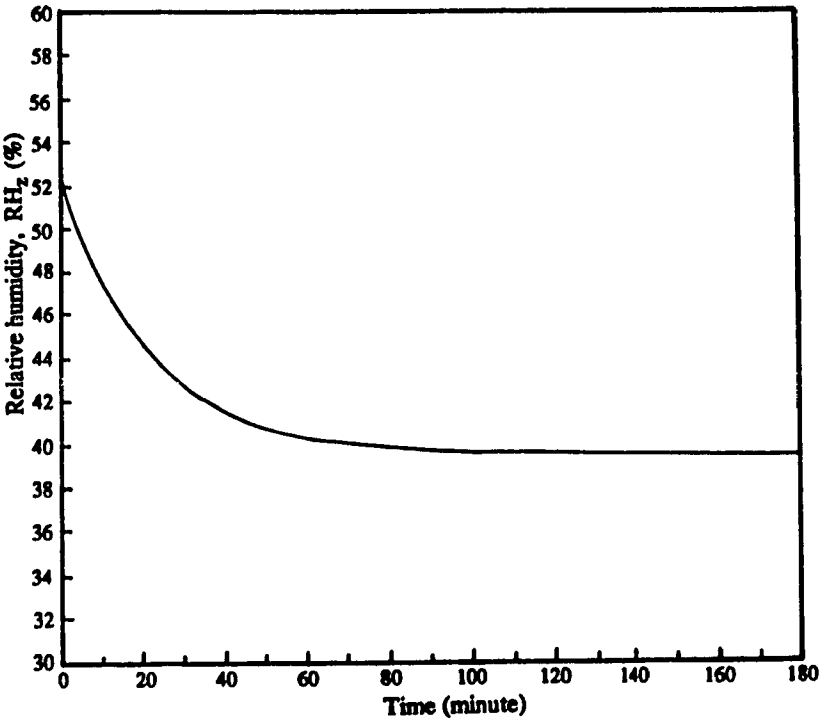

Figure 5.3d,e Closed-loop response with U_m and U_c
d) T_z response e) RH response

humidity response due to the step change. It may be noted from Figure 5.3d that the zone air temperature is brought close to the setpoint values in about 50 minutes. Also note that the peak overshoot in T_z is less than 0.5°C (1°F). With the two controllers operating together, the zone air relative humidity has reached to a final value of 41% (Figure 5.3e). This error compared to the setpoint value is about 9%. Although, the error is still somewhat large, it is nevertheless better than that shown in Figure 5.2c. The humidity response can be further improved by adding the face and bypass damper controller.

5.4.3 Implementation Of U_a, U_c And U_{fd} Controllers

With the implementation of the second controller (U_c) as in section 5.4.2, the zone air relative humidity improved considerably but still could not reach the setpoint value. The performance of the closed-loop system can be further improved by introducing the bypass control algorithm given by Equation (5.4) which can bypass fraction of return air (at high temperature and humidity ratio) which mixes with the leaving air from the coil (at low temperature and humidity ratio) to produce proper supply air conditions to meet the zone load.

The transient response of the system with controllers U_a, U_c and U_{fd} operating simultaneously is shown in Figures 5.4a, b, c, d, e, and f. In Figure 5.4a, we can see that the mass

(a)

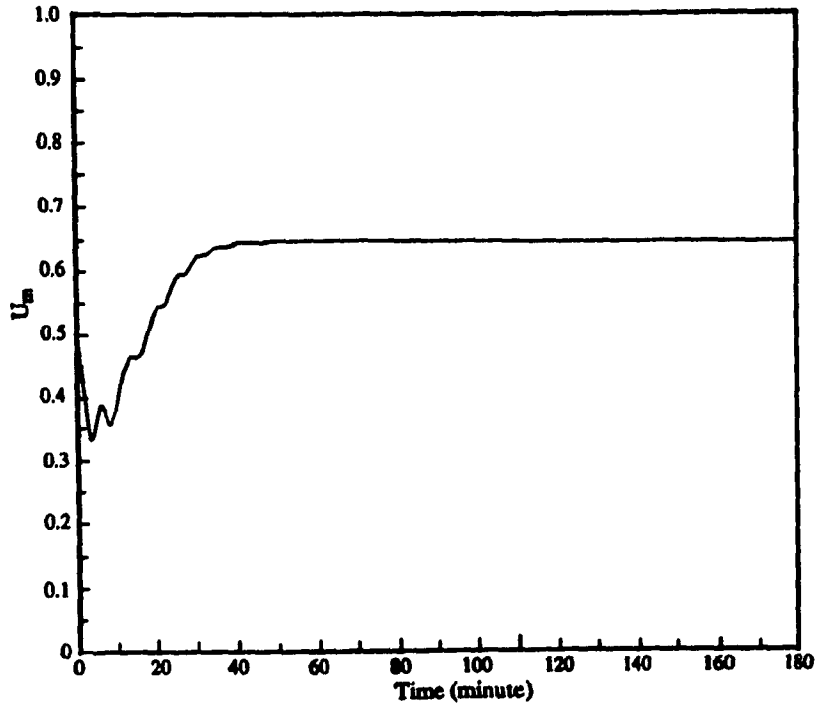

(b)

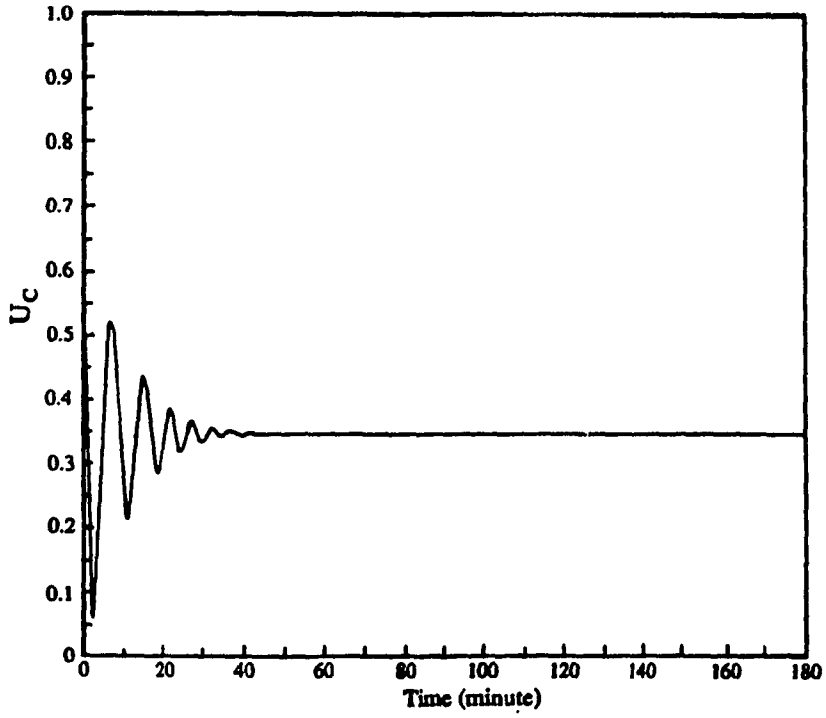

Figure 5.4a,b Closed-loop response with U_m, U_c and U_{fd}
a) U_m response b) U_c response

(c)

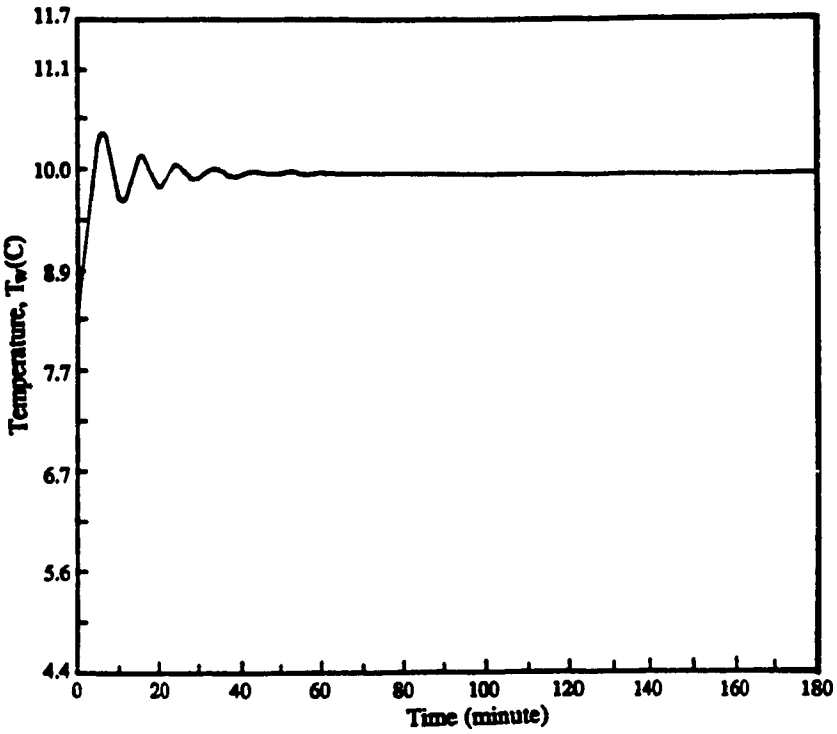

(d)

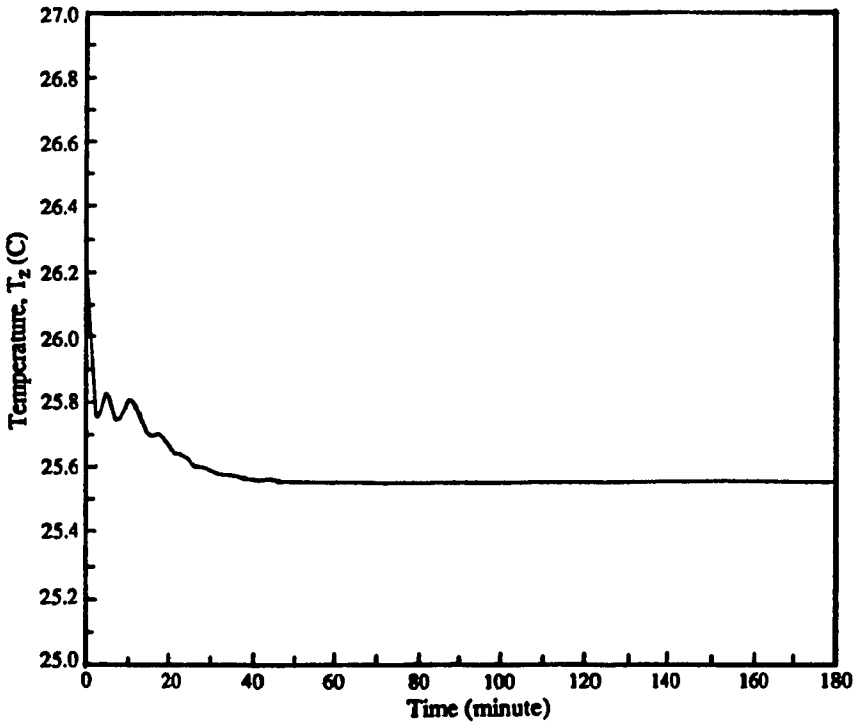

Figure 5.4c,d Closed-loop response with U_m, U_c and U_{fd}
c) T_w response d) T_z response

(e)

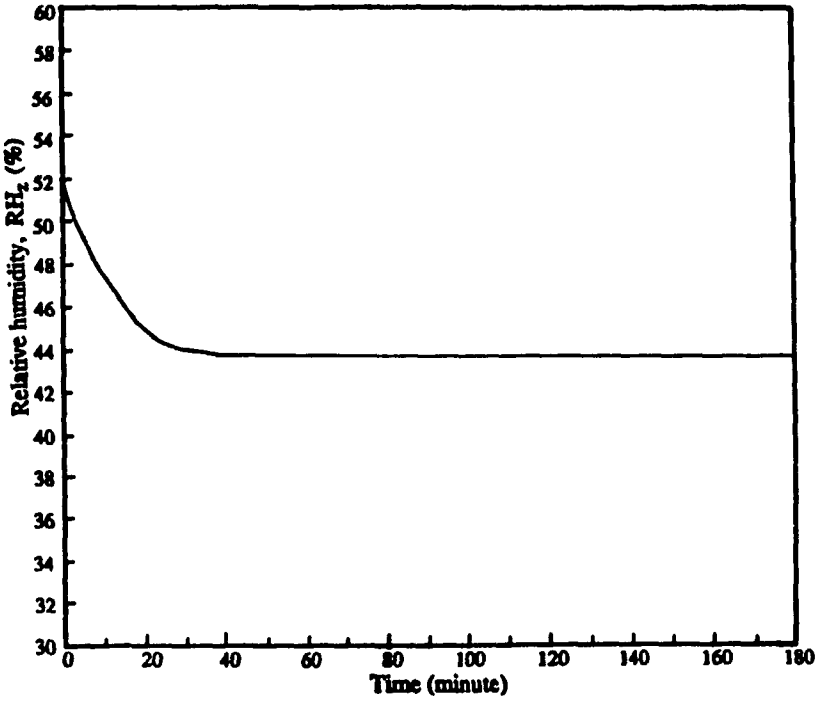

(f)

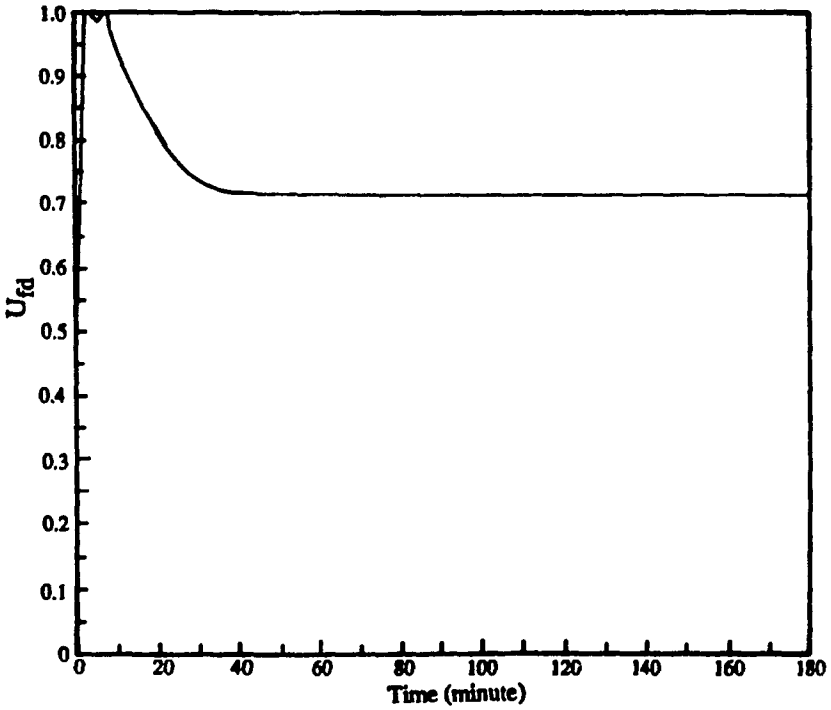

Figure 5.4e,f Closed-loop response with U_m, U_c and U_{fd}
e) RH response f) U_{fd} response

flow rate of air increases rapidly and then increase steadily to reach a final value of 0.63 (63% of rated mass flow rate). This increase in mass flow rate is because of the higher supply air temperature which is as a result of the mixing of bypass (return air with high temperature and humidity ratio) and leaving air from the coil to produce a suitable condition to meet the zone sensible and latent loads.

The chiller input energy consumption (U_c) remains the same as in the previous test (Figure 5.3b). It reaches to a final value of 0.35. Also T_w reaches to a steady state temperature of 10°C (50°F) and the response is shown in Figure 5.4c. The chilled water temperature rises slightly at first and then decreases to a value which is just sufficient to meet the load.

Figures 5.4d and e show the zone air temperature and relative humidity responses. It may be noted from the figures that the zone air temperature and relative humidity reach the setpoint values considerably faster than before. For example, the effect of adding the bypass control is to reduce the steady state time by about 10 minutes (compare Figures 5.3d and 5.4d). It may be noted that the addition of bypass control reduced the steady state error in relative humidity from 9% to about 1%. This was possible because of three simultaneous control actions (U_m, U_c and U_{fd}). Furthermore, it may be observed from Figure 5.4e that the bypass fraction is zero

during initial few minutes, then it starts to open when the zone air relative humidity is about 50% and gradually increases to about 30% at steady state. Whereas the result presented in Figure 5.3e was with no bypass. This explains the reason for the increase in relative humidity in Figure 5.4e (with bypass=0.3) compared to Figure 5.3e (bypass=0.0). The controller constants used in this simulation are listed in Table 5.1.

Thus, the combined action of U_m, U_c, and U_{fd} can significantly improve the VAV system performance. Note also that the control actions U_m, U_c, and U_{fd} are coupled in the sense the action of one influences the other through control algorithms given in Equations (5.1) to (5.6). The time response characteristic of the controllers indicates that the control strategy is able to respond to the changing loads quickly and efficiently.

Table 5.1 Controller constants used in the simulation.

Controller	Controller constant
Mass flow rate controller, U_m	K_{m1}=0.2, K_{m2}=0.8
Chiller energy input controller, U_c	K_{c1}=0.5, K_{c2}=0.5
Coil face damper controller, U_{fd}	K_{f1}=0.8, K_{f2}=0.2

5.5 Typical Daily Operating Performance Of The VAV System

In the following section, the combined response of U_a, U_c, and U_{fd} controllers to changing loads will be discussed. Three daily load profiles with different sensible heat ratios (SHR) will be used to study the VAV system performance with all three controllers operating simultaneously. The total load profile for this day is shown in Figure 5.5. Table 5.2 lists the sensible heat ratio for the three typical daily load profiles.

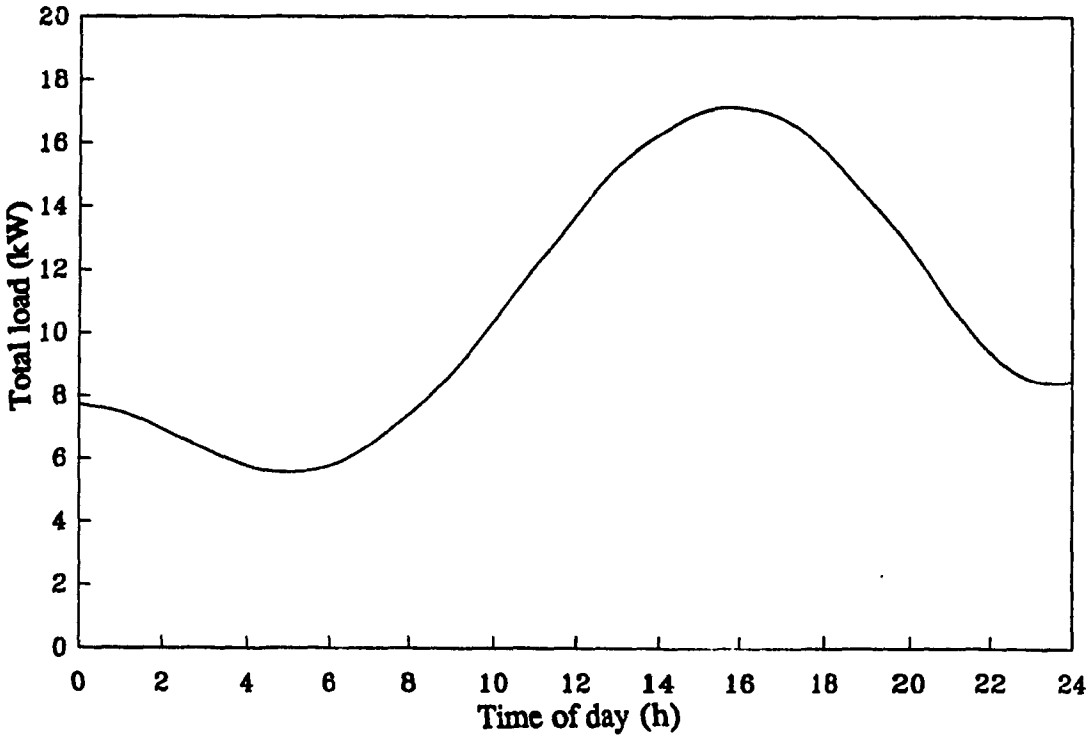

Figure 5.5 Typical daily total load profile.

Table 5.2 Sensible heat ratio for typical daily load profiles used in the simulation.

Time of day (h)	Sensible heat ratio (SHR)		
	Test 1	Test 2	Test 3
0 to 8:0	0.8	0.9	0.8
8:0 to 17:0			0.65
17:0 to 24:0			0.8

Figure 5.6 is the daily load profile with SHR=0.8. The combined response of U_m, U_c, and U_{fd} controllers operating simultaneously is shown in Figures 5.7a, b, c, d, e, and f. The first thing to note from Figure 5.7a is that the zone air temperature is maintained close to setpoint value throughout the 24 hours except for an initial overshoot. This is attributed to the fact that a sudden increase in load at time zero is likely to cause a large error. The zone air relative humidity is gradually varied and maintained close to setpoint value as shown in Figure 5.7b. In terms of absolute values the relative humidity variation during this time is about ±1.0% which is not unreasonable especially during peak hours with higher latent load. The mass flow rate control fraction is increased rapidly and maintained at about 65% of rated mass flow rate throughout the day (Figure 5.7c). Figure 5.7d shows the chiller input energy increases during the peak hours (9 to 18 h) which is consistent with the load. The chilled water

tank temperature should show the opposite trend of the chiller energy input, as the U_c increases T_w decreases, and this is shown in Figure 5.7e. The coil face damper opening fraction is shown in Figure 5.7f and it corresponds to the trend exhibited by the load. For example, at low load the coil face damper opening should be smaller (higher bypass) and vice versa.

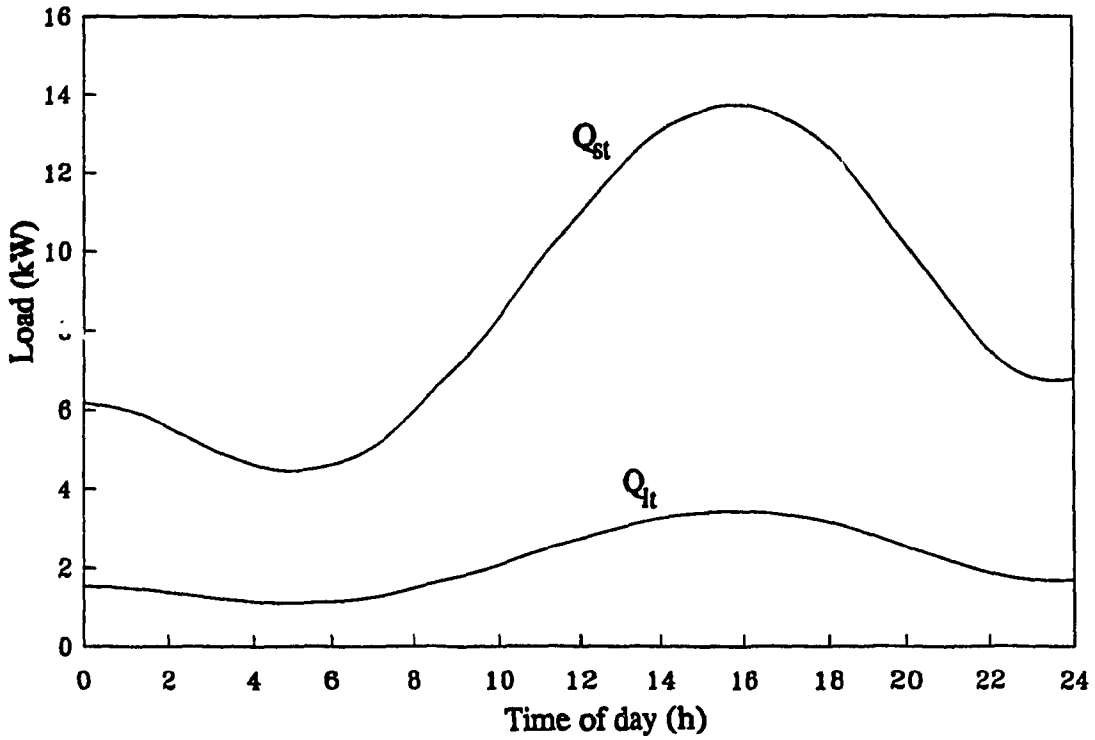

Figure 5.6 Load profile for the day with SHR=0.8

(a)

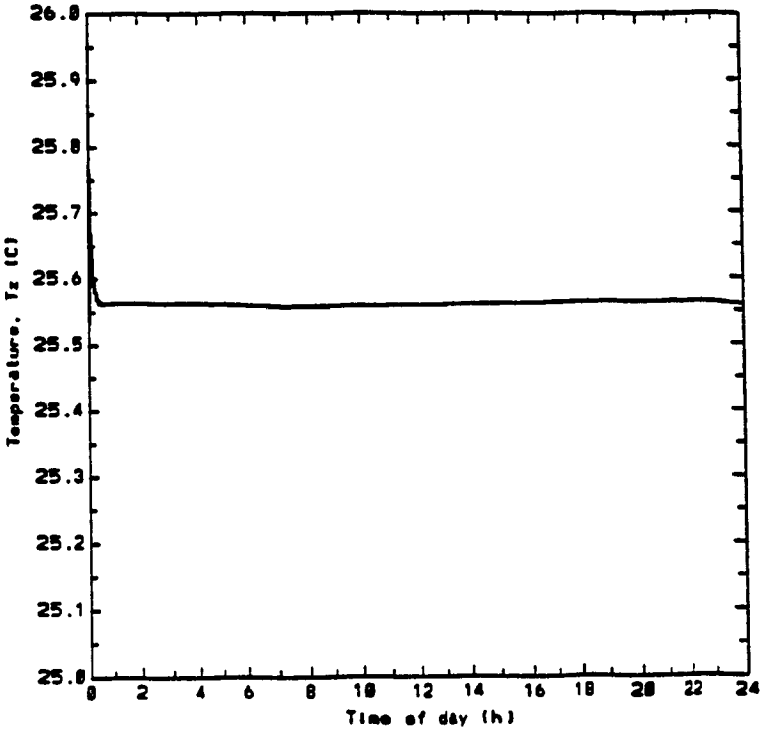

(b)

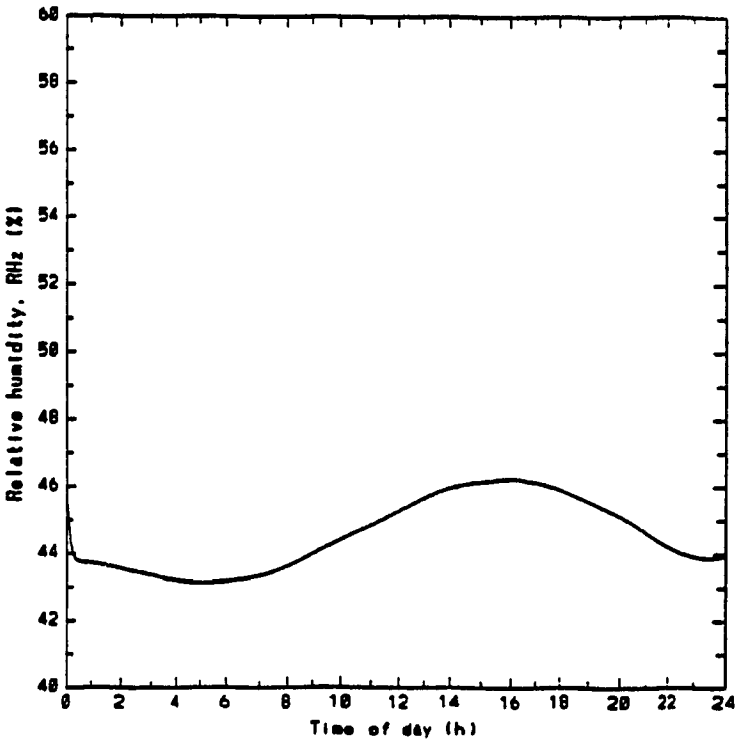

Figure 5.7a,b Closed-loop response for the day with SHR=0.8
a) T_z response b) RH response

(c)

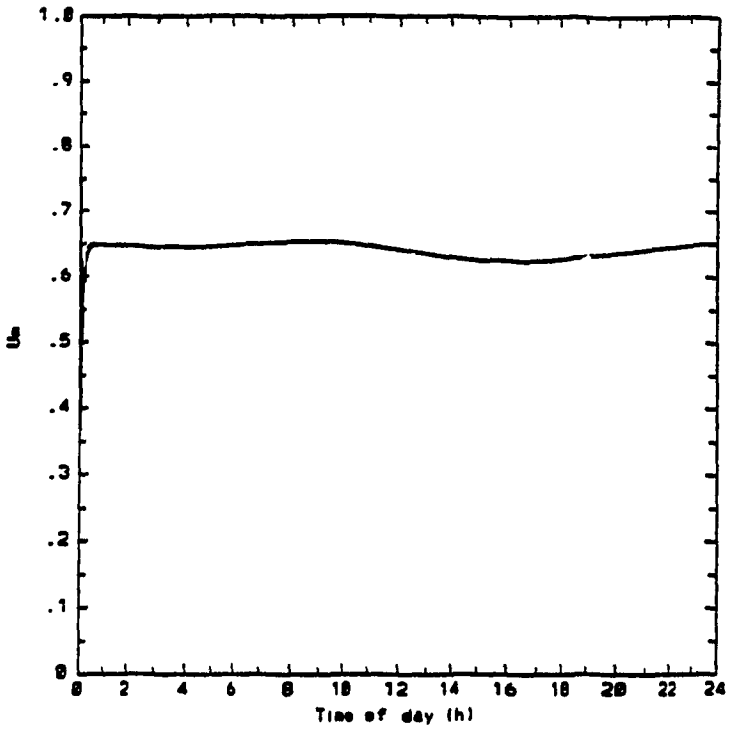

(d)

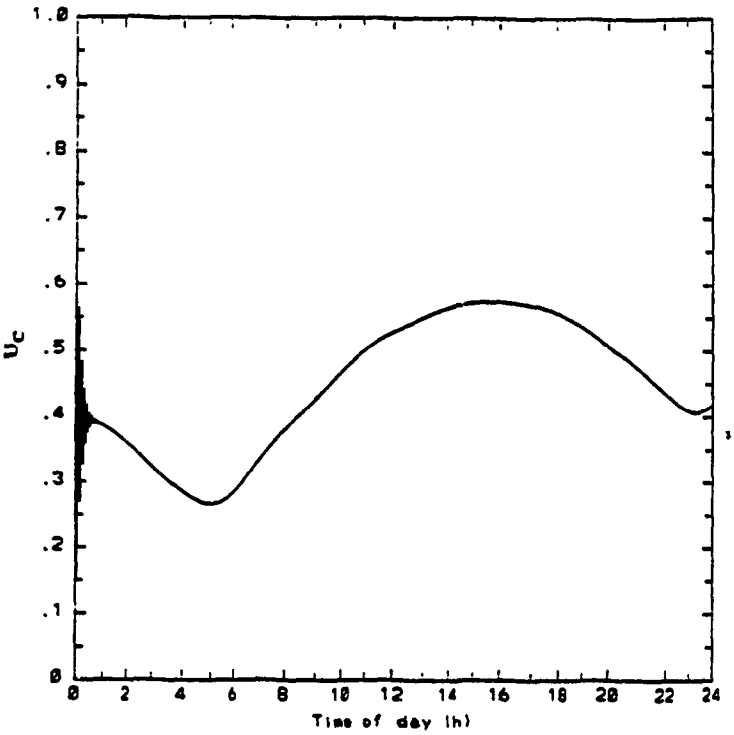

Figure 5.7c,d Closed-loop response for the day with SHR=0.8
c) U_m response d) U_c response

(e)

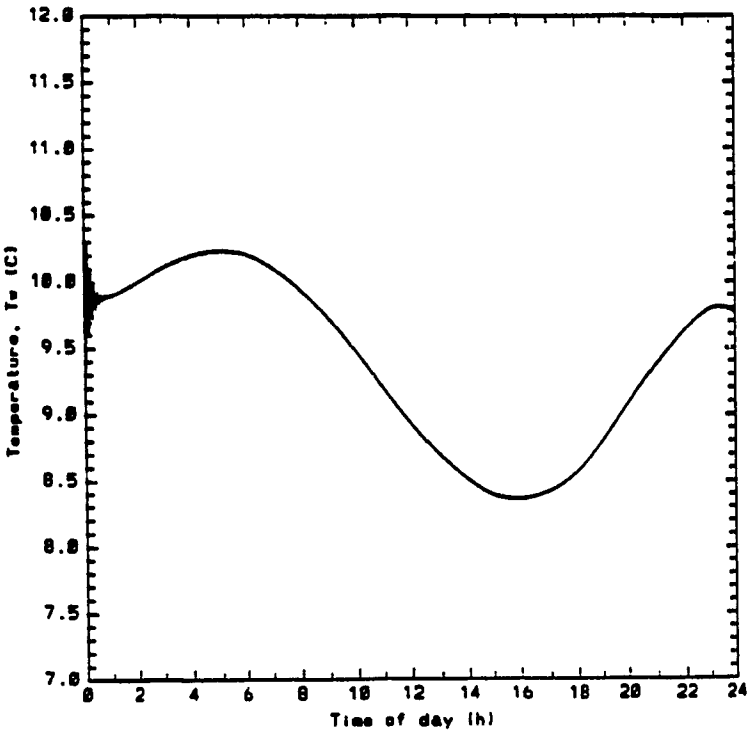

(f)

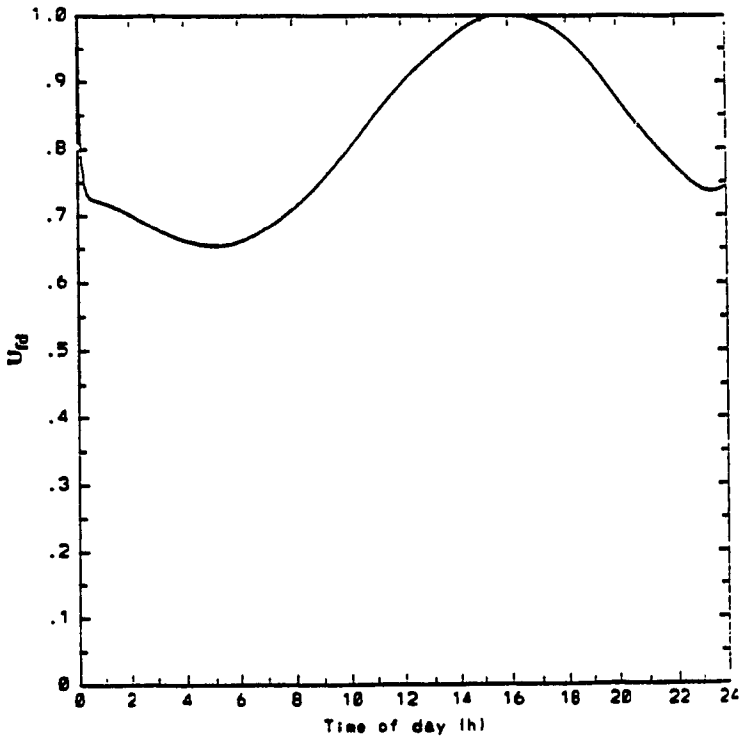

Figure 5.7e,f Closed-loop response for the day with SHR=0.8
e) T_w response f) U_{fd} response

Figures 5.9a to f show the daily operating performance of the VAV system for high sensible heat ratio (SHR=0.9) load profile. The load profile for this day is shown in Figure 5.8. It may be noted that the zone air temperature and relative humidity are maintained close to the setpoint values. Note that the zone air relative humidity is always below the setpoint value even though the bypass fraction is increased (Figure 5.9f). This can be attributed to the insensitivity of the bypass controller algorithm in which the wet bulb temperature difference is used. For example, a small change in zone air humidity ratio (ΔW_z=0.0005) may not cause a big difference in $T_{wb,z}-T_{wb,z,set}$.

On the other hand the mass flow rate fraction increases considerably and varies between 0.8 and 0.9 compared to previous value of 0.65 (Figure 5.7c). This is because of higher sensible load which causes a high air (dry bulb) temperature rise and hence higher air mass flow rate required to satisfy the high sensible load. This can be understood by examining Equation 5.6. For example, an increase in zone air temperature (T_z) caused by high sensible load resulted in large temperature difference between zone air temperature and the setpoint value ($T_z-T_{z,set}>0$) in Equation 5.6. This results an increase in mass flow rate fraction (U_m).

Figure 5.9d shows the chiller energy consumption profile which is consistent with the load profile. It shows that

chiller operates at higher capacity at peak hours and lower capacity at low loads. The chilled water tank temperature profile is shown in Figure 5.9e.

Figure 5.9f shows the coil face and bypass dampers position as a function of time. The figure indicates that the coil bypass damper opening increases as the sensible heat ratio increases. This is because of low latent loads in the zone. Under these circumstances, the bypass dampers open to allow more (humid) return air to bypass the coil to maintain proper humidity level in the zone.

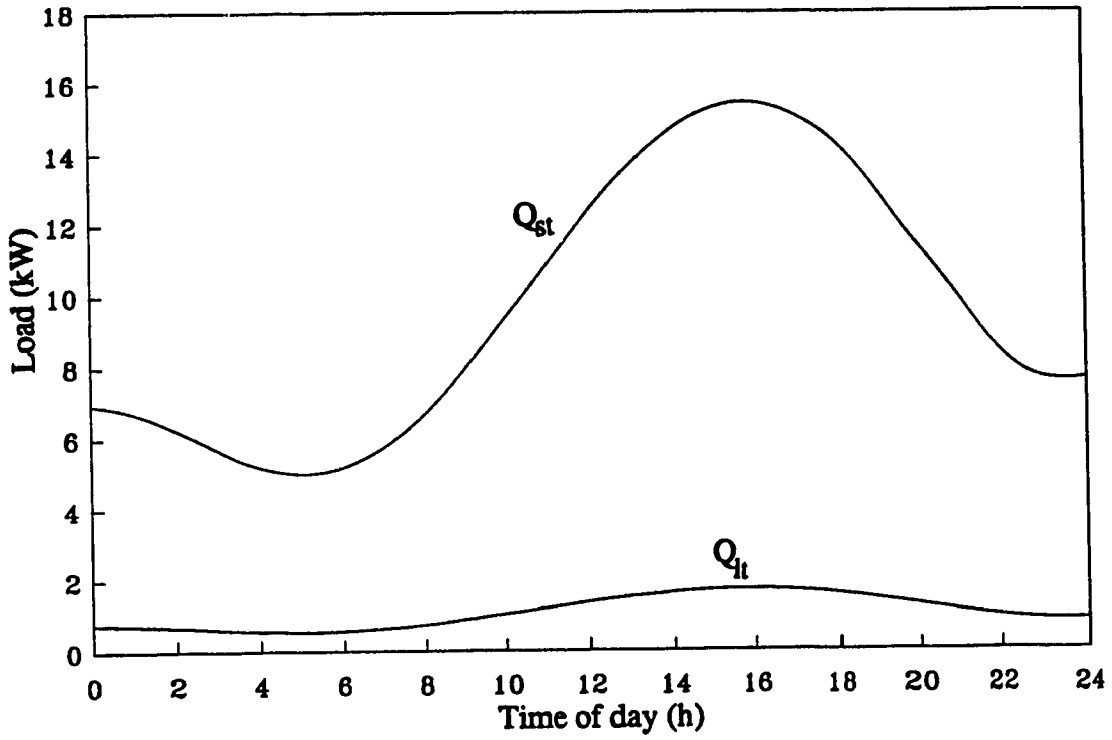

Figure 5.8 Load profile for the day with SHR=0.9

(a)

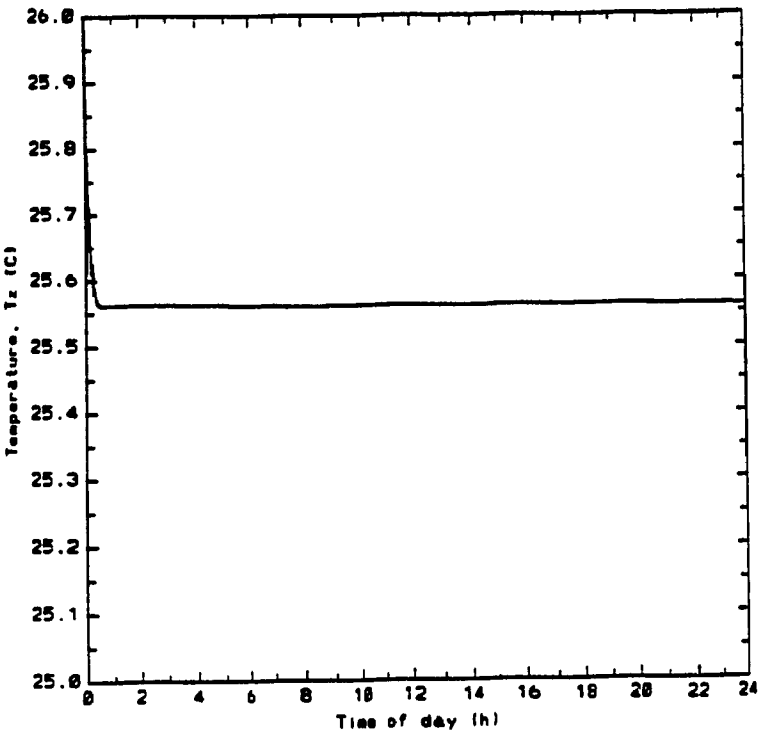

(b)

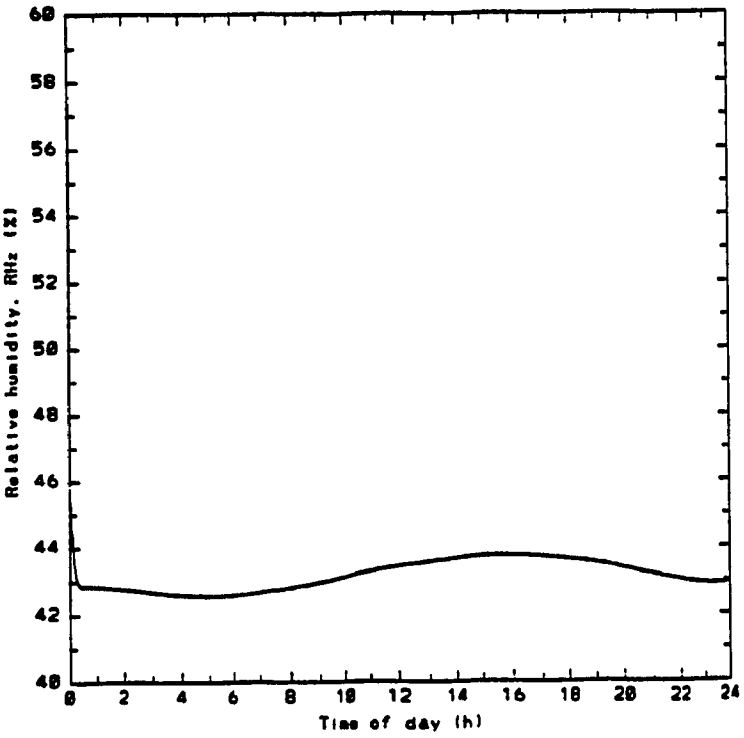

Figure 5.9a,b Closed-loop response for the day with SHR=0.9
a) T_z response b) RH response

(c)

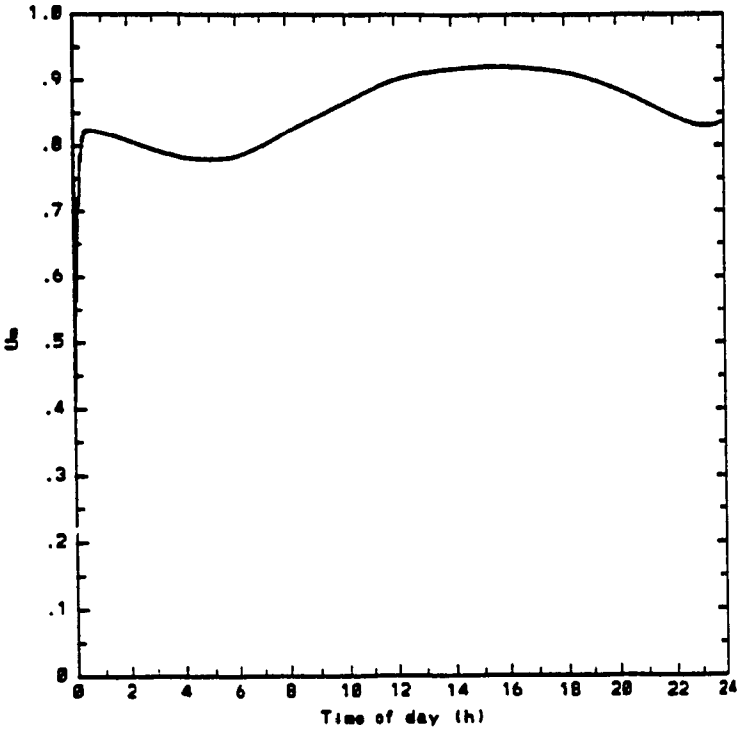

(d)

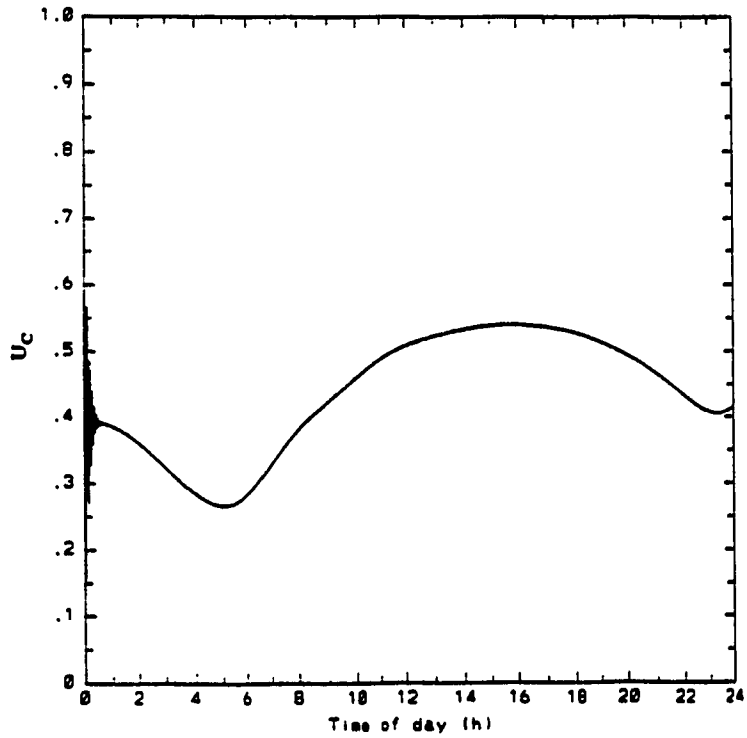

Figure 5.9c,d Closed-loop response for the day with SHR=0.9
c) U_m response d) U_c response

(e)

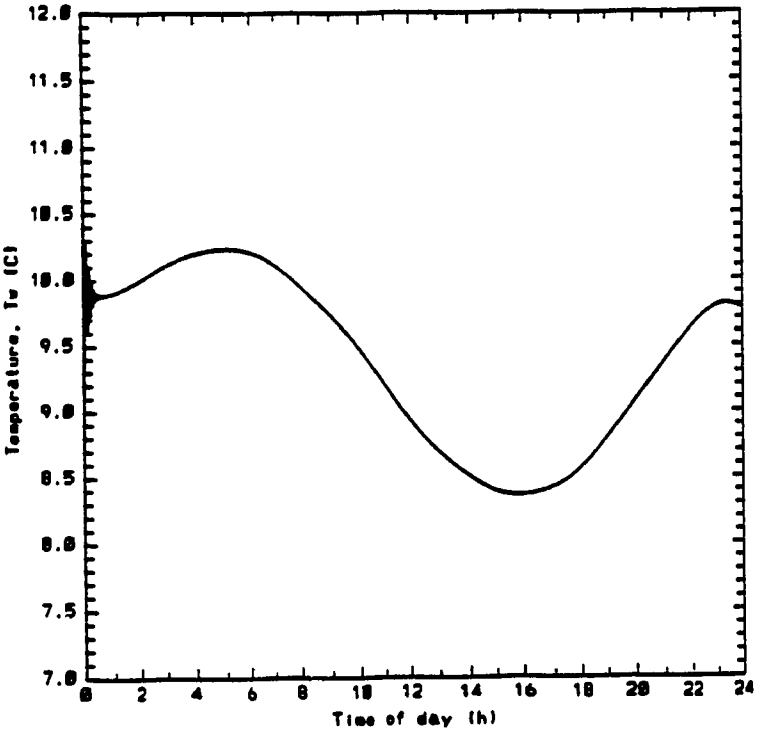

(f)

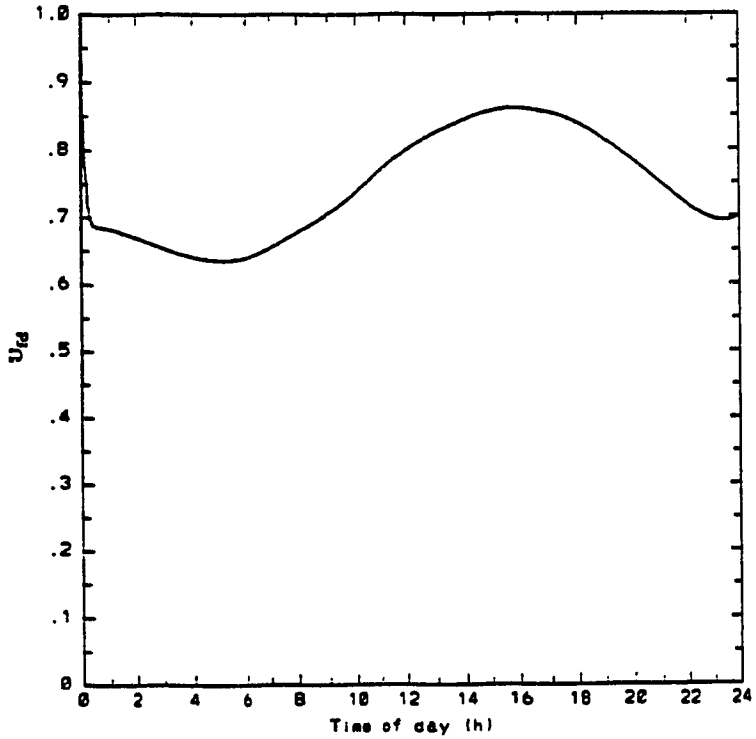

Figure 5.9e,f Closed-loop response for the day with SHR=0.9
e) T_w response f) U_{fd} response

The results for the third typical day are shown in Figures 5.11a, b, c, d, e, and f. The variable sensible heat ratio load profile for this day is shown in Figure 5.10. The results show that the zone air temperature is maintained close to the setpoint value inspite of changing sensible heat ratio (Figure 5.11a). However, the relative humidity is increasing especially during the peak hours (9 to 18 h) with high latent load (low SHR=0.65). Nevertheless it is still in the acceptable range set by ASHRAE Comfort Standard 55-1981 for summer cooling. U_m is maintained close to 50% of rated mass flow rate which is much less compared to previous two results during peak hours. The chiller input energy and chilled water temperature response are the same as before (Figures 5.11d and e) This is because U_c is function of total load. Since the total load profile is kept constant while changing the sensible or latent load fractions.

The coil face damper position profile is shown in Figure 5.11f. It can be noted that the bypass fraction is zero during the peak hours (11-19 h). This is because the warm and humid return air at low air mass flow rate must go through the coil in order to satisfy the space sensible and latent loads. Eventhough, there is no air bypassing the coil, the zone humidity level is still higher than the set point value as shown in Figure 5.11b.

The results suggest that the control algorithms through

their dynamic gain factor and feedback path are able to bring the zone air temperature and relative humidity close to the desired setpoint values. It must be pointed out here that the response of the controllers can be improved somewhat by fine tuning the parameters K_{mi}, K_{ci}, and K_{fi} in Equations (5.1), (5.4) and (5.6). However, care must be taken to avoid oscillatory response which is likely to occur during sudden changes in loads. It was found that when the load variation is gradual, a value of $K_{c1}=K_{c2}=0.5$ is satisfactory. It was also found that for rapidly changing loads, the magnitude of K_{c2} has to be reduced while that of K_{c1} has to be increased with $K_{c1}+K_{c2}=1.0$. The same guide lines may be followed for choosing values of K_{mi}, and K_{fi}.

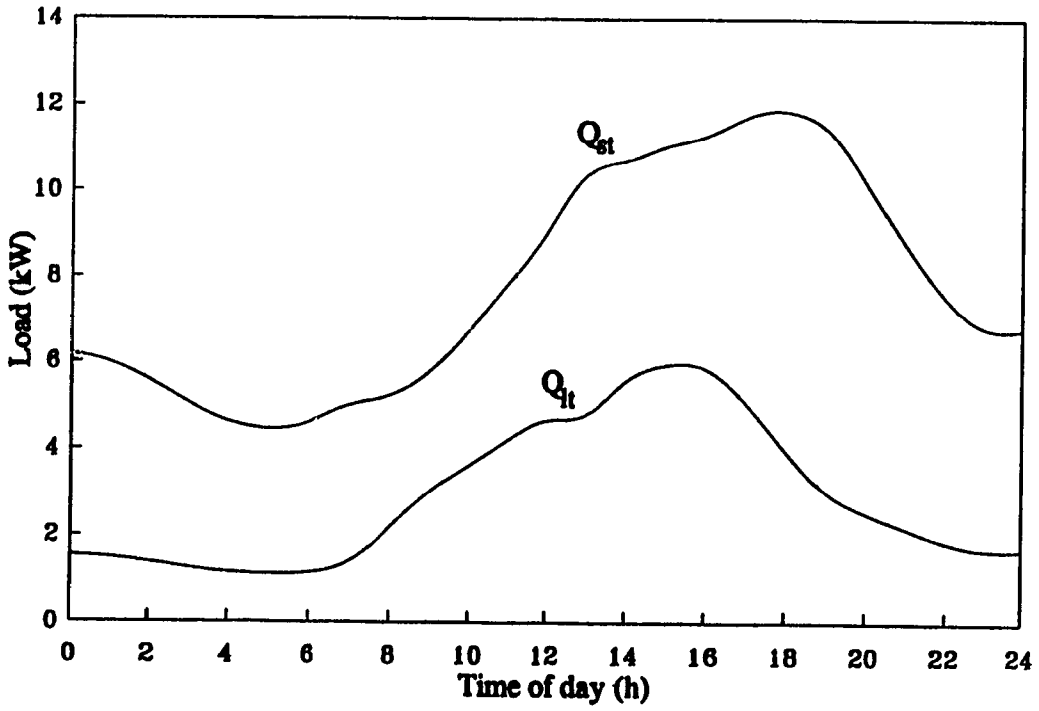

Figure 5.10 Load profile for the day with SHR=0.65

(a)

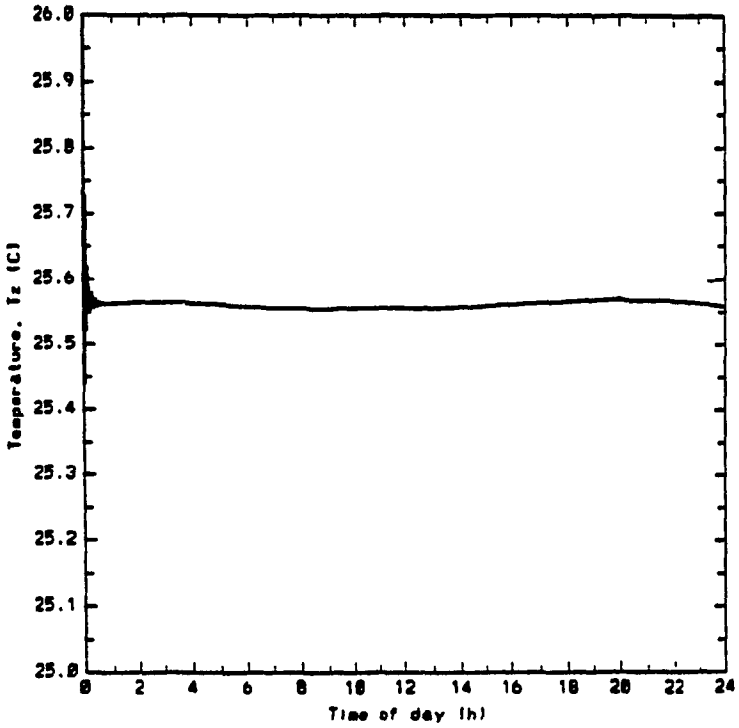

(b)

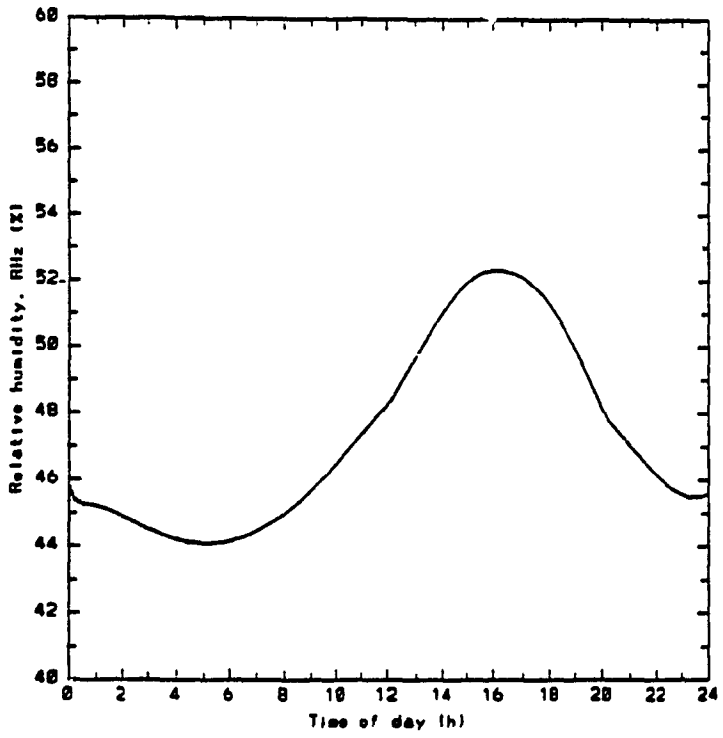

Figure 5.11a,b Closed-loop response for the day with SHR=0.65
a) T_z response b) RH response

(c)

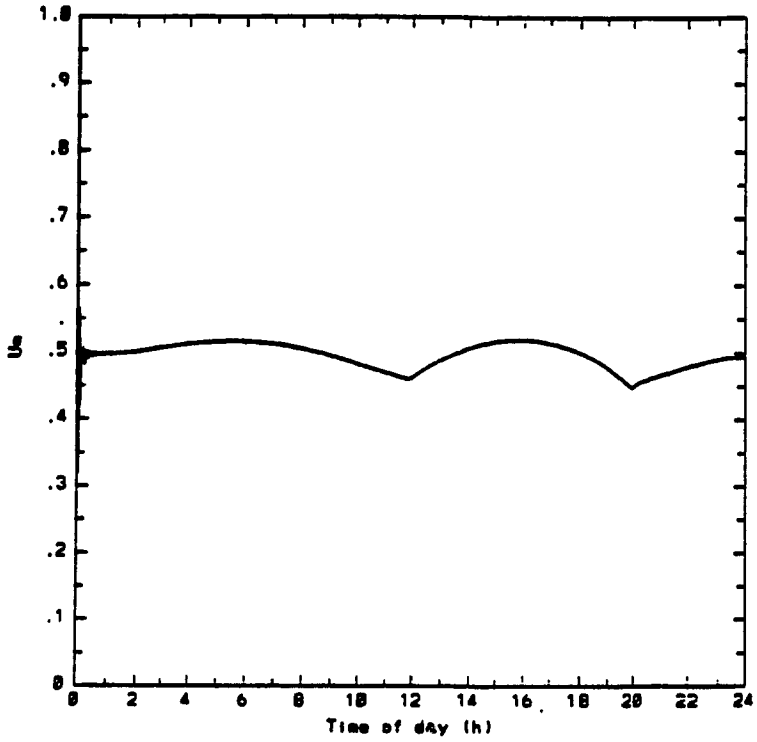

(d)

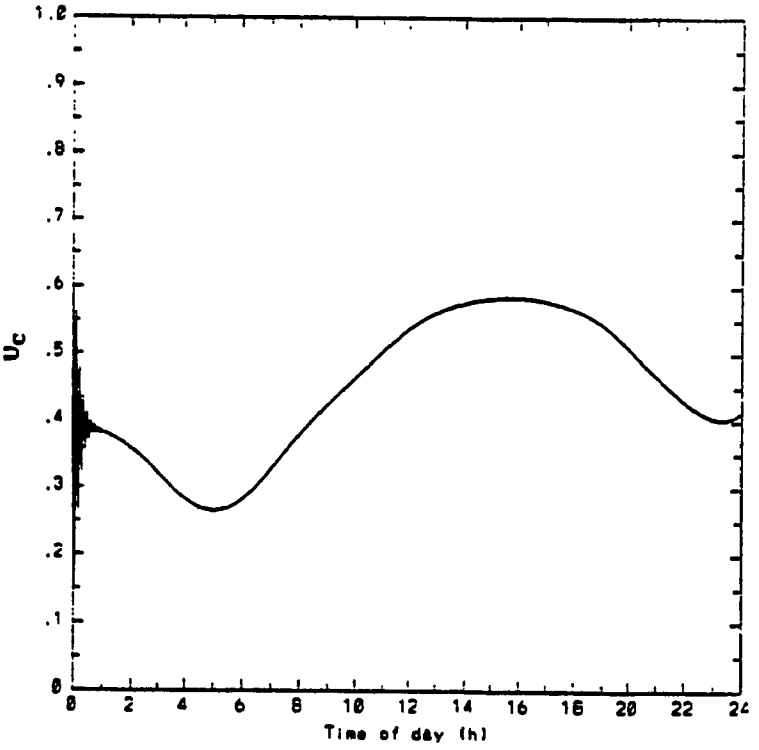

Figure 5.11c,d Closed-loop response for the day with SHR=0.65
c) U_m response d) U_c response

(e)

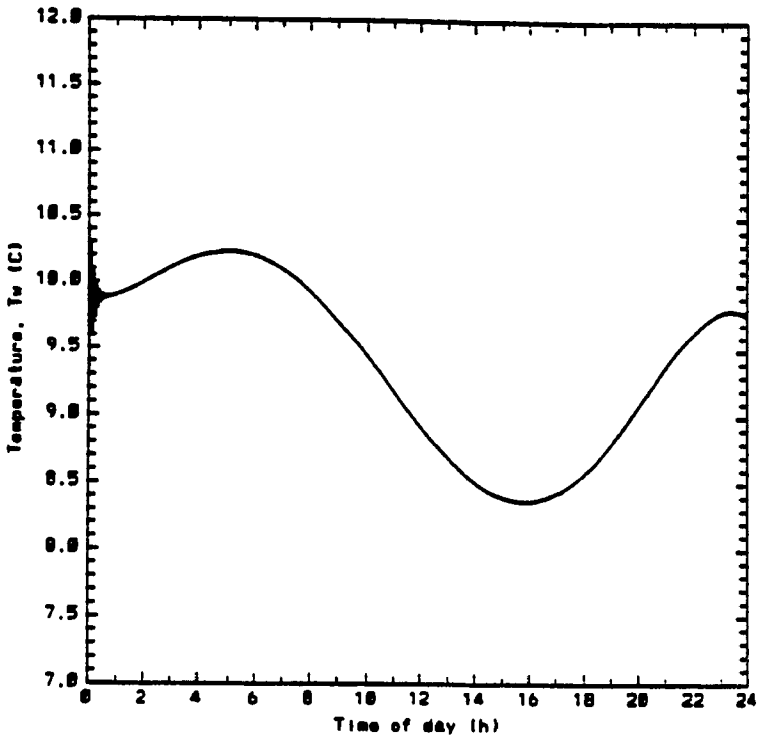

(f)

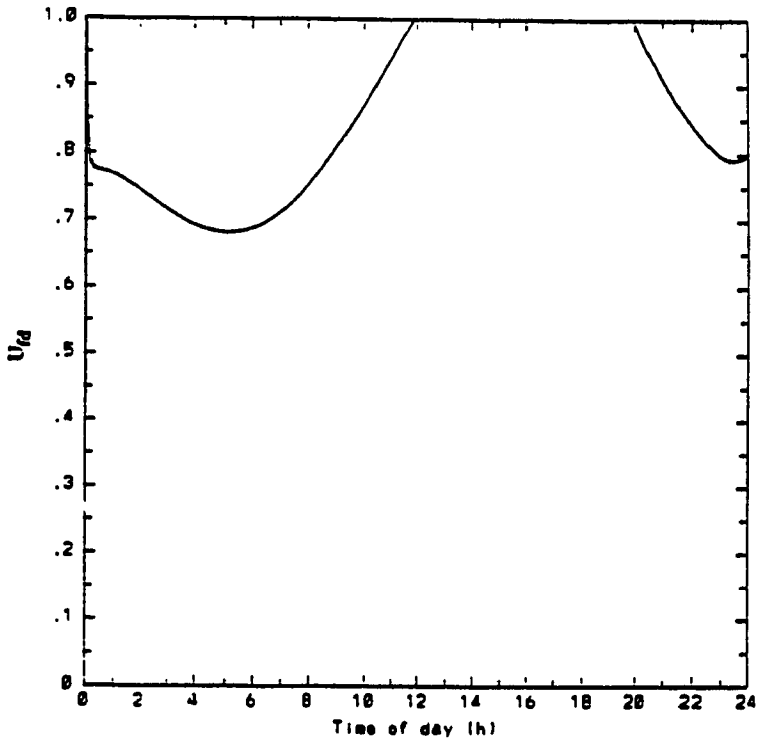

Figure 5.11e,f Closed-loop response for the day with SHR=0.65
e) T_w response f) U_{fd} response

CHAPTER 6

CONCLUSIONS AND RECOMMENDATIONS

6.1 Conclusions

The simulation of HVAC system components in Chapter 3 has demonstrated that each sub-system has its own operating characteristics. It became evident that the studies of individual components offer significant information and understanding about their performance and stability.

The major findings from the simulations of the sub-systems can be summarized as follows.

1. It was found that the steady-state time constant of the coil is approximately 45 to 55 seconds. The transient response was dominant in the first 15 seconds. It was also found that the leaving coil air conditions can be altered by regulating the chilled water temperature and/or it mass flow rate and also by varying the mass flow rate of air flowing through the coil.
2. The transient response of the duct depends on the rate of losses or gains from the surrounding and the capacitance effects offered by the duct material.
3. Also, the simulation results have shown that the time

constant of the occupied space is a function of the mass of air in the zone and the rate of heat losses/gain to the zone.

The computer models were combined to develop an overall VAV system model. The dynamic interactions between the components was studied. It was observed that:

1. The net effect of adding all sub-systems resulted in increase the time constant of the integrated system.
2. The time constant of the occupied space was dominant compared to other components' time constants, and
3. The steady state values of zone air temperature and relative humidity reached well below the setpoint values. The reason was that the temperature of the chilled water flowing in the coil was set at a constant value corresponding to the maximum peak load conditions. Furthermore, there was no feedback to take corrective action.
4. This indicated that a feedback control system is required to modulate either one or more of the control variables (U_m, U_2 and U_3) to remedy the error and improve the overall VAV system response.

The algorithms for controlling the mass flow rate of supply air, the position of bypass dampers and the input

energy to the chiller were implemented. The results from the closed-loop VAV model suggest that

1. The control algorithms through their dynamic gain factor and feedback path are able to bring the zone air temperature and relative humidity close to the desired setpoint values.
2. The time response characteristic of the controllers indicate that the control strategy is able to respond to the changing loads quickly and efficiently.
3. The maximum overshoot in zone air temperature was found to be 0.5°C (1°F) and the time required to reach steady state was found to be about 20 minutes.
4. The results also suggest that in order to control the zone relative humidity, the temperature of chilled water (via U_2 control), bypass damper setting (via U_3 control), and mass flow rate (via U_m control) have to be controlled simultaneously.

6.2 Recommendations

Numerous previous studies have focused attention on the stability of coil discharge air temperature and individual component dynamics. The examination of the dynamic interactions between HVAC system components as a whole has, however, received limited attention. These dynamic

interactions need to be further studied and exploited extensively. With good understanding the dynamic interactions it is possible to design improved control strategies for energy conservation and thermal comfort.

In order to improve the present study the following recommendations are made.

1. The work should be extended to multi-zones systems.
2. The simulation and control of static pressure in the duct has to be included in the overall model.
3. Transportation effect needs to be investigated.
4. To show the potential energy savings that can be obtained by implementing the control strategy it would be useful to carry out ecomomic analysis.
5. Experimental studies could be performed to validate the control strategy.

REFERENCES

AMCA Fan Application Manual, Air Movement and Control Association, Inc., 1985, p. 9.

ASHRAE, "1988 Equipment Handbook", Atlanta: American Society of Heating, Refrigerating and Air-Conditioning Engineers, pp. 3.1-3.14.

ASHRAE, "1977 Fundamentals Handbooks", American Society of Heating, Refrigerating and Air-Conditioning Engineers, NE., Atlanta, GA. 30329, Chapter 31.

ASHRAE, "1989 Fundamentals Handbooks", American Society of Heating, Refrigerating and Air-Conditioning Engineers, NE., Atlanta, GA. 30329, pp. 8.1-8.32.

ASHRAE Standard 55-1981, "Standard for Thermal Environmental Conditions for Human Occupancy", American Society of Heating, Refrigerating and Air-Conditioning Engineers, NE., Atlanta, GA. 30329.

ASHRAE, "1987 System Handbooks", American Society of Heating, Refrigerating and Air-Conditioning Engineers, NE., Atlanta, GA. 30329.

ASHRAE/IES Standard 90.1A-1989, "Energy Efficient Design of New Buildings Except Low-Rise Residential Buildings", American Society of Heating, Refrigerating and Air-Conditioning Engineers, NE., Atlanta, GA. 30329.

Athienitis, A.K., "A Predictive Control Algorithm for Massive Buildings", ASHRAE Transactions 1988, Vol. 94, Part 2, pp. 1050-1068.

Athienitis, A.K., Sullivan, H.F., and Hollands, K.G.T., "Passive Solar Simulation for Multizone Buildings: A Frequency Domain Approach", Proc. Solar Energy Society of Canada Conference, 1986, pp. 107-112.

"BESA: Building Energy Systems Analysis; Technical Reference", CandaPlan Group Inc., Ontario, Canada, 1987.

Beatty, K.O., Jr., and Katz, D.L., "Condensation of Vapours on Outside of Finned Tubes", Chem. Eng. Prog., January 1984, pp. 55-68.

REFERENCES

Blankenbaker J.E., " VAV Re-trofit", Heating/Piping/Air Conditioning, August 1982, pp. 75-81.

BLAST 3.0: Building Loads Analysis and System Thermodynamics Program, User Manual, Support Office, Dept. of Mechanical and Industrial Engineering, University of Illinois, Urbana-Champaign, Il, 1979.

Borresen, B.A., "Thermal Room Models for Control Analysis", ASHRAE Transactions 1981, Vol. 87, Part 2, pp. 251-260.

Brant, S.G., "Adaptive Control Implementation Issues", ASHRAE Transactions 1986, Vol. 92, Part 2B, pp. 211-219.

Braun, J.E., Mitchell, J.W., Klein, S.A., and Beckman, W.A., "Performance and Control Characteristics of a Large Cooling System", ASHRAE Transactions 1987, Vol. 93, Part 2, pp. 1830-1852.

Braun, J.E., Mitchell, J.W., Klein, S.A., and Beckman, W.A., "Models for Variable-Speed Centrifugal Chillers", ASHRAE Transactions 1987, Vol. 93, Part 2, pp. 1794-1813.

Brickman, H., "Understanding the Basics is Essential", ASHRAE Journal 1987, Vol. 29, No. 8, pp.28-30.

Briggs, D.E., and Young, E.H., "Convection Heat Transfer and Pressure Drop of Air Flowing Across Triangular Pitch Banks of Finned Tubes", Chemical Engineering Progress Symposium series-Heat Transfer 1963, Vol. 59, No. 41, pp. 1-10.

Brothers, P.W. and Warren, M.L., "Fan Energy use in Variable Air Volume Systems", ASHRAE Transactions 1986, Vol.92, Part 2B, pp. 19-29.

Cherchas, D.B., Abdelmessih, A., and Townsend, M., "A Direct Digital Control Algorithm for Control of a Single Environmental Space", ASME Transactions 1985, Vol. 107, December, pp. 324-331.

Cincinnati Fan and Ventilator Company, Inc., Cat. No. J489, Cincinnati, OH, 1989.

REFERENCES

Clark, D.R., "HVACSIM+ -- Building Systems and Equipment Simulation Program Reference Manual", National Information Service, NBSIR 84-2996, 1985.

Clark, D.R., Hurley, C.W. and Hill C.R., "Dynamic Models for HVAC System Component", ASHRAE Transactions 1985, Vol. 91, Part 1B, pp. 737-751.

Cooper, K.W., "Fan Controls for Variable Air Volume System", Borg-Warner Corporation, New York, Pennsylvania 17405, 1976.

DOE-2: Building Energy User Analysis Program, Engineering Manual, Version 2.1A, Laurence Berkley Laboratory, 1981.

Dusinberge, G.M., "Calculation of Transients in a Cross-Flow Heat Exchanger", ASME Journal of Heat Transfer, Vol. 81, No. 1, 1959, pp. 61-67.

Elmahdy, A.H., "Analytical and Experimental Multi-Row finned tube Heat Exchanger Performance During Cooling and Dehumidifying Processes", Ph. D. Thesis, Carleton University, Ottawa, Canada, Dec. 1975.

Elmahdy, A.H., and Mitalas, G.P., "FORTRAN IV program to Simulate Cooling and Dehumidifying Finned-Tube Multi-Row Heat Exchangers", Computer program No. 43, NRC Canada, 1977.

Fanger, P.O., "Conditions for Thermal Comfort", Thermal Comfort and Moderate Heat Stress: Proceedings of the CIB Commission W45, 13-15 September 1972, (London: Building Research Establishment, Her Majesty's Stationary Office, 1973), pp. 3-13.

Flanagan R.W., "Air Handling Equipment Design and Its Impact on Performance", ASHRAE Journal, Vol. 32, No. 3, 1990, pp. 53-59.

Gagge, A.P., Stolwijk, J.A.J., and Hardy, J.D., "Comfort Responses and Thermal Sensations and Associated Physiological Responses at Various Ambient Temperatures", Environmental Research 1967, Vol. 1, pp. 1-20.

REFERENCES

Gartner, J.R., "Simplified Dynamic Response Relation for Finned-Coil Heat Exchangers", ASHRAE Transactions 1972, Vol.78, Part 2, pp. 163-169.

Gartner, J.R., and Daane, L.E., "Dynamic Response Relations for a Serpentine Crossflow Heat Exchanger with Water Velocity Disturbance", ASHRAE Transactions 1969, Vol. 75, Part 1, pp. 53-68.

Gartner, J.R., and Harrison, H.L., " Dynamic Characteristics of Water-to-Air Cross-flow Heat Exchangers", ASHRAE Transactions 1965, Vol. 71, pp. 212-224.

Gartner, J. R., and Harrison, H. L., "Frequency Response Transfer Functions for a Tube in Crossflow", ASHRAE Transactions 1963, Vol. 69, pp. 320-330.

Geake L.W., "Controls for Single-Duct Variable Air Volume Terminal Units", ASHRAE Transactions 1980, Vol. 86, Part 2, pp. 825-838.

Grot, R.A., and Harrje D.T., "The Transient Performance of a Forced Warm Air Duct System", ASHRAE Transactions 1981, Vol. 87, Part 1, pp. 795-804.

Gupta, V.K., "Despite Popularity Problems Do Exist", ASHRAE Journal 1987, Vol. 29, No. 8, pp. 22-24.

Guntermann, W.E., "VAV System Enhancements", Heating, Piping and Air-Conditioning, August 1986, pp. 67-78.

Haines, R.W., "HVAC Systems Design Handbook", TAB Books Inc., 1988, Blue Ridge Summit, PA, pp. 229-248.

Hamilton D.C., Leonard R.G., and Pearson T.J., "Dynamic Response Characteristics of Discharge Air Temperature Control System at Near Full and Part Heating Load", ASHRAE Transactions 1974, Vol. 80, Part 2, pp. 180-194.

Harriott, P., "Process Control", McGraw-Hill, 1964, Chapter II.

REFERENCES

Harrje, D.T., "Retrofitting: Plan Action and Early Results Using the Temperatures at Twin Rivers", Princeton University, Center for Energy and Environmental Studies Report No. 29, June 1976.

Harrje, D.T., Socolow, R.H., and Sonderegger, R.C., "Residential Energy Conservation-The Twin Rivers Project", ASHRAE Transactions 1977, Vol. 83, Part 1, pp. 458-477.

Hay, J.E., "A Revised Method for Determining the Direct and Diffuse Components of the Total Short Wave Radiation", Atmosphere, Vol. 14, 1976.

Healthy Building Manual: "System, Parameters, Problems and Solutions", Ontario, Canada, 1987.

Hise, E.C., and Holman, A.S., "Heat Balance and Efficiency Measurements of Central, Forced-Air, Residential Gas Furnaces", ASHRAE Transactions 1977, Vol. 83, Part 1, pp. 865-880.

Howell, R.H., "Variation in Relative Humidity in a Conditioned Space due to Coil Bypass Control Systems", ASHRAE Transactions 1986, Vol. 92, Part 1B, pp. 499-508.

HVACSIM+: Building Systems and Equipment simulation Program Reference Manual, U.S. Department of Commerce, National Technical Information Service, 1985.

IAQU: "Indoor Air Quality Update", Cuttle Information Corp., Vol.3, No. 6, 1990, pp. 1-7.

Int-Hout III, D., "A Move Toward Digital Controls", ASHRAE Journal 1987, Vol. 29, No. 8, pp. 24-25.

Jackson, W.L., Chen, F.C., and Hwang, B.C., "The Simulation and Performance of a Centrifugal Chiller", ASHRAE Transactions 1987, Vol 93, Part 2, pp. 1751-1767.

Johnson, G.A., "Optimization Techniques for a Centrifugal Chiller Plant Using a Programmable Controller", ASHRAE Transactions 1985, Vol. 91, Part 2B, pp. 835-847.

REFERENCES

Kays, M.W., "Loss Coefficients for Abrupt Change in Flow Cross Section with Low Reynolds Number Flow in Multiple Tube Systems", Heat Transfer and Fluid Mechanics Institute Transactions, ASME, 1949.

Kays, W.M., and London, A.L., "Compact Heat Exchangers", McGraw-Hill Book Co., Inc., New York, N. Y., 1964.

Kays, M.W., and London, A.L., "Heat Transfer and Flow Friction Characteristics of some Compact Heat Exchanger, Part 1, Test System Procedure", ASME Transactions 1950, Vol. 72, p. 1075.

Kirshenbaum, M., "Variable Flow Chilled Water Systems", ASHRAE Journal, August 1987, pp. 32-36.

Knudsen, H.N., and Fanger, P.O., "The Impact of Temperature Step-Change on Thermal Comfort",

Kuo, B.C., "Automatic Control Systems", 5th. Ed., 1987, Prentice-Hall, Inc., Englewood Cliffs, NJ.

Kusuda, T., "Algorithms for Psychometric Calculations, NBS Report 9818, U.S. Department of Commerce, NBS, Washington DC., March 1969.

Le, H., Zaheer-uddin, M., Gourishankar, V., and Rink, R., "Near-Optimal Control of a Bilinear Solar-Assisted Heat Pump System", ASME Journal of Solar Energy Engineering, Vol. 109, pp.259-266, 1987.

Liu, B.Y.H., and Jordan, R.C., "The Interrelationship and Characteristic Distribution of Direct, Diffuse and Total Radiation", Solar Energy, Vol. 4, 1960.

Ljung, L., and Soderstrom, T., "Theory and Practice of Recursive Identification", Cambridge MA: MIT Press, 1983.

London, A.L., Kays, M.W., and Johson, "Heat Transfer and Flow Friction Characteristics of some Compact Heat Exchanger Surfaces, Part 3 Design Data for Five Surfaces", ASME Transactions 1952, Vol. 74, p. 1167.

Lujan P., "Variable Air Volume: Where are We?", ASHRAE Transactions, 1977, Part 1, Vol. 83, pp. 581 - 584.

REFERENCES

Maxwell, G.M., Shapiro, H.N., and Westra, D.G., "Dynamics and Control of a Chilled Water Coil", ASHRAE Transactions 1989, Vol. 95, Part 1, pp. 1243-1255.

Mayer, E., "Physical Causes for Draft: Some New Findings", ASHRAE Transactions 1987, Vol. 93, Part 1, pp. 540-548.

McClive, J.R., "Fan Selection and Performance", ASHRAE Transactions 1974, Part 1, Vol. 80, pp. 491-498.

McCullagh, K.R., Green, G.H., and Chandrasekar, S., "An Analysis of Chill Water Cooling Dehumidifying Coils Using Dynamic Relations", ASHRAE Transactions 1969, Vol. 75, Part 2, pp. 200-209.

McQuiston, F.C., "Correlation of Heat, Mass and Momentum Transport Coefficients for Plate-Fin-Tube Heat Transfer Surfaces with Staggered Tubes", ASHRAE Transactions 1978, Vol. 84, Part 1, pp. 294-309

McQuiston, F.C. and Parker, J.D., "Heating Ventilating and Air-Conditioning", John Wiley & Sons Inc., 3ed., 1988.

Metha D.P., "Dynamic Performance of PI Controllers: Experimental Validation", ASHRAE Transactions 1987, Vol. 93, Part 1B, pp. 1775-1793.

Metha, D.P., "Dynamic Thermal Responses of Buildings and Systems", dissertation Iowa State University, 1980.

Metha, D.P., Woods, J.E., "An Experimental Validation of a Rational Model for Dynamic Responses of Buildings", ASHRAE Transactions 1980, Vol. 86, Part 2, pp. 497-520.

Miller, D.E., "A Simulation to Study HVAC Process Dynamics", ASHRAE Transactions 1982, Vol. 88, Part 2, pp. 809-825.

Mitchell, J., "Analysis of Energy Use and Control Characteristics of a Large Variable Speed Drive Chiller System", ASHRAE Journal, January 1988, pp. 33-34.

Myers, G.E., Mitchell, J.W., and Lindeman JR., C.F., "The Transient Response of Heat Exchangers Having an Infinite Capacitance Rate Fluid", ASME Journal of Heat Transfer, Vol. 92. No. 2, 1970.

REFERENCES

Myers, G.E., Mitchell, J.W., and Norman, R.F., "The Transient Response of Crossflow Heat Exchangers, Evaporators, and Condensers", ASME Journal of Heat Transfer, Vol. 89, No. 1, 1967, pp. 75-80.

Nesler, C.G., "Automated Controller Tuning for HVAC Applications", ASHRAE Transactions 1986, Vol. 92, Part 2B, pp. 189-200.

Nesler C.G. and Stoecker W.F., "Selecting the Proportional and Integral Constants in the Direct Digital Control of Discharge Air temperature", ASHRAE Transactions 1984, Vol. 90, Part 2B, pp. 834-845.

O'Neill, P.J., "Thermal Performance Analysis of Finned Tube Heat Exchangers at Low Temperatures and Airflow Rates", ASHRAE Transactions 1988, Vol. 94, Part 2, pp. 244-260.

Park, C., and David, A.J., "An Adaptive Controller for Heating and Cooling Systems: Modelling, Implementation, and Testing", ASME Journal, 1983, pp. 1-8.

Patterson, N.R., "Fan Selection and Control in High Velocity Variable Air Volume Systems", ASHRAE Transactions 1977, Vol. 83, Part 1, pp. 585-597.

Pearson T.J. and Leonard R.G., "Gain and Time Constant for Finned Serpentine Crossflow Heat Exchangers", ASHRAE Transactions 1974, Vol. 80, Part 2, pp. 255-267.

Pinnella, M.J., Wechselberger, E., Hittle, D.C., and Pedersen, C.O., "self-Tuning Digital Integral Control", ASHRAE Transactions 1986, Vol. 92, Part 2B, pp. 202-209.

Procell, C.J., "VAV Systems-Loads and Psychometrics", ASHRAE Transactions 1980, Vol. 80, Part 1, pp. 473-479.

Roberts, M.M., "Opportunities Exist to Improve Design", ASHRAE Journal 1987, Vol. 29, No. 8, pp. 25-27.

Shavit, G., and Brandt S.G., "The Dynamic Performance of a Discharge Air Temperature System with a PI Controller", ASHRAE Transactions 1982, Vol. 88, Part 2, pp. 826-838.

REFERENCES

Shuttleworth, R., "Mechanical and Electrical Systems for Construction", McGraw-Hill Book Company, Inc., N.Y., 1983.

Spethmann, D.H., "Optimized Control of Multiple Chillers", ASHRAE Transactions 1985, Vol. 91, Part 2B, pp. 848-856.

Spitler, J.D., Pedersen, C.O., Hittle, D.C., and Johnson, D.C., "Fan Electricity Consumption for Variable Air Volume", ASHRAE Transactions 1986, Part 2B, Vol. 92, pp. 5-17.

Stoecker, W.F., Rosario, L.A., Heidenreich, M.E., and Phelan, T.R., "Stability of An Air-Temperature Control Loop", ASHRAE Transactions 1978, Vol. 84, Part 1, pp. 35-53.

Tamm, H., "Dynamic Response Relations for Multi-Row Cross Flow Heat Exchangers", ASHRAE Transactions 1969, Vol. 75, Part 1, pp. 69-80.

Tamm, H., and Green, G.H., "Experimental Multi-row Crossflow Heat Exchanger Dynamic", ASHRAE Paper No. 2276, 1973.

Thompson, G., "The Effect of Room and Control Systems Dynamics on Energy Consumption", ASHRAE Transactions 1981, Vol. 87, Part 2, pp. 883-896.

Tobias, J.R., "Simplified Transfer Function for Temperature Response of Fluids Flowing Through Coils, Pipes or Ducts", ASHRAE Transactions 1973, Vol. 79, Part 2, pp. 19-22.

Waeldner, W., "Recent Increases in Scope and Reality", ASHRAE Journal 1987, Vol. 29, No. 8, pp. 30-31.

Waller, B., "Various Flow Rates in Condenser Water Cycle", ASHRAE Journal, January 1988, pp. 30-32.

Walton, G.N., "Thermal Analysis Research Program (TARP)", Reference Manual, U. S. Department of Commerce, national Bureau of Standards, National Engineering Laboratory, Washington, DC., March 1983.

REFERENCES

Ward, D.J., and Young, E.H., "Heat Transfer and Pressure Drop Across Triangular Pitch Banks of Finned Tubes", Chemical Engineering Progress Symposium Series-Heat Transfer 1959, Vol. 55, No. 29.

Wessel, D.J., "Electronic Controls Revolutionize VAV", ASHRAE Journal 1987, Vol. 29, No. 8, pp. 27-78.

Williams, V.A., "Optimization of Chiller Plant's Energy Consumption Utilizing a Central EMCS and DDC", ASHRAE Transactions 1985, Vol. 91, Part 2B, pp. 857-861.

Witt, D.R., "Simulation of An All-Electric Self Contained Multi-Zone HVAC Unit for Annual Energy Analysis", ASHRAE Transactions 1972, Vol. 78, Part I, pp. 38-74.

Wong, S.P.W., and Wang, S.K., "System Simulation of the Performance of a Centrifugal Chiller Using a Shell-and-Tube-Type Water-Cooled Condenser and R-11 as Refrigerant", ASHRAE Transactions 1989, Vol. 95, Part 1, pp. 445-454.

Yilmaz, Z., "Evaluation of Built Environmental From the Thermal Comfort Viewpoint", ASHRAE Transactions 1987, Vol. 93, Part 1, pp. 549-563.

Zaheer-Uddin, M., "A Two-Component Thermal Model for a Direct Gain Passive House with a Heated Basement", Building and Environment, Vol. 21, No. 1, 1986.

Zaheer-uddin, M., "Sub-Optimal Controller for a Space Heating System", ASHRAE Transactions 1989, Vol. 95, Part 2, pp. 201-208.

Zaheer-uddin, M., and Goh, P.A., "A Control Strategy for a Variable Air Volume System", Proceedings of the Fifth Conference on Building Science and Technology, Toronto, Ontario, pp. 219-236, 1990.

Zhang, X. and Warren, M.L., "Use of a General Control Simulation Program", ASHRAE Transactions 1988, Vol. 94, Part 1, pp. 1776-1791.

APPENDIX

Listing Of Computer Program

```
************************************************************
*
*     HVAC SYSTEM COOLING AND DEHUMIDIFYING CASE SIMULATION
*
*    PROGRAM ANALYSIS IS THE MAIN PROGRAM FOR HVAC SYSTEM AIR
*     LOOP CONTROL SIMULATION ACCORDING TO THE SCHEMATIC
*     DIAGRAM IN THE THESIS.
*
*     PURPOSE:
*          TO SIMULATE THE ZONE AIR DYNAMIC CHARACTERISTICS
*          WITH AIR MASS (Um), BYPASS (U3) AND CHILLER (U2)
*          CONTROLLERS.
*
*     SUBROUTINES AND FUNCTION SUBPROGRAMS REQUIRED
*
*          SUBROUTINE  CHILL
*              "       COCOIL
*              "       DBDP
*              "       DBW
*              "       DBWB
*              "       DTFAN
*              "       DUCTAIR
*              "       RHMIX
*              "       RPMBHP
*              "       SUFED
*
*     DATA REQUIRED:
*            COIL PARAMETER (SEE i.e. COCOIL SUBROUTINE)
*            DUCT     "     (SEE i.e. DUCTAIR    "     )
*
*     TDBR      : ASSUMED RETURN AIR DRY BULB TEMPERATURE
*     TWBR      : ASSUMED RETURN AIR WET BULB TEMPERATURE
*     TDBOA     : OUTDOOR AIR DRY BULB TEMPERATURE
*     TWBOA     : OUTDOOR AIR WET BULB TEMPERATURE
*     TZSET     : ZONE AIR DRY BULB TEMPERATURE SET
*     WZSET     : ZONE AIR HUMIDITY RATIO SET
*
************************************************************

      PROGRAM ANALYSIS

      DIMENSION COF(5),U3(5000),UM(5000)
      DIMENSION HZ1(5000),WZ1(5000),UW(5000),TTD(5000)
      REAL Cpa,MINOA,Qc,TDBOA,TWBOA,CFMOA,TWBZSET
      REAL LH,LWB,LDB,LWT,MZ,M5,mw,PHY,UU
      REAL CFMRA,QSL,QLL,QTSL,MAR,K1,TZ,WO,MO
      REAL Vo,W1,W2,W3,HOA,H1,H2,H3,Mao,Ma2,Ma4
      REAL FFLP(8),ENGCON(8)
      INTEGER COUNT
```

```
      OPEN(9,FILE='L1.DAT',STATUS='OLD')
      OPEN(4,FILE='MODELST.DAT',STATUS='OLD')
      OPEN(2,FILE='MODELST.OUT',STATUS='UNKNOWN')
      OPEN(11,FILE='DTFAN.OUT',STATUS='UNKNOWN')
      OPEN(13,FILE='ove.OUT',STATUS='UNKNOWN')
      OPEN(16,FILE='ove1.OUT',STATUS='UNKNOWN')
      OPEN(14,FILE='OVE2.OUT',STATUS='UNKNOWN')

      Cpa=0.24
      PB=29.92
      SAAT=0.0
      COUNT=1
      I=1
      TZSET=78.
      HZSET=30.
      WZSET=0.009
      TSSET=53.
      WSSET=0.006
      HSSET=19.2
      HS=HSSET
      UM(1)=0.5
      uw(1)=0.3
      U3(1)=0.5
      TTD(1)=0.

*     ICOIL SHOULD BE EITHER '0' OR '1'    ..... COIL INPUT
      READ(4,*) ICOIL
      READ(4,*)AP,AS,AI,FLFA,FCON,FA,FPI,NPR,NOR
      IF (ICOIL) 12,12,11
  12  CONTINUE
      READ(4,*) TDO,TDI,FTH,HD,ST,SL,FLE,COID
      FD=SQRT(4.0*FLE*COID/(3.142*NOR*NPR))
      GOTO 20
  11  CONTINUE
      READ(4,*) TDO,TDI,FTH,HD,ST,SL,FD
  20  CONTINUE
      READ(4,*)TCON
C     COIL INPUT PARAMETERS.
      HE=2.0
*                                    ..... DUCT INPUT
      READ(4,*)NINT,Z1,Z2,Z3
      Read(4,*)TDT,DDT,Re,Ri
      Read(4,*)Te
      REO=0.
      FS=1.0/(12.0*FPI)
      AO=AP+AS
      ESFA=ES/(FA*NOR)
      SREI=ES/AI
      FSES=AS/AO
      ROH=TDO/FD
      CALL SUFED(ROH,COF)
```

```
      FH=0.5*(FD-TDO)
*                                  ........  C1 & C2
      C1=0.159*(FTH/HD)**(-0.065)*(FTH/FH)**0.141
      C2=-0.323*(FS/FH)**0.049*(FD/SL)**0.549
     &     *(FTH/FS)**(-0.028)

*                      ....  WATER FLOW RATE & TEMP.
      READ(4,*) USGPM,EWT
      FMR=USGPM*0.13368*62.316*60

C     OUTDOOR AIR DRY AND WET BULB TEMP  ... O.A CONDITIONS

      TDBOA=92.
      TWBOA=85.
      CALL DBWB(TDBOA,TWBOA,PB,WO,HOA,SO,VO,PVO,DPO,RHO)
      WRITE(2,50) TDBOA,TWBOA,WO,HOA,SO,VO,PVO,DPO,RHO
50    FORMAT(//,10X,'OUTDOOR AIR DRY BULB TEMPERATURE
     +=',F6.2,' F',/,
     +10X,'OUTDOOR AIR WET BULB TEMPERATURE =',F6.2,' F',/,
     +10X,'HUMIDITY RATIO OF OUTDOOR AIR =',F7.5,' LB H2O/LB
     +DRY AIR',/,
     +10X,'OUTDOOR AIR ENTHALPY =',F7.3,' BTU/LB DRY AIR ',/,
     +10X,'ENTROPY OF OUTDOOR AIR =',F7.5,' BTU/LB F',/,
     +10X,'VOLUME OF OUTDOOR MOIST AIR =',F7.3,' CU FT/IB DRY
     +AIR',/,
     +10X,'VAPOR PRESSURE OF LIQUID WATER IN OUTDOOR MOIST AIR
     +=',F6.4,' IN HG',/,
     +10X,'OUTDOOR AIR DEW-POINT TEMPERATURE =',F6.2,' F',/,
     +10X,'OUTDOOR AIR RELATIVE HUMIDITY =', F7.3,'%')

C     THE SPACE IS MAINTAINED AT 78 F dB AND 64 F wB OR
C     RH=45%.
*                           .......... SPACE CONDITIONS
      TDBR=78.
      TWBR=64.
      TWBZ=TWBR
      TWBZSET=63.5
C     initial assumption of the return air dry bulb and
C     humidity ratio
*                      ..... STEP 1     INITIAL ASSUMPTION
*                           POINT R  RETURN AIR CONDITIONS
      CALL DBWB(TDBR,TWBR,PB,WZ,HZ,SR,VZ,PVR,DPR,RHR)
      WRITE(2,60) TDBR,TWBR,WZ,HZ,SR,VZ,PVR,DPR,RHR
60    FORMAT(//,10X,'RETURN AIR DRY BULB TEMPERATURE =',F6.2,'
     +F',/,
     +10X,'ASSUMED RETURN AIR WET BULB TEMPERATURE =',F6.2,'
     +F',/,
     +10X,'HUMIDITY RATIO OF RETURN AIR =',F7.5,' LB H2O/LB
     +DRY AIR',/,
     +10X,'ASSUMED RETURN AIR ENTHALPY =',F7.2,' BTU/LB DRY
     +AIR ',/,
```

```
     +10X,'ENTROPY OF ASSUMED RETURN AIR =',F7.5,' BTU/LB
     +F',/,
     +10X,'VOLUME OF RETURN MOIST AIR =',F7.3,' CU FT/IB DRY
     +AIR',/,
     +10X,'VAPOR PRESSURE OF LIQUID WATER IN RETURN MOIST AIR
     +=',F6.4,' IN HG',/,
     +10X,'RETURN AIR DEW-POINT TEMPERATURE =',F6.2,' F',/,
     +10X,'RETURN AIR RELATIVE HUMIDITY =', F7.3,'%')

*                                  ......... QSL & QLL
      READ(9,*) QSLr,QLLr

      SACFMR=QSLR/(1.08*(TZSET-TSSET))
      MAR=SACFMR*60./VZ
      WRITE(16,*)'     BPASS       U3     TDBMBP      HMBP
     &WMBP       SACFM         FMA'

C       WRITE(13,*)'   I        TZ        WZ       RH      PHY
     & UM         HZ       SAAT       w3'
98    FORMAT(2X,F7.3,2X,F5.2,2X,F5.3,2X,F7.2,2X,
     &F7.2,2X,F7.3,2X,F5.3,2X,F5.3)

1     CONTINUE
      RT=(SAAT/60.)
      QTSL=26356.46+778.6867*RT-1550.12*RT**2+295.9168*RT**3
     &     -17.0272*RT**4+0.3058343*RT**5
      QSL=0.9*QTSL
      QLL=0.1*QTSL
      IF(I.EQ.1)       SACFM=QSL/(1.08*(TZSET-TSSET))
c     By using the duct model, the leaving air and duct
c     temperatures leaving the duct are determined. These
C     temperatures are the recirculating air temperatures.
*                                  ...... Z1   POINT 4
      W4=WZ
      TDTR=TDBR
      Call DuctAir(z1,Nint,TDBR,TDTR,SACFM,TDT,DDT,REO,RI
     &,TDB4,TD4,Te,VDU)
      Call DBW(TDB4,W4,RH4,DP4)
      CALL DBDP(TDB4,TWB4,PB,W4,H4,S4,V4,PV4,DP4,RH4)

      SAAT=SAAT+(Z1/VDU*60.)
*                                  ...... MIN.  O.A 20%
      CFMOA=.20*SACFM
      MO=CFMOA*60./VO
      CFM5=SACFM-CFMOA
      M5=CFM5*60./VZ
      FMA=MO+M5
C     DETERMINE PROPERTIES OF MIXED AIR
*                             ..... STEP 2    POINT 5
      W5=WZ
      TD4=TDB4
```

```
      Call DuctAir(Z2,Nint,TDB4,Td4,CFM5,TDT,DDT,REO,RI
     &,TDB5,Td5,Te,VDU)
      Call DBW(TDB5,W5,RH5,DP5)
      CALL DBDP(TDB5,TWB5,PB,W5,H5,S5,V5,PV5,DP5,RH5)
      SAAT=SAAT+Z2/VDU*60.

*                          ........    MIXING BOX
*                          ........    POINT  1
     H1=(MO*HOA+M5*H5)/FMA
     W1=(MO*WO+M5*W5)/FMA
     T1=(H1-1061.2*W1)/(0.24+0.444*W1)

     CALL RHMIX(TDBOA,TDB5,WO,W5,CFMOA,CFM5,T1,PB,TDP1)
     CALL DBDP(T1,TWB1,PB,W1,H1,S1,V1,PV1,TDP1,RH1)
          IF(I.EQ.1) THEN
             HZ1(1)=HZ
             WZ1(1)=WZ
          WZZZ=W1/0.0202*100.
          RHZZ=W1/.0202
          ENDIF

C     DETERMINE SATURATED TUBE HUMIDITY RATIO INPUT
      WSTIN=-0.00793+0.00031*EWT+0.0000075*(EWT-53)**2

      CALL COCOIL(TDO,TDI,FTH,FD,FCON,FLFA,AS,AO,AI,FA,
     &COID,FLE,AP,NPR,NOR,C1,C2,COF,EWT,FMR,T1,H1,FMA,
     &DBL,WTL,TCON,HD,W1,SAAT,TDP1,WL,WSTIN,QTSL)
      Call DBW(DBL,WL,RHL,DPL)
      CALL DBDP(DBL,WBL,PB,WL,HLL,SL,VL,PVL,DPL,RHL)

      K1=(FMA*U3(I)*(HZ-HLL))/(MAR*(HZ-HS))
      U3(I+1)=0.8*U3(I)+0.2*K1*(1+TWBZ-TWBZSET)
      IF(U3(I+1).GT.1) U3(I+1)=1.
      IF(U3(I+1).LT.0) U3(I+1)=0.
      IF(U3(I+1).EQ.1.) THEN
      RHMBP=RHL
      TDBMBP=DBL
      HMBP=HLL
      WMBP=WL
      GOTO 222
      ELSE
      CFMCL=U3(I+1)*SACFM
      CFMBP=SACFM-CFMCL
      TDBMBP=U3(I+1)*DBL+(1-U3(I+1))*T1
      CALL RHMIX(DBL,T1,WL,W1,CFMCL,CFMBP,TDBMBP,PB,TDPMBP)
      CALL DBDP(TDBMBP,TWBMBP,PB,WMBP,HMBP,SMBP,VMBP,PVMBP,
     &TDPMBP,RHMBP)
      ENDIF
222   CONTINUE
      WRITE(16,55)K1,U3(I+1),TDBMBP,HMBP,WMBP,SACFM,FMA
```

```
55    FORMAT(2X,F9.2,2X,F6.2,2X,F7.2,2X,F7.2,2X,F7.4,2X,
     &F8.1,2X,F8.1)
*                                ..... LEAVING  COIL
*                                ..... POINT     L
*                           FAN  ........    POINT  3

      CALL DTFAN(RHMBP,PB,TDBMBP,TFAN,SACFM)
      T3=TDBMBP+TFAN
      TDT3=T3
      W3=WMBP
      Call DBW(T3,W3,RH3,TDP3)
      CALL DBDP(T3,TWB3,PB,W3,H3,S3,V3,PV3,TDP3,RH3)
C     By using the duct air temperature  model leaving air and
C     duct temperatures leaving the duct are determined. These
C     temperature are also the entering space air temperature.

      TDT3=T3
      Call DuctAir(z3,Nint,T3,Tdt3,SACFM,TDT,DDT,RE,RI,
     &TDBS,TdS,Te,VDU)
      SAAT=SAAT+Z3/VDU*60.
      TTD(I+1)=SAAT
      CALL DBW(TdBS,W3,RHs,DPs)
      CALL DBDP(TdbS,TWBs,PB,WS,Hs,Ss,Vs,PVs,DPs,RHs)
           DCT=(TTD(I+1)-TTD(I))/60.
           z11=DCT/(0.075*22500.)
           z12=-FMA
      MW=QLL/(1061.2*TZSET)
      HZ1(I+1)=HZ1(I)+Z11*(Z12*(HZ1(I)-HS)+QSL+QLL)
      WZ1(I+1)=WZ1(I)+Z11*(Z12*(WZ1(I)-WL)+MW/DCT)
      TZ=(HZ1(I+1)-WZ1(I+1)*1061.2)
     &                  /(0.24+0.444*WZ1(I+1))
           WZ=WZ1(I+1)
           HZ=HZ1(I+1)
           CALL DBW(TZ,WZ,RHZ,DPZ)
           CALL DBDP(TZ,TWBZ,PB,WZ,HZ,SZ,VZ,PVZ,DPZ,RHZ)

           PHY=(QSL+QLL)/(MAR*(HZ1(I+1)-HS))
           UM(I+1)=0.2*UM(I)+0.8*PHY*(1+TZ-TZSET)
           IF(UM(I+1).GT.1.) UM(I+1)=1.
           IF(UM(I+1).LT.0.3) UM(I+1)=0.3
           SACFM=UM(I+1)*SACFMR
           FMA=SACFM*60./VZ
      CALL CHILL(I,FMR,QSL,QLL,WTL,EWT,TSSET,H3,MAR,HZ,FMA,
     &TDBS,UU2)
      CALL RPMBHP(SACFM,RPM,BHP)
      GOH14=(TZ-32.)*5/9.
      WZZZ=(WZ1(I+1)/0.0208)*100.
      WRITE(13,98)GOH14,WZZZ,UM(I+1),HZ1(I+1)
     &,SAAT,EWT,UU2,U3(I+1)
```

```
c     By using the duct air temperature model leaving air and
C     duct temperatures leaving the duct are determined. These
C     temperature are also the recirculating air temperatures.
      TDBR=TZ
      I=I+1
      IF(SAAT.LT.1440.) GOTO 1
 99   STOP
      END


**********************************************************
*
*     THIS PROGRAM DETERMINE OUTGOING CHILLED WATER
*     TEMPERATURE AND CHILLER OPERATING FRACTION.
*
*     INPUT DATA:
*
*       Cw      : STORAGE TANK CAPACITY
*       U1MAX   : CHILLED WATER FLOW RATE
*       UAW     : STORAGE TANK HEAT TRANSFER COEFFICIENT
*       U2MAX   : CHILLER CAPACITY
*       TA      : MECHANICAL ROOM TEMPERATURE
*
*     OUTPUT:
*
*       TWS     : OUTGOING CHILLED WATER TEMPERATURE
*
**********************************************************


      SUBROUTINE CHILL(I,U1MAX,QS,QL,TWR,TWS,TSSET,HS,MAR,HZ,
     &FMA,TDBS,UU2)
      DIMENSION TW(5000),COP(5000),U2(5000)
      REAL K(5000),TWR,MAR,QS,QL,TDBS,SAAT,UU2
      INTEGER I
      OPEN (10,FILE='CHILLER.DAT',STATUS='OLD')
      OPEN(11,FILE='CH.OUT',STATUS='UNKNOWN')

      READ(10,*)CW,UCW,UAW
      READ(10,*)TA,TMAX,U2MAX
      DT=0.2
      U2(1)=0.5
      TW(1)=50.
      TSMIN=52.
      COP(I)=3.5*(1.-(68.-TW(I))/TMAX)

      K(I)=(U1MAX*0.8*(TWR-TW(I))+UAW*(85.-TW(I)))
     &     /(COP(I)*U2MAX)
      IF(TDBS.LT.TSMIN) THEN
      TWSTAR=40.
      ELSE
```

```
      TWSTAR=TSMIN-((QS+QL)/(U1MAX*UCW))
      ENDIF
      U2(I+1)=0.6*U2(I)+0.4*K(I)*(1+TW(I)-TWSTAR)
      IF(U2(I+1).GT.1.) U2(I+1)=1.
      IF(U2(I+1).LT.0.) U2(I+1)=0.
      UU2=U2(I+1)
      TW(I+1)=TW(I)-U1MAX*UCW*DT/CW*(TW(I)-(TWR))
     &       -U2(I)*U2MAX*DT/CW*(COP(I))
     &       +UAW*DT/CW*(85.-TW(I))
      IF(TW(I+1).LT.40.) TW(I+1)=40.
      IF(I.EQ.1) THEN
      WRITE(11,*)'     i    COP     K     U2     TW
     &    TWSTAR'
      ENDIF
      WRITE(11,5)K(I),U2(I+1),TW(I+1),TWSTAR
5     FORMAT(2X,F6.1,2X,F4.2,2X,F5.2,2X,F7.2)
      CLOSE(10)
      TWS=TW(I+1)
      RETURN
      END


*****************************************************************
*
*     THIS PROGRAM DETERMINES FAN SPEED (RPM) AND FAN BRAKE
*     HORSE POWER (BHP) REQUIRED TO DELIVER THE SUPPLY AIR
*     FLOW RATE.
*
*     INPUT DATA:
*
*         SACFM : SUPPLY AIR FLOW RATE
*
*     OUTPUT:
*
*         RPM   : FAN SPEED
*         BHP   : FAN BRAKE HORSE POWER
*
*****************************************************************

      SUBROUTINE RPMBHP(SACFM,RPM,BHP)
      REAL SACFM,RPM,BHP
      OPEN(15,FILE='RPMBHP.OUT',STATUS='UNKNOWN')

      DATA A0,A1,A2,A3,A4/783.983,-0.1193927,0.0004806511,
     &                    -0.00000013237,0.00000000001411779/
      DATA E0,E1,E2,E3,E4/0.05993158,-0.00003366251,
     &     0.0000000857166,0.00000000001382296,
     &     0.000000000000002756514/

      RPM=A0+A1*SACFM+A2*SACFM**2+A3*SACFM**3+A4*SACFM**4
      BHP=E0+E1*SACFM+E2*SACFM**2+E3*SACFM**3+E4*SACFM**4
```

```
      WRITE(15,*) SACFM,RPM,BHP
      RETURN
      END

************************************************************
*
*     COOLING AND DEHUMIDIFYING COIL SIMULATION PROGRAM
*
*     PURPOSE:
*        TO SIMULATE THE PERFORMANCE OF FINNED TUBE HEAT
*        EXCHANGERS IN THE CASE OF COOLING AND
*        DEHUMIDIFICATION PROCESSES
*
*     REMARKS:
*        - THE NUMBER OF ROWS SHOULD EQUAL TO OR BE GREATER
*          THAN 4
*        - THIS PROGRAM IS RESTRICTED TO THE CIRCULAR FINNED
*          OR CONTINUOUS FINNED TUBE HEAT EXCHANGERS
*
*     INPUT DATA:
*        - COIL IDENTIFICATION:     ICOIL
*                                ICOIL=0 FLAT PLATE FINS
*                                ICOIL=1 CIRCULAR FINS
*
*           AS    - SECONDARY SURFACE AREA
*           AP    - PRIMARY SURFACE AREA
*           AI    - INTERNAL SURFACE AREA
*                   (WATER SIDE)
*           FLFA  - MINIMUM FLOW OVER FACE AREA
*           FCON  - THERMAL CONDUCTIVITY OF FIN MATERIAL
*           FA    - COIL FACE AREA
*           FPI   - # OF FINS PER CENTIMETER
*           NPR   - NUMBER OF TUBES PER ROW
*           NOR   - NUMBER OF ROWS PER COIL
*           TDO   - TUBE OUTSIDE DIAMETER
*           TDI   - TUBE INSIDE DIAMETER
*           FTH   - FIN THICKNESS
*           HD    - COIL HYDRAULIC DIAMETER
*           ST    - TUBE TRAVERSE SPACING
*           SL    - TUBE LONGITUTINAL SPACING
*     IF ICOIL=1
*           FD    - FIN DIAMETER
*     IF ICOIL=0
*           FLE   - LENGTH OF CONTINUOUS FIN
*           COID  - COIL DEPTH (DISTANCE IN DIRECTION OF
*                   FLOW OF AIR)
*           TCON  - THERMAL CONDUCTIVITY OF TUBE MATERIAL
*
*        - AIR AND CHILLED WATER ENTRY CONDITIONS
*
```

```
*            FMR   - CHILLED WATER FLOW RATE
*            EWT   - INLET WATER TEMPERATURE
*            FMA   - DRY AIR FLOW RATE
*            EDB   - DRY BULB TEMPERATURE OF AIR AT INLET
*            EWB   - WET BULB TEMPERATURE OF AIR AT INLET
*
*      OUTPUT
*
*            LDB   - DRY BULB TEMPERATURE OF AIR LEAVING THE
*                    COIL
*            LWT   - WATER TEMPERATURE LEAVING COOLING COIL
*            WAL   - HUMIDITY RATIO OF AIR LEAVING THE COIL
*
************************************************************

      SUBROUTINE COCOIL(TDO,TDI,FTH,FD,FCON,FLFA,AS,
     &AO,AI,FA,COID,FLE,ap,NTPR,NOR,C1,C2,COF,EWT,CWFR,TAE,
     &HAE,FMA,TALL,TWL,TCON,HD,W,SAAT,DP,WAL,WSTIN,QTOT)

      REAL LE,IG,WTOST,QTOT,dt,mt,mf
      INTEGER N,NOP,NTPR,COUNT
      DIMENSION COF(5),TAL(100,13),TTO(100,13)
      DIMENSION TWLL(100,13),WA(100,13)
      DIMENSION WTOST(100,100),WAA(100,100)
      DIMENSION WAAF(100,100)
      OPEN(39,FILE='CFILE.OUT',STATUS='UNKNOWN')

*    SIMULATION OF:
*      COUNTERFLOW CHILLED WATER COOLING/DEHUMIDIFYING COIL
*
      DATA VISC,CP/0.0437,0.243/
      DATA CP,H0/0.243,-7.55/
      DATA ADP0,ADP1,ADP2,ADP3/11.471,6875.333,-280479.327,
     &                         5025099.039/
      DATA AN0,AN1,AN2,AN3/-0.0000253518,0.000000002233617,
     & -0.00000000000003540414,0.0000000000000000000190324/
C
C     INITIALIZE
C
      FOULF=0.0003
      cv=0.45
      vo=cp/cv
      dcu=556.
      dal=171.
      cpcu=0.092
      cpal=0.214

      MF=(As/2*FTH*dAL)/(COID/2)
      mt=3.141592654/4*(tdo**2-tdi**2)*nor*ntpr*fle*dcu
     &   /(COID/2 )
      LE=0.92
```

```
      CW=1.
      dy=.114
      DX=-DY
      PB=29.92
C     CALCULATE THERMAL RESISTANCE ON THE AIR SIDE + FOULING
      RFOULA=(AO/AI)*(0.5*(TDO-TDI)/TCON+foulf)

C     CALCULATE CHILLED WATER VELOCITY     ... ft/s
*
      V=CWFR*4/(3.14159*TDI*TDI*NTPR*62.4*3600)
C     CALCULATE COIL FACE VELOCITY   .....   ft/hr
      FV=FMA/(0.075*FA)
*                          .........   DT in hr
      DT=(COID)/(FV*8.)
      DTW=AN0+AN1*QTOT+AN2*QTOT**2+AN3*QTOT**3
C     CALCULATE MASS VELOCITY (Gc = lb/(hr*ft**2)
*     FLFA is the minflow area / Frontal area : dimensionless
      VM=(1-W)*FMA/(FLFA*FA)
      FRAT=CWFR/FMA
C     CALCULATE CMIN OR CMAX = CHOT
      FMACP=FMA*CP
C     CALCULATE REYNOLDS NO. -- AIR SIDE
      RENR=HD*VM/VISC
      DIA2=(TDI*12)**0.2
      HCR1=(150./DIA2)*V**0.8
      aocoid=ao/(ntpr*nor*fa/fle)
C     CHECK IF COMPLETELY DRY
      XEWT=EWT+5
      IF(DP-XEWT) 30,30,40
C     COMPLETELY DRY COIL
30    CONTINUE
         ICM=-1
C     CALCULATE HCD (DRY SURFACE COEF.) 0.3=Cpa/Pr**2/3
C     lb/(h*ft**2)
33    CONTINUE
      HCD=0.3*C1*RENR**C2*VM
C     CALCULATE FIN EFFICIENCY
C     CALCULATE THE DRY FIN EFFICIENCY
      FAI=.5*(FD-TDO)*SQRT(2*HCD/(FTH*FCON))
      EFFD=0.0
      DO 200 I=1,5
      EFFD=EFFD+COF(I)*FAI**(I-1)
200   CONTINUE
      FID=AS/AO*EFFD+(1.055-AS/AO)
      RA=(1/(HCD*As))/coid
           IF (ICM) 31,1000,1000
31           CONTINUE
*     FIRST INITIALIZATION
*                          ......    SAAT in sec
      saat=13.2/60.
      do 230  j=1,1
```

```
      DO 220  I=1,1
          TAL(J,I)=TAE
          TWLL(j,I)=EWT
          TTO(j,i)=EWT
220   CONTINUE
230   continue
      SAAT=SAAT+COID/FV*60.
301   CONTINUE
      DO 210 NT=2,9
              DO 300 I=NT,NT
              HCRD=HCR1*(1.+0.0115*TWLL(NT-1,i-1))
              RW=(1/((HCRD*AI/1.6)/COID))
              VW=V*3600.
C     FUNCTION OF DISTANCE
      BB1=-dt*VO*FV/dy
      BB2=-DT*(VO*FID/(FMA/FV*CP*RA))
      IF (I.EQ.2) THEN
          TWD=TWLL(NT-1,I-1)
          TAD=TAL(NT-1,I-1)
      ELSE
          TWD=TWLL(NT-2,I-2)
          TAD=TAL(NT-2,I-2)
      ENDIF
      TAL(NT,I)=TAL(NT-1,I-1)+BB1*(TAD-TAL(NT-1,I-1))
     &             +BB2*(taL(NT-1,i-1)
     &             -tto(NT-1,i-1))
      CC1=(1-fid)/(FID+(MT*CPCU)/(MF*CPAL))
      CC2=DT*FID/(RA*(1-FID)*MF*CPAL)
      CC3=-DT/(RW*CPAL*MF*(fid))
      TTO(NT,i)=TTO(NT-1,i-1)+cc1*(tal(nt-1,i-1)-tal(nt,i))
     &             +CC1*CC2*(Tal(NT-1,I-1)-Tto(NT-1,i-1))
     &             +(Tto(NT-1,i-1)-twll(NT-1,i-1))*CC3*CC1
      AA1=-DTW*VW/DX
      AA2=-(1/(RW*CWFR/VW*CW))*DTW
      TWLL(NT,i)=TWLL(NT-1,i-1)+AA1*(TWD-TWLL(NT-1,i-1))
     &              +AA2*(Twll(NT-1,i-1)-Tto(NT-1,i-1))
300   CONTINUE
      WRITE(39,*)TWLL(NT,I),TTO(NT,I),TAL(NT,I)
210   CONTINUE
      TALL=TAL(9,9)
      WAL=W
      TWL=TWLL(9,9)
      RETURN
40    CONTINUE
C     CALCULATE HCW (WET SURFACE COEFF.)
C     CORRECTION FACTOR FOR H
      CFACT=1.425-0.00051*RENR+0.263*RENR*RENR*10**(-6)
      HCW=0.3*CFACT*C1*RENR**C2*Vm
      HCD=0.3*C1*RENR**C2*VM
C     CALCULATE FIN EFFICIENCY
C     CALCULATE THE DRY FIN EFFICIENCY
```

```
      FAI=.5*(FD-TDO)*SQRT(2*HCW/(FTH*FCON))
      EFFD=0.0
      DO 500 I=1,5
      EFFD=EFFD+COF(I)*FAI**(I-1)
500   CONTINUE
      FId=AS/AO*EFFd+(1.-AS/AO)
      RA=(1/(hcd*As))/COID

C     CALCUL TE THE WET FIN EFFICIENCY
C     LET TUBE TEMPERATURE .7 F ABOVE THE WATER TEMP.
C     THIS VALUE IS OBTAINED FROM DRY COIL TUBE TEMP.
      FTR=EWT+0.7
      AWSTR=FUAWST(FTR)
      SHR=.24*(TAE-FTR)/(.24*TAE+(1061+.444*TAE)*W-
     &    .24*FTR-(1061+.444*FTR)*AWSTR)
      SHR=ABS(SHR)
      AWD=W-AWSTR
      AWD=ABS(AWD)
      IF (TAE.LE.80.)  GOTO 601
      EFFW=EXP(-.41718)*SHR**(.09471)*AWD**(.0108)*
     &     FAI**(-.50303)
      GOTO 602
601   CONTINUE
      EFFW=EXP(-.3574)*SHR**(.16081)*AWD**(.01995)*
     &     FAI**(-.52951)
602   CONTINUE
C     OVERALL EFFICIENCY
      FIW=AS/AO*EFFW+(1.0-AS/AO)

      do 650  j=1,1
      DO 651  I=1,1
          TAL(J,I)=TAE
          WA(j,I)=W
          TWLL(j,I)=EWT
          TTO(j,I)=EWT+0.5
          WTOST(J,i)=WSTIN
651   CONTINUE
650   continue
      SAAT=SAAT+COID/FV*60.
      DO 652 NT=2,9
             DO 600 I=NT,NT

C     FUNCTION OF DISTANCE
            HCRD=HCR1*(1.+0.0115*TWLL(NT-1,i-1))+0.000003206
            RW=(1/((HCRD*AI/1.6)/COID))
            VW=V*3600.
            WTOST(NT,i)=-0.00793+0.00031*TTO(NT-1,i-1)
     &                  +0.0000075*(TTO(NT-1,i-1)-53)**2
            IG=1060.6+.444*TTO(NT-1,i-1)
            DD2=-FIW/(FMA/FV*CP*LE*RA)
        IF (I.EQ.2) THEN
```

```
            WAD=WA(NT-1,I-1)
          ELSE
            WAD=WA(NT-2,I-2)
          ENDIF
          WA(NT,I)=WA(NT-1,I-1)-DT*FV/DY*(WAD-WA(NT-1,I-1))
     &           +DT*DD2*(WA(NT-1,I-1)-WTOST(NT,i))
          IF((WA(NT,I)-WTOST(NT,i)).GT.0.) THEN
          WA(NT,I)=WA(NT,I)
          fiw=fiw
          ELSEIF((WA(NT-1,I-1)-WTOST(NT,I)).LT.0.) THEN
            WA(NT,I)=WA(NT-1,I-1)
            fiw=fid
            ELSE
            WA(NT,I)=WA(NT,I)
          ENDIF
          BB1=-dt*VO*FV/dy
          BB2=-DT*(VO*FID/(FMA/FV*CP*RA))
          BB3=(VO-1)
          IF (I.EQ.2) THEN
            TAD=TAL(NT-1,I-1)
            TWD=TWLL(NT-1,I-1)
          ELSE
            TAD=TAL(NT-2,I-2)
            TWD=TWLL(NT-2,I-2)
          ENDIF
          TAL(NT,I)=TAL(NT-1,I-1)+BB1*(TAD-TAL(NT-1,I-1))
     &           +BB2*(taL(NT-1,i-1)
     &           -tto(NT-1,i-1))
     &      +bb3*TAl(NT-1,I-1)*(WA(NT-1,I-1)-WA(NT,I))

          CC1=(1.15-fid)/(FID+(MT*CPCU)/(MF*CPAL))
          CC2=DT*FID/(RA*(1-FID)*MF*CPAL)
          CC3=-DT/(RW*CPAL*MF*(FID))
          CC4=DT*FIW*IG/(LE*RA*CP*MF*CPAL*(1-FIW))

          TTO(NT,i)=TTO(NT-1,i-1)+cc1*(tal(nt-1,i-1)-tal(nt,i))
     &           +CC1*CC2*(Tal(NT-1,I-1)-Tto(NT-1,i-1))
     &           +(Tto(NT-1,i-1)-twll(NT-1,i-1))*CC3*CC1
     &           +CC1*CC4*(WA(NT-1,I-1)-WTOST(nt-1,i-1))

          AA1=-DTW*VW/DX
          AA2=-(1/(RW*CWFR/VW*CW))*DTW
          TWLL(NT,i)=TWLL(NT-1,i-1)+AA1*(TWD-TWLL(NT-1,i-1))
     &           +AA2*(Twll(NT-1,i-1)-Tto(NT-1,i-1))

600       CONTINUE
          WRITE(39,*)TWLL(NT,I-1),TTO(NT,I-1),TAL(NT,I-1),
     &WA(NT,I-1),WTOST(NT,I-1)
652       CONTINUE
          TALL=TAL(9,9)
          WAL=WA(9,9)
```

```
      TWL=TWLL(9,9)
1000  RETURN
      END

*****************************************************************
*
*     SUBROUTINE DTFAN (RHO,PB,T1,TFAN,SACFM)
*
*     THIS SUBROUTINE DETERMINE FAN HEAT GAIN
*
*     RHO:   RELATIVE HUMIDITY OF AIR
*     PB:    BAROMETRIC PRESSURE IN INCH OF HG
*     T1:    AIR DRY BULB TEMPERATURE
*     SACFM: SUPPLY AIR VOLUME FLOW RATE
*
*     INPUT DATA:
*         DCFM   : RATED SUPPLY AIR FLOW RATE
*
*     OUTPUT:
*         TFAN   : FAN HEAT GAIN
*
*****************************************************************

      SUBROUTINE DTFAN(RHO,PB,T1,TFAN,SACFM)

      OPEN(44,FILE='DTFAN.DAT',STATUS='OLD')

      READ(44,*)DELTAP,EFF
      READ(44,*)DCFM

      DTS=DELTAP/EFF
      CON1=(.24+.44*RHO)*60.*PB/(.754*(T1+459.7)*
     &     (1.0+1.605*RHO))
      CON3=0.3996/CON1
      TFAN=DTS*CON3
      PLR=SACFM/DCFM
      TFAN=TFAN*PLR
      CLOSE(44)

      RETURN
      END

*****************************************************************

      FUNCTION FUAWST(T)
      FUAWST=-.00793+.00031*T+.0000075*(T-53.)**2
      RETURN
      END
```

```
************************************************************
*
*     SUBROUTINE DUCTAIR(Z,NINT,TAZ,TD0,SACFM,TDT,D,RE,RI,
*     +TAO,TDO,TE,V)
*
*     This program determines duct air temperature at a
*     giveN distance (z) at a time (t).
*
*        INPUT DATA:
*             TDT      : DUCT MATERIAL THICKNESS
*             DDT      : DUCT CROSS SECTION DIAMETER
*             RE       : OUTSIDE INSULATION RESISTANCE
*             RI       : INSIDE INSULATION RESISTANCE
*             TE       : AMBIENT TEMPERATURE
*             Z(I)     : DUCT LENGHT
*             NINT     : INTEGRATION STEP (NINT< 100)
*             TAZ      : LNLET DUCT AIR TEMPERATURE
*             TD0      : INITIAL DUCT SURFACE TEMPERATURE
*
*     OUTPUT:
*             TAO      : OUTLET DUCT AIR TEMPERATURE
*             TDO      : OUTDUCT SURFACE TEMPERATURE
*
************************************************************

      SUBROUTINE DUCTAIR(Z,NINT,TAZ,TD0,SACFM,TDT,D,RE,RI,
     +TAO,TDO,TE,V)

      DIMENSION Ta(100,100),Td(100,100),TADU(100,100)
      REAL*8 DX,DT

      Open(3,file='duc.dat',status='old')
      Open(5,file='duc.out',status='unknown')

      Cpa=0.243
      PB=29.92
      VOA=0.075
      VOD=500.0
      CPD=0.1
      A=3.14159*D**2/4.
      P=3.14159*D
      V=SACFM/A*60.
      hi=0.024*Cpa*(Voa*V)**.8/D**.2
      HE=2.0
      Ui=1/(Ri+1/hi)
      Ue=1/(Re+1/he)
      DX=Z/NINT
      Ta(1,1)=Taz
      Td(1,1)=Td0
      DT=DX/V
      WRITE(5,*)TA(1,1),TD(1,1)
```

```
      DO 100 I=2,NINT+1
           DO 200 J=I,I
                BETA=DT*Ue/(Cpd*Vod*TDT)
                BETA1=DT*Ui/(Cpd*Vod*TDT)
                Td(I,J)=Td(I-1,J-1)+BETA*(Te-Td(I-1,J-1))
     &                     +BETA1*(Ta(I-1,J-1)-Td(I-1,J-1))
                IF(I.EQ.2) THEN
                TADU(I,J)=TA(I-1,J-1)
                ELSE
                TADU(I,J)=TA(I-2,J-2)
                ENDIF
                UU=1/(1/UE+1/UI)
                GAMA=DT*P*UU/(Cpa*A*Voa)
                Ta(I,J)=Ta(I-1,J-1)+DT*V/DX*(TA(I-1,J-1)-
     &                    TADU(I,J))+GAMA*(Td(I-1,J-1)
     &                    -Ta(I-1,J-1))
200        CONTINUE
100   CONTINUE

      WRITE(5,*) Ta(11,11), Td(11,11),DDT,I
      TAO=TA(11,11)
      TDO=TD(11,11)

      RETURN
      END


*****************************************************************

       SUBROUTINE SUFED (ROH, COF)

       DIMENSION X(60),Y(60),COF(5)
       OPEN(3,FILE='SUFED.OUT',STATUS='UNKNOWN')

       WRITE (3,1)
 1     FORMAT(8X,'R1 ',8X,'R2',8X,'I02',8X,'I11',8X,'I12',8X,
      &'K02',8X,'K11',8X,'K12',//)
       FAI=.02
       DO 10 I=1,60
       FAI=FAI+.035
       R1=FAI/(1.-ROH)
       R2=R1*ROH
       RO=2.*ROH/(FAI*(1.+ROH))
       CALL BESI(R1,1,R1I1,IE1)
       CALL BESK(R2,1,R2K1,IE2)
       CALL BESI(R2,1,R2I1,IE3)
       CALL BESK(R1,1,R1K1,IE4)
       CALL BESI(R2,0,R2I0,IE5)
       CALL BESK(R2,0,R2K0,IE6)
       WRITE(3,2) R1,R2,R2I0,R1I1,R2I1,R2K0,R1K1,R2K1
 2     FORMAT(8(F8.4,4X))
```

```
      FED=R0*(R1I1*R2K1-R2I1*R1K1)/(R2I0*R1K1+R1I1*R2K0)
      X(I)=FAI
      Y(I)=FED
 10   CONTINUE
      CALL POLFIT (X,Y,60,.1E-4,4,COF)

      RETURN
      END


*****************************************************************
*
*     SUBROUTINE POLFIT FITS POLYNOMIAL OF ORDER FROM 1 TO
*     LAST TO THE ORDERED PAIRS OF DATA POINTS X,Y
*
*****************************************************************

      SUBROUTINE POLFIT(X,Y,N,TOL,LAST,COF)

      DIMENSION X(60),Y(60),A(10,10),SUMX(10),SUMY(10),COF(10)

 70   SUMX(1)=0.0
      SUMX(2)=0.0
      SUMX(3)=0.0
      SUMY(1)=0.0
      SUMY(2)=0.0
      DO 90 I=1,N
      SUMX(1) = SUMX(1) +1.
      SUMX(2) = SUMX(2) + X(I)
      SUMX(3) = SUMX(3) + X(I)*X(I)
      SUMY(1) = SUMY(1) + Y(I)
      SUMY(2) = SUMY(2) + X(I)*Y(I)
 90   CONTINUE
      NORD=1
 91   L=NORD + 1
      KK=L+1
      DO 101 I=1,L
      DO 100 J=1,L
      IK=J-1+I
      A(I,J)=SUMX(IK)
100   CONTINUE
      A(I,KK)=SUMY(I)
101   CONTINUE
      DO 140 I=1,L
      A(KK,I)=-1.0
      KKK=I+1
      DO 110 J=KKK,KK
      A(KK,J)=0.0
110   CONTINUE
      C=1.0/A(1,I)
      DO 120 II=2,KK
```

```
      DO 120 J=KKK,KK
      A(II,J)=A(II,J)-A(1,J)*A(II,I)*C
120   CONTINUE
      DO 140 II=1,L
      DO 140 J=KKK,KK
      A(II,J)=A(II+1,J)
140   CONTINUE
      S2=0.0
      DO 160 J=1,N
      S1=0.0
      S1=S1+A(1,KK)
      DO 150 I=1,NORD
      S1=S1+A(I+1,KK)*X(J)**I
150   CONTINUE
      S2=S2+(S1-Y(J))*(S1-Y(J))
160   CONTINUE
      B=N-L
      IF (ABS(S2).LE.0.0001) GOTO 968
161   CONTINUE
      S2=(S2/B)**.5
968   CONTINUE
      DO 164 I=1,L
      J=I-1
      COF(I)=A(I,KK)
164   CONTINUE
      IF (NORD-LAST) 170,173,173
170   IF (S2-TOL) 173,173,171
171   NORD=NORD+1
      J=2*NORD
      SUMX(J)=0.0
      SUMX(J+1)=0.0
      SUMY(NORD+1)=0.0
      DO 172 I=1,N
      SUMX(J) = SUMX(J) + X(I)**(J-1)
      SUMX(J+1) = SUMX(J+1) +X(I)**J
      SUMY(NORD+1) = SUMY(NORD+1) + Y(I)*X(I)**NORD
172   CONTINUE
      GOTO 91
173   CONTINUE
      RETURN
      END


*****************************************************************
*
*     SUBROUTINE BESI TO CALCULATE THE MODIFIED BESSEL
*     FUNCTION
*     OF ORDER 0 TO N
*
*     CALL BESI (X,N,BI,IER)
*
```

```
*      X    ARGUMENT OF BESSEL FUNCTION
*      N    ORDER OF BESSEL FUNCTION GREATER THAN OR =0
*      BI   RESULTANT VALUE OF I BESSEL FUNCTION
*      IER  RESULATNT ERROR CODE:
*
*      IER=0      NO ERROR
*      IER=1      N.LT.0
*      IER=2      X.LT.0
*      IER=3      BI .LT. 10**(-69)  RES IS SET TO 0
*      IER=4      X.GT.N . X.GT.170  BI IS SET TO 10**70
*
**********************************************************************

      SUBROUTINE BESI (X,N,BI,IER)

      IER=0
      BI=1.
      IF (N) 150,15,10
10    IF (X) 160,20,20
15    IF (X) 160,17,20
17    RETURN
20    TOL=1.E-6
      IF (X-12.) 40,40,30
30    IF (X-FLOAT(N)) 40,40,110
40    XX=X/2.
50    TERM=1.
      IF (N) 70,70,55
55    DO 60 I=1,N
      FI=I
      IF (ABS(TERM)-1.0D-32) 56,60,60
56    IER=3
      BI=0.
      RETURN
60    TERM=TERM*XX/FI
70    BI=TERM
      XX=XX*XX
      DO 90 K=1,1000
      IF (ABS(TERM)-ABS(BI*TOL)) 100,100,80
80    FK=K*(N+K)
      TERM=TERM*(XX/FK)
90    BI=BI+TERM
100   RETURN

110   FN=4*N*N
      IF(X-170.) 115,111,111
111   IER=4
      RETURN

115   XX=1./(8.*X)
      TERM=1.
      BI=1.
```

```
      DO 130 K=1,30
       IF (ABS(TERM)-ABS(TOL*BI)) 140,140,120
  120  FK=(2*K-1)**2
       TERM=TERM*XX*(FK-FN)/FLOAT(K)
  130  BI=BI+TERM
       GOTO 40
  140  PI=3.141592653
       BI=BI*EXP(X)/SQRT(2.*PI*X)
       GOTO 100
  150  IER=1
       GOTO 100
  160  IER=2
       GOTO 100

       END


************************************************************
*
*      SUBROUTINE BESK
*
*      COMPUTE THE K BESSEL FUNCTION FOR A GIVEN ARGUMENT AND
*      ORDER
*
*      USAGE
*      CALL BESK(X,N,BK,IER)
*
*      DESCRIPTION OF PARAMETERS
*      X  -THE ARGUMENT OF THE K BESSEL FUNCTION DESIRED
*      N  -THE OEDER OF THE K BESSEL FUNCTION DESIRED
*      BK -THE RESULTANT K BESSEL FUNCTION
*      IER-RESULTANT ERROR CODE WHERE
*          IER=0  NO ERROR
*          IER=1  N IS NEGATIVE
*          IER=2  X IS ZERO OR NEGATIVE
*          IER=3  X .GT. 170, MACHINE RANGE EXCEEDED
*          IER=4  BK .GT. 10**70
*
*      REMARKS
*      N MUST BE GREATER THAN OR EQUAL TO ZERO
*
*      SUBROUTINES AND FUNCTION SUBPROGRAMS REQUIRED
*      NONE
*
*      METHOD
*      COMPUTES ZERO ORDER AND FIRST ORDER BESSEL FUNCTIONS
*        USING SERIES APPROXIMATIONS AND THEN COMPUTES N TH
*        ORDER FUNCTION BY USING RECURRENCE RELATION.
*      RECURRENCE RELATION AND POLYNOMIAL APPROXIMATION
*       TECHNIQUE AS DESCRIBED BY A.J.M.HITCHCOCK,'POLYNOMIAL
*        APPROXIMATIONS TO BESSEL FUNCTIONS OF ORDER ZERO AND
```

```
*       ONE AND TO RELATED FUNCTIONS', M.T.A.C.,
*       V.11,1957,PP.86-88, AND G.N. WATSON,
*     'A TREATISE ON THE THEORY OF BESSEL FUNCTIONS',
*       CAMBRIDGE
*     UNIVERSITY PRESS, 1958, P.62
*
***********************************************************************

      SUBROUTINE BESK(X,N,BK,IER)

      REAL*8 GJ
      DIMENSION T(12)

      BK=0.
      IF (N) 10,11,11
 10   IER=1
      RETURN
 11   IF (X) 12,12,20
 12   IER=2
      RETURN

 20   IF (X-170.0) 22,22,21
 21   IER=3
      RETURN

 22   IER=0
      IF (X-1) 36,36,25
 25   A=EXP(-X)
      B=1./X
      C=SQRT(B)
      T(1)=B
      DO 26 L=2,12
 26   T(L)=T(L-1)*B
      IF (N-1) 27,29,27
C
C     COMPUTE KO USING POLYNOMIAL APPROXIMATION
C
 27   G0=A*(1.2533141-.1566642*T(1)+.08811128*T(2)
     &    -.09139095*T(3)+.1344596*T(4)-.2299850*T(5)
     &    +.3792410*T(6)-.5247277*T(7)+.5575368*T(8)
     &    -.4262633*T(9)+.2184518*T(10)-.06680977*T(11)
     &    +.009189383*T(12))*C
      IF (N) 20,28,29
 28   BK=G0
      RETURN
C
C     COMPUTE K1 USING POLYNOMIAL APPROXIMATION
C

 29   G1=A*(1.2533141+.4699927*T(1)-.1468583*T(2)
     &    +.1280427*T(3)-.1736432*T(4)+.2847618*T(5)
```

```
     &     -.4594342*T(6)+.6283381*T(7)-.6632295*T(8)
     &     +.5050239*T(9)-.2581304*T(10)+.07880001*T(11)
     &     -.01082418*T(12))*C
       IF (N-1) 20,30,31
 30    BK=G1
       RETURN
C
C      FROM KO,K1, COMPUTE KN USING RECURRENCE RELATION
C
 31    DO 35 J=2,N
       GJ=2.*(FLOAT(J)-1.)*G1/X+G0
       IF(GJ-1.0D32) 33,33,32
 32    IER=4
       GOTO 34
 33    G0=G1
 35    G1=GJ
 34    BK=GJ
       RETURN
 36    B=X/2.
       A=.5772157+ALOG(B)
       C=B*B
       IF (N-1) 37,43,37
C
C      COMPUTE KO USING SERIES EXPANSION
C
 37    G0=-A
       X2J=1.
       FACT=1.
       HJ=.0
       DO 40 J=1,6
       RJ=1./FLOAT(J)
       X2J=X2J*C
       FACT=FACT*RJ*RJ
       HJ=HJ+RJ
 40    G0=G0+X2J*FACT*(HJ-A)
       IF (N) 43,42,43
 42    BK=G0
       RETURN
C
C      COMPUTE K1 USING SERIES EXPANSION
C
 43    X2J=B
       FACT=1.
       HJ=1.
       G1=1./X+X2J*(.5+A-HJ)
       DO 50 J=2,8
       X2J=X2J*C
       RJ=1./FLOAT(J)
       FACT=FACT*RJ*RJ
       HJ=HJ+RJ
 50    G1=G1+X2J*FACT*(.5+(A-HJ)*FLOAT(J))
```

```
      IF (N-1) 31,52,31
 52   BK=G1

      RETURN
      END

*****************************************************************
*
*    SUBROUTINE PSYCH(PT,TEMP,PS,HA,HS,VA,VS,WS,FS,HWTR,TEST)
*
*     THIS SUBROUTINE IS KNOWN AS PSYCHROMETRIC CHART, CAPABLE
*      OF DETERMINE MOIST AIR PROPERTIES.
*
*       PT=PB=BAROMETRIC PRESSURE (IN OF HG)
*       TEMP=DRY-BULB TEMPERATURE F
*       HA=ENTHALPY OF DRY AIR
*       HS=ENTHALPY OF SATURATED AIR( BTU/LB OF DRY AIR)
*       VA=VOLUME OF DRY AIR(CU FT/LB)
*       VS=VOLUME OF SATURATED AIR(CU FT/LB OF DRY AIR)
*       WS=HUMIDITY OF SATURATED AIR(LB OF WATER/ LB OF DRY
*          AIR)
*       FS(AIR-WATER INTERACTION FACTOR)
*       HWTR=ENTHALPY OF LIQUID WATER(BTU/LB OF WATER)
*       THIS PROGRAM IS WRITTEN BASED UPON STANDARDIZATION OF
*       THERMODYMIC PROPERTIES OF MOIST AIR
*       TEST= THIS IS AN INDEX FORTABULAR CALCULATION
*       IF T=1 PROGRAM GENERATE ENTIRE TABLE FOR
*              WS,VA,VAS,VS,HA
*       HAS,HS,PS,HH2O,HWP,HFG,AND HWDP
*       WHERE
*       PS=VAPOR PRESSURE
*       HH2O=ENTHALPY OF WATER VAPOR(BTU/LB OF WATER)
*       HWP=ENTHALPY OF WATER (BASICALLY SAME AS HW)
*       HFG=HEAT OF VAPORIZATION(BTU/LB  OF WATER)
*       HWDP=BASICALLY SAME AS HW.
*       SAR = ENTROPY  OF DRY AIR
*       SS = ENTROPY OF SATURATED MOIST AIR
*       SAS =SS-SAR
*
*       SUBROUTINES AND FUNCTIONS REQUIRED
*
*        SUBROUTINE ENTRY
*        SUBROUTINE ALAH
*
*****************************************************************

      SUBROUTINE PSYCH(PT,TEMP,PS,HA,HS,VA,VS,WS,FS,HWTR,TEST)

      INTEGER TEST
      COMMON NTAPE,INPUT,SAR,SS,SAS
```

```
      DIMENSION TM(330),PSS(300),FSS(300),X20(300),HWP(300),
     &          HFG(300),HGP(300),HWDP(300)
      REAL SUM1(5),SUM2(5),HO(5),RINT(4),TINT(4)
      REAL C(5),AA(5),B(5),D(5),F(5),G(5),AF(4)
      REAL HW(4,6),A(4,6),V(4,6),XN(3,5),TH(3,5),AL(3,5),
     &     R(4,6)
      OPEN(6,FILE='PSY',STATUS='NEW')

      DATA HW/-114.25,-110.54,-106.64,-102.58,-102.
     +58,-98.34,-93.92,-89.34,-93.92,-89.34,-84.57,
     +-79.64,.02,10.06,20.06,30.04,30.04,40.03,50.01,
     +60.,60.,69.99,80.01,90.05/,A/-80.,-70.,-60.,-50.
     +,-50.,-40.,-30.,-20.,-30.,-20.,-10.,0.,0.,10.,20.,
     +30.,30.,40.,50.,60.,60.,70.,80.,90./,V/676.3,677.,
     +677.5,677.9,677.9,678.,678.,677.9,678.,677.9,677
     +.5,677.,597.31,591.7,586.,580.4,580.4,574.7,569.,
     +563.2,563.2,557.3,551.3,545.2/
      DATA C/3.5,3.5,2.5,3.5,4./,XN/1
     +.,0.,0.,1.,0.,0.,0.,0.,0.,2.,1.,1.,1.,1.,1./,TH
     +/2235.4,99999.,99999.,3352.69,99999.,99999.,99999.,
     +99999.,99999.,960.,1944.,3379.,2291.16,51
     +76.37,5445.59/,AA/1.073,.9580,0.,0.,5.011/,B
     +/0.,.09,0.,0.,0./,D/3.3E-6,2.023E-6,0.,0.,2.32E-5/,F
     +/.011,.009009,0.,0.,0./,G/1.2164,-.414686,1.867
     +,1.8945,-4.1083/,AL/0.,0.,0.,0.,0.,0.,0.,0.,0
     +.,0.,0.,0.,-.03958,.05353,.04/,AF/-7.90298,5.02808,-1.3
     +816E-7,8.1328E-3/,R/.44E-8,1.9E-8,.71E-7,2.35
     +E-7,2.35E-7,.7E-6,1.91E-6,.48E-5,1.91E-6,.48E-5,
     +1.11E-5,2.43E-5,2.37E-5,4.44E-5,.79E-4,1.34E-4,
     +1.34E-4,2.19E-4,3.46E-4,5.26E-4,5.26E
     +-4,.78E-3,1.12E-3,1.58E-3/

      PB=PT
      MQ=0
      JJ=0
      IF(TEST.NE.1) GOTO 70
      KT=-100
10    KL=KT+50
      WRITE(6,40)
20    FORMAT(1X,I5,2X,E9.4,1X,F8.3,1X,F8.3,2X,F8.3,3X,F8.3,
     +4X,F8.3,3X,F8.3,4X,F8.4,4X,F8.4)
30    FORMAT('TEMP(F)    WS       VA       VAS      VS      HA
     +         HAS      HS         SA         SS         SAS')
40    FORMAT ('72H1              THERMODYNAMIC      PROPERTIES
     + OF MOIST AIR    ' )
      WRITE(6,50) PB
50    FORMAT('                          AT BAROMETRIC PRESSURE
     +=  ' ,F5.2,'      IN. HG')
      WRITE(6,30)
      WRITE(6,30)
60    FORMAT(1H )
```

```
      GOTO 80
70    KT=1
      KL=1
80    DO 440 IT=KT,KL
      TT=IT
      IF(TEST.NE.1) TT=TEMP
      T=(TT-32.)/1.80+273.16
      U=1./T
      DO 160 I=1,5
      SUM1(I)=0.
      SUM2(I)=0.
      DO 130 J=1,3
      EX=EXP(-TH(J,I)*U)
      IF(XN(J,I))   110,100,110
100   PAULA=0.
      GOTO 120
110   PAULA=XN(J,I)*TH(J,I)*EX/(1.-EX)
120   SUM1(I)=SUM1(I)+PAULA
130   SUM2(I)=SUM2(I)+AL(J,I)*TH(J,I)*EX
      IF (F(I))   150,140,150
140   Q=0.
      GOTO 160
150   Q=F(I)*TH(1,I)*EXP(-TH(1,I)*U)/(EXP(-TH(1,I)*U)-1.)**2
160   HO(I)=1.98583*(C(I)/U+SUM1(I)-AA(I)-2.*B(I)*U+
     &      D(I)/U**2-Q+SUM2(I))
      HO(5)=HO(5)/18.016
      HOAIR=(.2095*HO(1)+.7809*HO(2)+.0093*HO(3)+
     &      .0003*HO(4))/28.966
      AAA=-40.7+13116.*U+12.E7*U**3
      BAA=-40.7+26232.*U+48.E7*U**3
      AWW=-33.97+55306.*U*10.**(72000.*U**2)
      BWW=-33.97+110612.*10.**(72000.*U**2)*U+
     &    55306.*U**3*144000.*ALOG(10.)*10.**(72000.*U**2)
      EP=EXP(-4416.5*U)
      AAW=-29.53+.00669*(1.-EP)/U+17546.*U+95300.*U**2+
     &    8.515E7*U**3
      BAW=-29.53+.00669*4416.5*EP+2.*17546.*U+3.*95300.*U**2
     &   +4.*8.515E7*U**3
      AWWW=0.0348*U*U*AWW**3
      BWWW=.1044*U*U*AWW*BWW
      P=PB/29.92
      HAIR=HOAIR-(BAA*P*.0242179)/28.966-60.99
      HAIR=HAIR*1.8
      B1=11.344*(1.-T/373.16)
      B2=-3.49149*(373.16/T-1.)
      IF (T-273.16)  200,200,190
190   Z=AF(1)*(373.16/T-1.)+AF(2)*ALOG10(373.16/T)+
     &  AF(3)*(10.**B1-1.)+AF(4)*(10.**B2-1.)
      PPP=1.
      GOTO 210
```

```
200    Z=9.09718*(1.-273.16/T)-3.56654*ALOG10(273.16/T)+
      &   .876793*(1.-T/273.16)
       PPP=.0060273
210    PS=10.**Z*PPP
       HH20=HO(5)-(BWW*PS*.0242179)/18.016+477.277
       HH20=HH20-0.5*(BWWW*PS*PS*0.0242179)/18.016
       HH20=HH20*1.8
       TX=T-273.16
       MG=0
       I=0
       IF(TX+50.)   400,220,220
220    IF(TX+25.)   390,230,230
230    IF(TX)    380,370,240
240    IF(TX-30.)    370,250,250
250    IF(TX-60.)    360,350,350
260    DO 270 KL=1,4
       TINT(KL)=A(KL,I)
270    RINT(KL)=R(KL,I)
       CALL ALAH(RINT,TINT,TX,BETA)
       ALPHA=(AAA-2.*AAW+AWW)*PS/(82.0567*T)+
      &       AWWW*PS**2/(82.0567*T)
       ZEP=ALPHA*(1.-PS/P)+BETA*(P/PS-1.)
       FS=EXP(ZEP)
       WS=(.62197*FS*PS/P)/(1.-FS*PS/P)
       YS=18.016/(28.966*WS+18.016)
       HS=YS*HOAIR*28.966+(1.-YS)*HO(5)*18.016-(YS**2*BAA+
      &    2.*YS*(1.-YS)*BAW+(1.-YS)**2*BWW)*P*.0242179
       HS=HS-.5*(1.-YS)**3*BWWW*P*P*0.0242179
       VS=82.0567*T/P-(YS**2*AAA+2.*YS*(1.-YS)*AAW+
      &    (1.-YS)**2*AWW)
       VS=VS-(1.-YS)**3*AWWW*P
       OM1=(1./252.)/(28.966*(1./453.5924))
       HSP=OM1*HS/YS+859.099*WS-109.782
       OM2=(1./28316.85)/(28.966*(1./453.5924))
       VSP=OM2*VS/YS
       VA=(82.0567*T/P-AAA)*OM2
       HASP=HSP-HAIR
       VASP=VSP-VA
       CALL ENTPY(TH,U,XN,AL,F,C,B,D,G,AAA,BAA,P,AWWW,BWWW,AWW,
      &      BWW,AAW,BAW,YS,WS)
280    JJ=JJ+1
       I=0
       MG=1
       IF(TX+50.)    400,290,290
290    IF(TX+25.)    390,300,300
300    IF(TX)    380,310,330
310    IF (MQ)   370,320,370
320    MQ=1
       GOTO 380
330    IF(TX-30.)    370,340,340
340    IF(TX-60.)    360,350,350
```

```
350   I=I+1
360   I=I+1
370   I=I+1
      MQ=0
380   I=I+1
390   I=I+1
400   I=I+1
      IF(MG.EQ.0) GOTO 260
      DO 410 KL=1,4
      TINT(KL)=A(KL,I)
410   RINT(KL)=HW(KL,I)
      CALL ALAH(RINT,TINT,TX,HWW)
      HWP(JJ)=HWW*1.8
      HGP(JJ)=HH20
      HFG(JJ)=HGP(JJ)-HWP(JJ)
      DO 420 KL=1,4
      RINT(KL)=V(KL,I)
420   TINT(KL)=A(KL,I)
      CALL ALAH(RINT,TINT,TX,TOM)
      HWDP(JJ)=HGP(JJ)-TOM*1.8
      ITT=TT
      TM(JJ)=TT
      PSS(JJ)=PS*29.921
      FSS(JJ)=FS
      X20(JJ)=HH20
      IF(MQ.EQ.1) GOTO 280
      IF(TEST.NE.1) GOTO 530
      WRITE (6,20) ITT,WS,VA,VASP,VSP,HAIR,HASP,HSP,SAR,SS,SAS
440   CONTINUE
      KT=KT+50
      IF (KT.LT.140) GOTO 10
      IF(PB)   530,450,530
450   KP=1
      DO 520 JM=1,5
      WRITE (6,460)
460   FORMAT(1H1,'                    THERMODYNAMIC     PROPERTIES
     + OF WATER AT SATURATION')
      WRITE (6,470)
470   FORMAT(1H1,'                          BAROMETRIC PRESSUR
     +E =29.92 IN HG')
      WRITE(6,60)
C       WRITE(6,480)
C480    FORMAT(123H   T(F)                PS              FSC
C     +      HH20        HWP          HFG    H    W
C     +DP  )
      WRITE(6,60)
      KPP=KP+50
      DO 500 JJ=KP,KPP
500   WRITE(6,510) TM(JJ),PSS(JJ),FSS(JJ),X20(JJ),HWP(JJ),
     &      HFG(JJ),HWDP(JJ)
510   FORMAT(F5.0,1X,2(9X,E9.4),4(10X,F10.2))
```

```
520    KP=KP+51
530    HA=HAIR
       HS=HSP
       VS=VSP
       PS=PSS(1)
       HWTR=HWP(1)

       RETURN
       END


*****************************************************************
*
*      SUBROUTINE DBDP(DB,WB,PT,W,H,S,V,PV,DP,RH)
*
*      THIS SUBROUTINE CALCULATES AIR PROPERTIES FOR A GIVEN
*      SET OF AIR DRY BULB (DB) AND DEW POINT (DP)
*      TEMPERATURES.
*
*      INPUT PARAMETERS
*
*         DB=DRY BULB TEMPERATURE F
*         DP=THERMODYNAMIC DEW-POINT TEMPERATURE( ASHRAE
*            DEFINATION)
*         PT=BAROMETRIC PRESSURE IN OF HG
*
*      OUTPUT PARAMETERS
*
*         W=HUMIDITY RATIO
*         H=MOIST AIR ENTHALPY
*         V=MOIST AIR VOLUME
*         SAR= ENTROPY OF DRY AIR
*         SS= ENTROPY OF SATURATED MOIST AIR
*         SAS= SS-SAR
*
*      SUBROUTINES AND FUNCTIONS REQUIRED
*
*        SUBROUTINE PSYCH
*        SUBROUTINE OF
*
*****************************************************************

       SUBROUTINE DBDP(DB,WB,PT,W,H,S,V,PV,DP,RH)

       COMMON NTAPE,INPUT,SAR,SS,SAS
       REAL MU

       CALL PSYCH(PT,DP,PSP,HAP,HSP,VAP,VSP,WSP,FSP,HWP,0)
       PV=PSP
       IF(DB.NE.DP) GOTO 16
       H=HSP
```

```
      S=SS
      V=VSP
      W=WSP
      WB=DP
      RH=100.
      GOTO 14
16    W=WSP
      CALL PSYCH(PT,DB,PS,HA,HS,VA,VS,WS,FS,HW,0)
      H=HA+W/WS*(HS-HA)
      V=VA+W*(VS-VA)/WS
      S=SAR+SAS*W/WS
      IF(DB.LT.96.) GO TO 1
      CALL OF(DB,W,WS,VV,HH,SSS)
      H=H+HH
      V=V+VV
      S=S+SSS
1     MU=W/WS
      RH=MU/(1.-(1.-MU)*FS*PS/PT)*100.
      WB1=DB
      DT=10.
      CALL PSYCH(PT,WB1,PS1,HA1,HS1,VA1,VS1,WS1,FS1,HW1,0)
      Y1=HS1-H-(WS1-W)*HW1
13    WB2=WB1-DT
      CALL PSYCH(PT,WB2,PS2,HA2,HS2,VA2,VS2,WS2,FS2,HW2,0)
      Y2=HS2-H-(WS2-W)*HW2
      IF(Y1*Y2) 10,11,12
11    IF(Y1.EQ.0) WB=WB1
      IF(Y2.EQ.0.) WB=WB2
      GOTO 14
12    Y1=Y2
      WB1=WB2
      GOTO 13
10    IF(DT.LT.0.005) GOTO 15
      DT=DT/2.
      GOTO 13
15    Z=ABS(Y1/Y2)
      WB=(WB1+WB2*Z)/(1.+Z)

14    RETURN
      END


**********************************************************
*
*     SUBROUTINE DBWB(DB,WB,PT,W,H,S,V,PV,DP,RH)
*
*     THIS SUBROUTINE CALCULATES AIR PROPERTIES FOR A GIVEN
*    SET OF AIR DRY BULB (DB) AND WET BULB (WB) TEMPERATURES.
*
*     INPUT PARAMETERS
*
```

```
*         DB=DRY BULB TEMPERATURE (F)
*         WB=THERMODYNAMIC WET-BULB TEMPERATURE( ASHRAE
*            DEFINATION)
*         PT=BAROMETRIC PRESSURE IN OF HG
*
*      OUTPUT PARAMETERS
*
*         W=HUMIDITY RATIO
*         H=MOIST AIR ENTHALPY
*         V=MOIST AIR VOLUME
*         SAR= ENTROPY OF DRY AIR
*         SS= ENTROPY OF SATURATED MOIST AIR
*         SAS= SS-SAR
*
*      SUBROUTINES AND FUNCTIONS REQUIRED
*
*        SUBROUTINE PSYCH
*        SUBROUTINE ALAH
*        SUBROUTINE OF
*
*****************************************************************

      SUBROUTINE DBWB(DB,WB,PT,W,H,S,V,PV,DP,RH)

      REAL MU,BX(7),TY(4),BY(4)
      INTEGER*4 TX(7)
      COMMON NTAPE,INPUT,SAR,SS,SAS

      DATA BX/0.0268,0.0650,0.1439,0.3149,0.6969,1.636,4.607/
      DATA TX/96,112,128,144,160,176,192/

      CALL PSYCH(PT,DB,PS,HA,HS,VA,VS,WS,FS,HW,0)
      S1=SAR
      S2=SAS
      IF(DB.NE.WB) GOTO 16
      DP=DB
      PV=PS
      H=HS
      V=VS
      W=WS
      RH=100.
      S=SS
      GOTO 17
16    CALL PSYCH(PT,WB,PSTAR,HASTR,HSTAR,VASTR,VSTR,WSTR,
     &FSTR,HWSTR,0)
      W=(HSTAR-HA-HWSTR*WSTR)/(HS-HA-HWSTR*WS)*WS
      IF(W.LT.0) W=0.
      H=HA+W/WS*(HS-HA)
      V=VA+W/WS*(VS-VA)
      S=S1+S2*W/WS
      IF(DB.LT.96) GOTO 1
```

```
      IF(DB.GT.150) GOTO 18
      DO 19 J=1,4
      TY(J)=TX(J)
19    BY(J)=BX(J)
      GOTO 20
18    DO 21 J=1,4
      JJ=J+3
      TY(J)=TX(JJ)
21    BY(J)=BX(JJ)
20    CALL ALAH(BY,TY,DB,B)
      AA=B/WSTR**2+1.6078*HWSTR
      BB=B/WSTR+HWSTR*(1.-1.6078*W)
      CC=W*HWSTR
      W=(-BB+SQRT(BB*BB+4*AA*CC))/2/AA
      CALL OF(DB,W,WS,VV,HH,SSS)
      H=H+HH
      V=V+VV
      S=S+SSS
1     MU=W/WS
      RH=MU/(1.-(1.-MU)*FS*(PS/PT))*100.
      DT=10.
      DP1=DB
      CALL PSYCH(PT,DP1,PS1,HA1,HS1,VA1,VS1,WS1,FS1,HW1,0)
      Y1=WS1-W
13    DP2=DP1-DT
      CALL PSYCH(PT,DP2,PS2,HA2,HS2,VA2,VS2,WS2,FS2,HW2,0)
      Y2=WS2-W
      IF(Y1*Y2)  10,11,12
11    IF(YI.EQ.0.) DP=DP1
      IF(Y2.EQ.0.) DP=DP2
      GOTO 14
12    Y1=Y2
      DP1=DP2
      GOTO 13
10    IF(DT.LT.0.001) GOTO 15
      DT=DT/2.
      GOTO 13
15    Z=ABS(Y1/Y2)
      DP=(DP1+DP2*Z)/(1.+Z)
14    CALL PSYCH(PT,DP,PV,HA,HS,VA,VS,WS,FS,HW,0)

17    RETURN
      END


**********************************************************************
*
*     SUBROUTINE ALAH(P.C,X,Y)
*
*     FOUR POINT LAGRANGEAN INTERPOLATION
```

```
*
*****************************************************************

      SUBROUTINE ALAH(R,C,X,Y)

      DIMENSION R(4),C(4)

      X1=X-C(1)
      X2=X-C(2)
      X3=X-C(3)
      X4=X-C(4)
      Q12=C(1)-C(2)
      Q13=C(1)-C(3)
      Q14=C(1)-C(4)
      Q21=C(2)-C(1)
      Q23=C(2)-C(3)
      Q24=C(2)-C(4)
      Q31=C(3)-C(1)
      Q32=C(3)-C(2)
      Q34=C(3)-C(4)
      Q41=C(4)-C(1)
      Q42=C(4)-C(2)
      Q43=C(4)-C(3)
      Y=R(1)*X2*X3*X4/Q12/Q13/Q14+R(2)*X1*X3*X4/Q21/Q23/Q24
      Y=Y+R(3)*X1*X2*X4/Q31/Q32/Q34+R(4)*X1*X2*X3/Q41/Q42/Q43

      RETURN
      END


*****************************************************************
*
*     SUBROUTINE OF(T,W,WS,V,H,S)
*
*     IF(T.GT.114) OF IS USED TO FIND CORRECTION FOR H,V,S
*     CALCULATED
*     BY H=HA+W*HAS/WS+H, V=VA+W*VAS/WS+V, S=SAR+W*SAS/WS+S
*     T=DRY BULB TEMPERATURE F
*     W=HUMIDITY RATIO LB/LB OF WA
*     W=LB/LB OF DRY AIR
*     WS=SATURATED AIR HUMIDITY RATIO
*     V=CORRECTED VOLUME OF MOIST AIR
*     H=CORRECTED ENTHALPY OF MOIST AIR (BTU/LB OF DRY AIR)
*
*****************************************************************

      SUBROUTINE OF(T,W,WS,V,H,S)

      REAL  A(7),B(7),C(7),AX(4),BX(4),CX(4),TY(4)
      INTEGER TX(7)
      COMMON NTAPE,INPUT,SAR,SA,SAS
```

```
      DATA A/0.0018,0.0042,0.0096,0.0215,0.0487,0.1169,
     &0.3363/,B/0.0260,0.0650,0.1439,0.3149,0.6969,
     &1.639,4.608/,C/0.00004,0.00009,.0002,0.00042,
     &0.00091,0.00207,0.00567/

      DATA TX/96,112,128,144,160,176,192/

      XC=W*(1.-W/WS)/(1.+1.6078*W)/WS
      IF(T-150.)1,1,2
1     DO 3 J=1,4
      TY(J)=TX(J)
      AX(J)=A(J)
      BX(J)=B(J)
3     CX(J)=C(J)
      GOTO 6
2     DO 4 J=1,4
      JJ=J+3
      AX(J)=A(JJ)
      BX(J)=B(JJ)
      CX(J)=C(JJ)
4     TY(J)=TX(JJ)
6     CALL ALAH(AX,TY,T,AY)
      CALL ALAH(BX,TY,T,AY)
      CALL ALAH(CX,TY,T,CY)
      V=XC*AY
      H=XC*BY
      S=XC*CY

      RETURN
      END



*****************************************************************
*
*     SUBROUTINE ENTPY(TH,U,XN,AL,F,C,B,D,G,AAA,BAA,P,AWWW,
*                 BWWW,AWW,BWW,AAW,BAW,YS,WS)
*
*     THIS SUBROUTINE FINDS ENTROPIES
*
*****************************************************************

      SUBROUTINE ENTPY(TH,U,XN,AL,F,C,B,D,G,AAA,BAA,P,AWWW,
     &            BWWW,AWW,BWW,AAW,BAW,YS,WS)

      COMMON NTAPE,INPUT,SAR,SS,SAS
      DIMENSION TH(3,5),B(5),D(5),F(5),G(5),C(5),XN(3,5),
     &AL(3,5),SO(5)

      DO 1 I=1,5
      SUM1=0
```

```
      SUM2=0
      DO 2 J=1,3
      EX=EXP(-TH(J,I)*U)
      IF(XN(J,I))3,8,3
8     PAULA=0.
      GOTO 4
3     PAULA=XN(J,I)*(TH(J,I)*U*EX-(1.-EX)*ALOG(1.-EX))
     &      /(1.-EX)
4     SUM1=SUM1+PAULA
2     SUM2=SUM2+AL(J,I)*EX*(1.+TH(J,I)*U)
      EX=EXP(-TH(J,I)*U)
      IF(F(I))5,6,5
6     Q=0
      GOTO 1
5     Q=F(I)*(EX*(1.-EX)-1.)/(EX-1.)**2
1     SO(I)=1.98583*((C(I)*(1.-ALOG(U)))+SUM1+SUM2-
     &      (B(I)*U**2)+(2.*D(I)/U)+Q+(G(I)))
      SO(5)=SO(5)/18.016
      CAA=U*(AAA-BAA)
      SOAIR=(.2095*SO(1)+.7809*SO(2)+.0093*SO(3)+
     &      .0003*SO(4))/28.966+.03947
      SAR=SOAIR+.0242179*CAA*P/28.966-1.98583/28.966*
     &    ALOG(P)-1.60096
      CWWW=U*(AWWW-BWWW)
      CWW=U*(AWW-BWW)
      CAW=(AAW-BAW)*U
      IF(YS.GE.1.) GOTO 1000
      IF(YS)9,9,10
9     SS=0.
      GOTO 11
10    SS=((28.966*YS*SOAIR+18.016*(1.-YS)*SO(5))+
     &   .0242179*((YS**2*CAA+2.*YS*(1.-YS)*CAW+
     &   (1.-YS)**2*CWW)*P+.5*(1.-YS)**3*CWWW*P**2)-1.985
     &   83*(YS*ALOG(YS)+(1.-YS)*ALOG(1.-YS)+ALOG(P)))/
     &   28.966/YS-1.60096-.8396*WS

11    SAS=SS-SAR

1000  RETURN
      END


*****************************************************************
*
*     SUBROUTINE RHMIX(DB1,DB2,W1,W2,CFM1,CFM2,DBMIX,PB,DP)
*
*     THIS SUBROUTINE DETERMINES THE AIR DRY BULB AND DEW
*     POINT TEMPERATURES OF A MIXED AIR.
*
*     INPUT PARAMETERS
*
```

```
*       DB1:    DRY BULB TEMPERATURE OF AIR 1
*       DB2:  DRY BULB TEMPERATURE OF AIR 2
*       W1:   HUMIDITY RATIO OF AIR 1
*       W2:   HUMIDITY RATIO OF AIR 2
*       CFM1:   VOLUME FIOW RATE OF AIR 1
*       CFM2:   VOLUME FLOW RATE OF AIR 2
*
*      OUTPUT PARAMETERS
*
*       DBMIX:  MIXED AIR DRY BULB TEMPERATURE
*       DP:     MIXED AIR DEW POINT TEMPERATURE
*
*****************************************************************

      SUBROUTINE RHMIX(DB1,DB2,W1,W2,CFM1,CFM2,DBMIX,PB,DP)

      REAL*8 W3

      CALL PSYCH(PB,DB1,PS,HA,HS,V1,VS,WS,FS,HW,0)
      CALL PSYCH(PB,DB2,PS,HA,HS,V2,VS,WS,FS,HW,0)
      BTU1=CFM1/V1*.24
      BTU2=CFM2/V2*.24
      BTU3=BTU1+BTU2
      PER1=BTU1/BTU3
      PER2=BTU2/BTU3
      CALL PSYCH(PB,DBMIX,PS,HA,HS,V2,VS,WS,FS,HW,0)
      W3=PER1*W1+PER2*W2
      DP=-1.393723D 00+1.2316782D 04*W3-
     &   1.1517287D 06*W3*W3+7.116057D 07
     &   *W3**3-2.389548D 09*W3**4+3.301402D 10*W3**5

      RETURN
      END


*****************************************************************
*
*       SUBROUTINE DBW(DB,W,RH,DP)
*
*       THIS SUBROUTINE IS USED TO DETERMINE DEW-POINT TEMP.
*      BY CALLING DEW-POINT FUNCTION FOR GIVEN DRY-BULB TEMP.
*       AND HUMIDITY RATIO.
*
*      DB: INPUT DRY BULB TEMPERATURE
*      W:  INPUT HUMIDITY RATIO
*      RH: OUTPUT RELATIVE HUMIDITY IN %
*      DP: OUTPUT DEW-POINT TEMPERATURE
*
*      SUBROUTINES AND FUNTION SUBPROGRAMS REQUIRED
*
*          FUNCTION PVSF(X)
```

```
*          FUNCTION DPF(V)
*
*****************************************************************

      SUBROUTINE DBW(DB,W,RH,DP)

          PVS=PVSF(DB)
          PV=29.92*W/(0.622+W)
          RH=PV*100/PVS
          DP=DPF(PV)

          RETURN
          END


*****************************************************************
*
*         FUNCTION DPF(PV)
*
*       THIS SUBROUTINE CALCULATES DEW-POINT TEMP. FOR A GIVEN
*         VAPOR PRESSURE
*
*     PV:  A GIVEN PRESSURE VAPOUR
*     DPF: DEW-POINT TEMPERATURE
*
*****************************************************************



      FUNCTION DPF(PV)

          IF (PV) 10,10,20
10        GOTO 40

20        CONTINUE
          Y=LOG(PV)
          IF(PV.GT.0.1836) GOTO 30
          DPF=71.98+24.873*Y+0.8927*Y*Y
          GOTO 40
30        DPF=79.047+30.579*Y+1.8893*Y*Y

40        RETURN
          END


*****************************************************************
*
*         FUNCTION PVSF(X)
*
*       THIS FUNCTION IS USED TO DEFERMINE THE SATURATED VAPOR
*         PRESSURE FOR A GIVEN DRY BULB TEMPERATURE
```

```
*
*     PVSF:      SATURATED VAPOUR PRESSURE
*     X:    A GIVEN DRY BULB TEMPERATURE
*
*****************************************************************

      FUNCTION PVSF(X)

         DIMENSION A(6),B(4),P(4)

        DATA A/-7.90298,5.02808,-1.3816E-7,11.344,
     & 8.1328E-3,-3.49149/, B /-9.09718,-3.56654,0.876793,
     & 0.0060273/

         T=(X+459.688)/1.8
         IF (T.LT.273.16) GO TO 10
         Z=373.16/T
         P(1)=A(1)*(Z-1)
         P(2)=A(2)*LOG10(Z)
         Z1=A(4)*(1-1/Z)
         P(3)=A(3)*(10**Z1-1)
         Z1=A(6)*(Z-1)
         P(4)=A(5)*(10**Z1-1)
         GOTO 20

10       Z=273.16/T
         P(1)=B(1)*(Z-1)
         P(2)=B(2)*LOG10(Z)
         P(3)=B(3)*(1-1/Z)
         P(4)=LOG10(B(4))
20       SUM=0
         DO 30 I=1,4
30       SUM=SUM+P(I)

         PVSF=29.921*10**SUM
         RETURN
         END
```